

Chromospheric activity and rotation of FGK stars in the solar vicinity^{★ ★★}

An estimation of the radial velocity jitter

R. Martínez-Arnáiz¹, J. Maldonado², D. Montes¹, C. Eiroa², B. Montesinos³

¹ Universidad Complutense de Madrid, Facultad de Ciencias Físicas, Dpt. Astrofísica, av. Complutense s/n. 28040 Madrid, Spain
e-mail: rma@astrax.fis.ucm.es

² Universidad Autónoma de Madrid, Departamento de Física Teórica, Módulo 15, 28049 Cantoblanco, Madrid, Spain

³ LAEX, CAB (CSIC-INTA), ESAC Campus, P.O. BOX 78, 28691 Villanueva de la Cañada, Madrid, Spain

Preprint online version: October 22, 2018

ABSTRACT

Context. Chromospheric activity produces both photometric and spectroscopic variations that can be mistaken as planets. Large spots crossing the stellar disc can produce planet-like periodic variations in the light curve of a star. These spots clearly affect the spectral line profiles and their perturbations alter the line centroids creating a radial velocity jitter that might “contaminate” the variations induced by a planet. Precise chromospheric activity measurements are needed to estimate the activity-induced noise that should be expected for a given star.

Aims. We obtain precise chromospheric activity measurements and projected rotational velocities for nearby ($d \leq 25$ pc) cool (spectral types F to K) stars, to estimate their expected activity-related jitter. As a complementary objective, we attempt to obtain relationships between fluxes in different activity indicator lines, that permit a transformation of traditional activity indicators, *i.e.*, Ca II H & K lines, to others that hold noteworthy advantages.

Methods. We used high resolution (~ 50000) *echelle* optical spectra. Standard data reduction was performed using the IRAF *ECHELLE* package. To determine the chromospheric emission of the stars in the sample, we used the spectral subtraction technique. We measured the equivalent widths of the chromospheric emission lines in the subtracted spectrum and transformed them into fluxes by applying empirical equivalent width and flux relationships. Rotational velocities were determined using the cross-correlation technique. To infer activity-related radial velocity (*RV*) jitter, we used empirical relationships between this jitter and the R'_{HK} index.

Results. We measured chromospheric activity, as given by different indicators throughout the optical spectra, and projected rotational velocities for 371 nearby cool stars. We have built empirical relationships among the most important chromospheric emission lines. Finally, we used the measured chromospheric activity to estimate the expected *RV* jitter for the active stars in the sample.

Key words. Galaxy: solar neighbourhood – Stars: late-type – Stars: activity – Stars: chromospheres – Stars: rotation – Stars: planetary systems

1. Introduction

Exoplanetary science is living a golden era characterized by the enormous rate at which new exoplanets are being discovered. This impressive advancement would not have been possible without parallel technological developments. Improved precision in both radial velocity and photometric measurements has extended the area around the star in which a planet can be found and has increased the probability of detecting low mass exoplanets. These improvements have created, however, a new and noteworthy problem, *i.e.*, the possibility of misidentifying plan-

ets. Chromospheric activity, in particular, the presence of spots and/or alteration of the granulation pattern in active regions, create a time-variable photometric and spectroscopic signature (Saar & Donahue 1997; Santos et al. 2000; Saar 2003) that might be misinterpreted as an exoplanet. Moreover, the minimum detectable mass of a planet orbiting a star is limited by the *rms* velocity jitter caused by stellar sources (Narayan et al. 2005). Therefore, a thorough analysis of activity levels, as only different activity indicators can provide, must be performed for those stars that constitute the natural targets of planet-search surveys.

When searching for exoplanets using the radial velocity (*RV*) technique, the possibility of jitter caused by chromospheric activity must be considered. When modeling stellar activity, Saar & Donahue (1997) were the first to quantitatively estimate the impact of stellar spots on the *RV* curve and showed that they could produce peak-to-peak *RV* amplitudes of up to a few hundred m s^{-1} , depending on spot size and the rotational velocity of the star. Subsequent studies (Santos et al. 2000; Saar et al. 2003; Paulson et al. 2004; Desert et al. 2007) obtained similar results. Several attempts to reduce *RV* noise levels by using an activity-based correction have been made (Saar & Donahue 1997; Saar et al. 1998; Santos et al. 2000; Saar & Fischer 2000; Saar et al.

Send offprint requests to: R. Martínez-Arnáiz (rma@astrax.fis.ucm.es)

[★] Based on observations made with the 2.2 m telescope at the Centro Astronómico Hispano Alemán (CAHA) at Calar Alto (Spain) and the Telescopio Nazionale Galileo (TNG) operated on the island of La Palma by the Istituto Nazionale de Astrofisica Italiano (INAF), in the Spanish Observatorio del Roque de los Muchachos. This research has been supported by the Programa de Acceso a Infraestructuras Científicas y Tecnológicas Singulares (ICTS).

^{★★} Tables A.1 to A.4 are only available in electronic form at the CDS via anonymous ftp to cdsarc.u-strasbg.fr (130.79.128.5) or via <http://cdsweb.u-strasbg.fr/cgi-bin/qcat?J/A+A/>

2003; Wright 2005). To use these corrections and to test and calibrate the relations, high precision, homogeneous chromospheric activity measurements are needed.

Transit searches for exoplanets are also affected by the temporal evolution and modulation of active regions across the stellar disc. The amplitude of variations can reach more than 1% when a large spot crosses the solar disc at activity maximum. This decrease in signal, combined with the modulation caused by stellar rotation can mimic the signal of a planet orbiting the star. Therefore Sun-like variability, not to mention that of stars more active than the Sun, can significantly affect the detection performance of photometric planet searches (Henry et al. 1997; Baliunas et al. 1997; Henry et al. 2000; Aigrain et al. 2004).

Hence, chromospheric activity is a *proxy* for predicting variability levels expected for a star, therefore allowing the estimation of a lower limit for planet detections in its vicinity. In this paper, we present spectroscopic-based chromospheric activity measurements for 371 nearby ($d \leq 25$ pc), cool (spectral types F to K) stars. These stars are the natural targets for exoplanet searches: their proximity ensures the ability to get an adequate signal-to-noise ratio (hereafter S/N), and solar-like stars are more likely to host so-called habitable planets (Kasting et al. 1993; Doyle et al. 1998; Turnbull & Tarter 2003). In this study, we considered not only the traditional chromospheric activity indicators, *i.e.*, R'_{HK} or $H\alpha$, but also other less common indicators, such as the Ca II IRT lines, which allow us to exploit peak-to-peak RV amplitude variations caused by spots being less significant at longer wavelengths (Desort et al. 2007; Reiners et al. 2009).

2. The stellar sample

The stellar sample comprises 371 cool stars in the solar vicinity, constrained to be at distances closer than 25 pc (see Table A.1). Distances were obtained from the Hipparcos Catalogue (ESA 1997) and the *New Reduction of the Raw Data* (van Leeuwen 2007). The spectral type distribution of the sample is 56 F type stars, 126 G type stars, 186 K stars, and 3 M type stars. Since our study is based on solar-like stars, only F, G and K spectral types stars with trigonometric parallax $\pi \geq 40$ mas were retrieved. To avoid misclassified stars, we used colour index as a complementary criteria, *i.e.*, $B-V$ colour index in the range 0.25-0.58 mag (F stars), 0.52-0.81 mag (G stars), and 0.74-1.40 mag (K stars). To establish the main-sequence character of the stars, we used a cutoff of ± 1 mag from the main sequence (Wright 2005). Finally, stars in multiple systems were removed from the sample. We used the CCDM (Dommanget & Nys 1994, 2002) and SB9 (Pourbaix et al. 2004) catalogues to identify astrometric and spectroscopic binaries, respectively.

These stars are potential targets for present and future projects that aim to detect Earth-like planets or exo-solar analogues to the Edgeworth-Kuiper Belt. In this context, most of our stars will be observed in the framework of DUNES (DUst around NEarby Stars), an approved Herschel Open Time Key Project with the aim of detecting cool faint dusty disks, at flux levels as low as the Solar EKB. Some preliminary results can be found in Martínez-Arnáiz et al. (2009), Maldonado et al. (2010), and Montes et al. (2010).

3. Observations and data reduction

The present work is based on data extracted from high resolution *echelle* spectra. Most of the spectra were obtained in several observing runs but we also used S^4N spectra (Allende Prieto et al.

2004). The latter have similar spectral resolution (~ 45000) to those obtained by us and were consequently used in an analogous manner to measure and analyse the stellar parameters and properties of the stars.

Observations were obtained at two different observatories: the German-Spanish Astronomical Observatory, CAHA, (Almería, Spain) and La Palma Observatory (La Palma, Spain). Observations were taken at the former 2 m telescope using the *Fibre optics Cassegrain Echelle Spectrograph* (FOCES) (Pfeiffer et al. 1998) with a 2048×2048 $24 \mu\text{m}$ SITE#1d-15, and at the latter with the 3.5 m Telescopio Nazionale Galileo (TNG) using the *Spectrografo di Alta Risoluzione Galileo* (SARG), the grid R4 (31.6 lines/mm), the red cross-dispersor (200 lines/mm), and a CCD detector mosaic of total surface 2048×4096 and $13.5 \mu\text{m}$ pixels.

We carried out four observing runs at CAHA (July 2005, January 2006, December 2006 and February-May 2007). FOCES spectra have a wavelength range from 3600 to 10700 Å in 106 orders with a typical resolution of 40000 (reciprocal dispersion from 0.08-0.13 Å/pixel in the red and blue region of the spectrum, respectively). The total number of stars observed using this spectrograph is 198. At La Palma Observatory, we performed three observing runs (February 2006, April 2007 and, November 2008). SARG spectra have a wavelength range from 5540 to 7340 Å in 50 orders with a resolution of 57000 (reciprocal dispersion from 0.01 to 0.04 Å/pixel in the red and blue region of the spectrum, respectively). We observed 129 stars using the SARG spectrograph.

As mentioned before, we used S^4N (Allende Prieto et al. 2004) spectra. These spectra were taken between October 2000 and November 2001 in six observing runs at the Harlan J. Smith 2.7 m telescope (McDonald Observatory) and two at the 1.52 m telescope at La Silla (Chile). At McDonald Observatory, the 2dcoudé (Tull et al. 1995) spectrograph with the Tektronix 2048×2048 $24 \mu\text{m}$ CCD detector was used. The spectral coverage was 3600-5100 Å with a typical resolution of 50000. At La Silla Observatory, the *Fiber-fed Extended Range Optical Spectrograph* (FEROS) (Kaufer et al. 2000) with the CCD detector EEV 2048×2048 $15 \mu\text{m}$ was used. The wavelength coverage in this case is 3500-9200 Å and the resolution ~ 45000 . The total number of studied S^4N stars is 106. Of them, 79 were observed at McDonald Observatory, while the rest were observed with FEROS at La Silla Observatory.

All the observed stars and the corresponding spectrograph used are listed in Table A.1. We note that some stars were observed more than once and using different spectrographs.

For the reduction, we used the standard procedures in the IRAF (*Image Reduction and Analysis Facility*) package (bias subtraction, extraction of the scattered light produced in the optical system, division by the normalized flat-field, and wavelength calibration). After the reduction process, the spectrum was normalized to the continuum order by order by fitting a polynomial function to remove the general shape of the aperture spectra.

4. Analysis and results

4.1. Rotational velocities

The determination of rotational velocities for stars in exoplanet surveys is crucial. Radial velocity variations induced by chromospherically active regions on the stellar surface are modulated by the rotation period of the star (Baliunas et al. 1997; Henry et al. 1997, 2000). Obtaining the rotational velocity of the star is thus

Table 1. A constant for FOCES, 2dcoudé (McDonald), FEROS and SARG spectra.

FOCES			2dcoudé			FEROS			SARG		
Name	SpT	A	Name	SpT	A	Name	SpT	A	Name	SpT	A
HIP 104217	K7V	0.500 ± 0.130	HIP 67422	K2V	0.550 ± 0.009	HIP 99461	K3V	0.640 ± 0.015	HIP 98698	K4V	0.523 ± 0.007
HIP 117779	K5V	0.436 ± 0.095	HIP 3765	K2V	0.610 ± 0.008	HIP 10138	K1V	0.620 ± 0.008	HIP 3765	K2V	0.605 ± 0.005
HIP 3765	K2V	0.616 ± 0.100	HIP 7981	K1V	0.580 ± 0.008	HIP 99825	K0V	0.600 ± 0.008	HIP 88972	K2V	0.501 ± 0.003
HIP 7981	K1V	0.574 ± 0.100	HIP 3093	K0V	0.570 ± 0.008	HIP 84720	G8V	0.640 ± 0.008	HIP 3093	K0V	0.607 ± 0.006
HIP 3093	K0V	0.557 ± 0.100	HIP 56997	G8V	0.630 ± 0.016	HIP 57443	G5V	0.660 ± 0.008	HIP 64924	G5V	0.606 ± 0.010
HIP 95319	G8V	0.648 ± 0.100	HIP 10798	G5V	0.620 ± 0.008	HIP 91438	G5V	0.650 ± 0.008	HIP 23835	G4V	0.646 ± 0.008
HIP 9269	G5V	0.581 ± 0.224	HIP 64924	G5V	0.600 ± 0.008	HIP 71683	G2V	0.640 ± 0.008			
HIP 48113	G0.5V	0.680 ± 0.280	HIP 7918	G1V	0.640 ± 0.008	HIP 1599	F9V	0.680 ± 0.007			
$\langle A \rangle = 0.574 \pm 0.004$			$\langle A \rangle = 0.598 \pm 0.003$			$\langle A \rangle = 0.643 \pm 0.003$			$\langle A \rangle = 0.581 \pm 0.082$		

essential to test whether detected RV variations have a stellar or a planetary origin.

The widths and shapes of spectral lines contain information that allow us to deduce physical information about the star, including its rotation rate. To measure this width, the most commonly used parameter is the line FWHM (Full Width Half Maximum) because it can be easily measured. The Fourier domain offers, however, some advantages over the wavelength one. Signatures of certain physical processes, such as the Doppler-shift distribution produced by rotation or macroturbulence, are more readily detected in that domain. The cross-correlation function (CCF) was therefore used to measure rotational velocities. The width (σ) of the CCF peak for a star when correlated with itself depends on the instrumental profile and several broadening mechanisms such as gravity, effective temperature, or rotation. To measure the rotational contribution, and hence determine the star’s projected rotational velocity, the contribution of other broadening mechanisms has to be modelled. For $v \sin i \leq 50 \text{ km s}^{-1}$, the CCF is well approximated by a Gaussian (Soderblom et al. 1989) and consequently the rotational broadening corresponds to a quadratic broadening of the CCF. In that case, the observed width of the CCF can be written as (see Queloz et al. 1998, and references therein)

$$\sigma_{\text{obs}}^2 = \sigma_{\text{rot}}^2 + \sigma_0^2, \quad (1)$$

where σ_{rot} is the rotational broadening and σ_0 is the width of the CCF of a similar non-rotating star. Projected rotational velocities, $v \sin i$, can be derived from the above expression as

$$v \sin i = A(\sigma_{\text{obs}}^2 - \sigma_0^2)^{1/2}, \quad (2)$$

where A is a coupling constant that depends on the spectrograph and its configuration. To determine A for each spectrograph, non-rotating stars were used¹. Their spectra were broadened from $v \sin i = 1 \text{ km s}^{-1}$ to 50 km s^{-1} using the program `JSTARMOD`². The value of σ_{obs} was then determined as the equivalent width of the first peak in the CCF. The constant A was found by fitting the relation $v \sin i^2$ vs σ_{obs}^2 . The stars used to compute A , the measurements, and the mean values for each spectrograph are shown in Table 1.

It is well known that σ_0 is a function of the broadening mechanisms present in the atmosphere of the star, except rotation (Melo et al. 2004). Since the broadening mechanisms are a function of the temperature and gravity, we may expect the colour index, $B-V$ to depend on σ_0 , for stars in the main sequence. To

determine this dependence, we created morphed spectra with no rotational velocity using the `ATLAS9` code by Kurucz (1993) adapted to operate on a linux platform by Sbordone et al. (2004) and Sbordone (2005). Temperatures vary from 3500 K to 6500 K (in intervals of 250 K). Since the stars were selected to be on the main sequence, $\log g$ was fixed to be 4.5. Solar metallicity was assumed. The morphed spectra were broadened to match the instrumental profile of the real spectra using the FWHM of the calibration arc lines, which is a good approximation of the broadening for the instruments used. Given that each spectrograph has a different resolving power, different instrumental broadenings were applied to obtain a calibration curve for each instrument. These curves are shown in Fig. 1.

Color indices, $B-V$, were obtained from the Tycho-2 Catalogue (Høg et al. 2000) using the transformation from B_T and V_T to Johnson indices (see Sect. 1.3 from Hipparcos Catalogue, ESA 1997) and are listed in Table A.1.

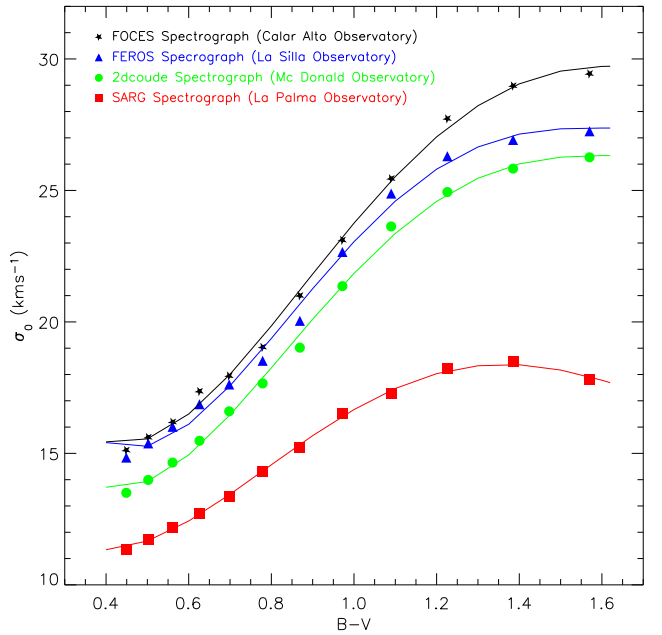


Fig. 1. Calibration between σ_0 and colour index $B-V$, where σ_0 represents the “natural” broadening of the spectrum lines and was obtained from synthetic spectra covering the spectral range of the observed stars. Given that the instrumental profile also contributes as a broadening mechanism and considering that each spectrograph has a different one, we had to derive a calibration relationship for each of them.

¹ Slow rotating stars with well known $v \sin i$.

² `JSTARMOD` is a modified version of the Fortran code `STARMOD` developed at the Penn State University (Huenemoerder & Barden 1984; Barden 1985). The modified code, implemented by J. López-Santiago, admits as input *echelle* spectra obtained with a CCD with more than 2048 pixels.

Once A and σ_0 were known for each star, $v \sin i$ could be directly derived by measuring σ_{obs} , *i.e.*, width of the CCF of the star when correlated with itself. Values for stars in the sample can be found in Table A.1. For slow rotating stars, it is important to mention that sometimes, the value of σ_0 is larger than that of σ_{obs} . In that case, $v \sin i$ cannot be measured using this method and we only provide an upper limit. This value was chosen by considering the minimum $v \sin i$ that could be measured with the same spectrograph for a star of the same spectral type, *i.e.*, the same σ_0 .

4.2. Chromospheric activity

We analyse different activity indicators throughout the optical spectra (from Ca II H&K to Ca II IRT). These lines form at different heights in the chromosphere hence provide information about different stellar properties. Some lines are present only during high energy processes such as flares. As shown in previous work (see Montes et al. 2000, 2001, and references therein), by performing a simultaneous analysis of different optical chromospheric activity indicators, a detailed study of the chromosphere's structure can be achieved and it becomes possible to discriminate between structures such as plages, prominences, flares, and microflares. The spectra used in this work have a spectral range that covers plages from Ca II H & K to Ca II IRT lines, including the Balmer lines.

4.2.1. Equivalent widths and fluxes

To determine the chromospheric contribution to the spectrum, and thus the chromospheric activity, the contribution of the photosphere must be removed. In order to achieve this, we used the spectral subtraction technique, described in detail by Montes et al. (1995a, 2000). This technique has been extensively used before because it permits the detection of weak emission features in the cores of chromospheric lines. In addition, it is the most effective means of identifying other chromospheric activity indicators such as the Balmer lines or the Ca II IRT, where no calibrations of the photospheric minimum flux exists (Barden 1985; Huenemoerder et al. 1989; Hall & Ramcey 1992; Frasca & Catalano 1994; Gunn & Doyle 1997; Lázaro & Arévalo 1997; Montes et al. 1995a, 1996b, 1997, 2000, 2001; Gálvez et al. 2002, 2007, 2009; López-Santiago et al. 2003, 2010). Inactive, slowly rotating stars, observed in the same observing run as the active stars, were used as reference to construct a morphed spectrum for each active star, using the program *ISTARMOD*. The program builds the morphed spectrum by shifting and broadening the reference spectrum to match that of the target star. This implies that the reference star must have a lower rotation rate than but a similar spectral type to the target star. A compilation of the inactive, slowly rotating stars used as references can be found in Table 2. Reference stars were initially chosen from the literature but some inactive, slowly rotating stars of the sample were also used as reference after confirming that they did not show chromospheric activity. To ensure that those stars were inactive, their values of total flux in Ca II H & K were compared to the lower boundary defined by Rutten (1984), which is traditionally used to correct flux measurements from the basal chromospheric flux (see Fig. 3). Maximum differences of 0.25 (F type stars), 0.3 (G type stars) and 0.35 (K type stars) in $\log(F_H + F_K)$ values between the stars used as references and the lower boundary of Rutten (1984) were allowed. The morphed spectrum was subtracted from that of the active star, obtaining a spectrum in which

only the chromospheric contribution is present, *i.e.*, the subtracted spectrum. The excess emission EW of the activity indicator lines were obtained from that spectrum. To estimate the errors in the measured EW , we followed Montes et al. (2001) and considered *ISTARMOD*'s typical internal precisions ($0.5\text{-}2 \text{ km s}^{-1}$ in velocity shifts and $\pm 5 \text{ km s}^{-1}$ in $v \sin i$), the *rms* in regions outside the chromospheric features (typically 0.01-0.03), and the standard deviations. The estimated errors for relatively strong emitters are in the range of 10-20% but for low activity stars errors are larger. Taking into consideration that S/N is lower in the blue spectral region, errors in the chromospheric features at these wavelengths are larger.

In Fig. 2, we plot an histogram for the total number of stars of each spectral type and the number that could be classified as active (displaying chromospheric features in the spectrum) or not active. In Table A.2, we give the excess emission EW and its er-

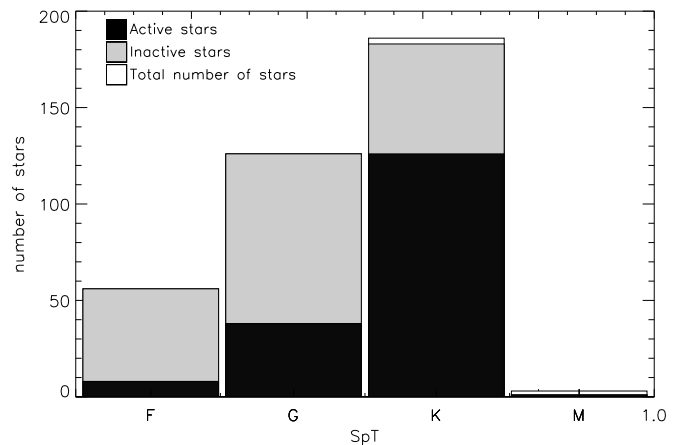


Fig. 2. Number of active (black) and inactive (grey) stars in the sample for each spectral type.

ror for the active stars in the sample. Of the complete sample of stars analysed (371 stars), 173 presented chromospheric activity features in their spectra. Of them, 8 were F type stars (14% of the analysed F stars), 38 G type stars (30% of the G type stars), 126 K type stars (68% of the analysed K stars) and 1 M star (33% of the analysed M stars). From the remaining, 193 could be classified as inactive because of the lack of any chromospheric activity feature in their spectra. Of them, 48 are F type stars (86% of the analysed F stars), 88 G type stars (70% of the total G type stars), and 57 K stars (31% of the analysed K type stars). The remaining 5 stars could not be classified as either active or inactive because of the low S/N of their spectra. We have included a column (Col. # 8) in Table A.1 to specify whether the star can be considered as active or not active. In 6 cases (5 K stars and 1 M star), we could not measure chromospheric activity due to the lack of a suitable non-active reference star to perform the subtraction technique, but chromospheric activity features were clearly present in the spectra. These stars were classified as active (and indicated with * in Table A.1) but chromospheric activity was not measured. It is also important to mention that due to the configuration used with the SARG spectrograph the spectral range corresponding to Ca II H & K was not covered and these lines could not be measured.

We must comment on eight special cases: HIP 3093, HIP 3765, HIP 7981, HIP 54646, HIP 60866, HIP 62523, HIP 77408 and HIP 85810. These stars were observed more than once and

Table 2. Inactive stars used as references in the subtraction technique to measure chromospheric activity

HIP	SpT	$B-V$	$v \sin i$ (km s ⁻¹)	Obs ¹ .	$\log(F_H + F_K)$ (erg cm ⁻² s ⁻¹)	HIP	SpT	$B-V$	$v \sin i$ (km s ⁻¹)	Obs ¹ .	$\log(F_H + F_K)$ (erg cm ⁻² s ⁻¹)
37279	F5V	0.420	5.38	Mc	0.76 ^a	8102	G8V	0.730	8.00	Mc	0.15 ^a , 0.14 ^d
910	F5V	0.489	4.88	S	...	79492	G8V	0.756	2.68	FO	0.12 ^a , 0.11 ^d
78072	F6IV	0.480	11.42	FO	0.57 ^a	95319	G8V	0.805	0.60	FO	-0.05 ^a , 0.01 ^d
22449	F6V	0.475	19.22	Mc	0.71 ^{a,d}	101997	G8V	0.730	3.50	S	0.16 ^d
40035	F7V	0.495	11.26	S	...	47080	G8V	0.779	6.97	FO/S/Mc	0.30 ^a
27072	F7V	0.498	...	FE	...	63366	G9V	0.780	...	FE	0.12 ^a
17147	F9V	0.538	9.70	FO	0.48 ^d	74537	K0V	0.761	2.12	S	...
57757	F9V	0.558	3.41	Mc	0.44 ^d	40693	K0V	0.766	≤ 6.79	Mc	0.09 ^d
16852	F9V	0.568	2.67	Mc	0.39 ^a , 0.37 ^d	84195	K0	0.940	8.58	FO	-0.20 ^d
1599	F9V	0.576	≤ 3.23	FE	0.45 ^b	112190	K0	0.968	≤ 3.35	FO	-0.12 ^d
64394	F9.5V	0.588	4.72	Mc	0.48 ^{a,d}	3093	K0.5V	0.853	9.38	FO/S/Mc	-0.05 ^a , -0.11 ^d
61317	G0V	0.589	2.00	Mc	0.43 ^a , 0.41 ^d	7981	K1V	0.834	6.50	FO/S/Mc	-0.01 ^a , -0.02 ^d
77257	G0IV	0.596	3.00	Mc	0.37 ^{a,d}	70016	K1V	0.867	8.15	S	-0.13 ^a , -0.07 ^d
14632	G0V	0.606	3.15	Mc	0.33 ^a , 0.32 ^d	79190	K1V	0.843	≤ 3.97	FE	...
77801	G0V	0.624	...	FO/S	0.37 ^d	71681	K1V	0.900	≤ 3.52	FE	...
1499	G0V	0.680	4.18	FO	0.21 ^d	3765	K2V	0.885	6.71	FO/S/Mc	-0.04 ^a
67904	G0V	0.697	...	FE	0.27 ^d	88972	K2V	0.886	4.82	S	-0.11 ^a , -0.13 ^d
10644	G0.5V	0.603	3.93	Mc	0.52 ^a , 0.50 ^d	105152	K2V	1.028	3.69	FO	-0.33 ^a
29860	G0.5V	0.611	2.98	S	0.34 ^{a,d}	114886	K2V	0.898	≤ 3.18	FO	-0.07 ^d
48113	G0.5IV	0.624	2.93	FO/S	0.23 ^a , 0.27 ^d	12114	K3V	0.918	6.45	S	-0.11 ^a , -0.04 ^d
15371	G1V	0.600	≤ 2.64	FE	0.42 ^c	114622	K3/K4 V	1.000	2.10	FO/S	-0.29 ^a
53721	G1V	0.613	2.80	Mc	0.31 ^a , 0.35 ^d	78843	K3/K4V	1.059	6.24	S	-0.38 ^d
24813	G1.5IV	0.613	2.00	Mc	0.31 ^{a,d}	73184	K4V	1.110	...	FE	-0.20 ^d
7918	G1.5V	0.620	2.10	FO/S/Mc	0.30 ^a	113718	K4V	0.948	6.22	FO	...
52369	G2/G3V	0.629	7.22	S	...	12929	K5	1.170	8.11	FO	0.01 ^a , -0.07 ^d
79672	G2Va	0.648	≤ 4.07	Mc	0.31 ^a , 0.30 ^d	50125	K5V	1.122	2.85	S	...
27435	G4V	0.639	2.61	S	0.32 ^d	54651	K5V	1.089	≤ 0.53	S	...
50505	G5	0.686	1.72	S	0.22 ^d	83591	K5V	1.120	3.70	FO/S	-0.20 ^d
64924	G5V	0.709	4.09	S	0.16 ^a , 0.15 ^d	93871	K5V	1.050	4.07	FO	...
171	G5V	0.660	3.00	Mc	0.30 ^a	104214	K5V	1.160	4.72	FO/S	-0.22 ^a
5336	G5V	0.700	8.00	Mc	0.19 ^a	80644	K6V	1.209	≤ 3.68	FO	-0.25 ^a , -0.26 ^d
62523	G7V	0.706	10.60	S	0.42 ^d	104217	K7V	1.360	1.70	FO/S	-0.50 ^a
2941	G7V	0.717	5.54	S	0.23 ^a , 0.19 ^d	54646	K8V	1.345	5.83	S	-0.37 ^d
58576	G8IV-V	0.757	...	Mc	0.03 ^a , 0.11 ^d	60661	M0V	1.451	...	FO	...
14150	G8V	0.715	4.08	S	0.22 ^d						

¹ Spectrograph used: Mc: Mc Donald; S: SARG; FO: FOCES; FE: FEROS

^a Duncan et al. 1991

^b Henry et al. 1996

^c Jenkins et al. 2006

^d Wright et al. 2004

with different instruments. Chromospheric activity features were detected in at least one of the observations, but not in all of them. Therefore, the stars are labelled as active and inactive depending on the observing run. In six of the cases (HIP 3093, HIP 3765, HIP 54646, HIP 60866, HIP 77408 and HIP 85810), the level of activity (when measured) is very low, which points to the use of a different reference star as the explanation for the inability to detect emission features in the subtracted spectrum. Two of these stars (HIP 3093 and HIP 3765) show levels of chromospheric activity so low that are generally considered inactive and used as reference stars to subtract the photospheric contribution from the spectrum. In the remaining cases, HIP 7981 and HIP 62523, variability appears to be the cause. The star HIP 7981 was previously classified as variable by Hall et al. (2007). Both stars were observed in three observing runs, two of them closer in time than the other. The stars exhibit no chromospheric emission features in observations carried out during the same epoch, whereas they do in data for other epoch. This indicates that the

lack of features appears to be real and not attributable to a different choice of the reference star. Variability therefore presents itself as a plausible explanation of the lack of detected activity in two of the observations. These stars are marked with \star in Table A.1. Fluxes can be derived from the measured EW by correcting the continuum flux

$$F_\lambda = EW_\lambda F_\lambda^{\text{cont}} \implies \log F_\lambda = \log(EW) + \log(F_\lambda^{\text{cont}}), \quad (3)$$

where the continuum flux, F_λ^{cont} , is obviously dependent on the wavelength and must therefore be determined for the region where the activity indicator line appears. We used the empirical relationships between F_λ^{cont} and colour index, $B-V$, (Hall 1996) to compute F_λ^{cont} for each line and star. We note that the aforementioned relationships are linear for the spectral type range of the sample stars. In Table A.3, we give the absolute flux at the stellar surface and its error for the active stars in the sample.

4.2.2. R'_{HK} index

Chromospheric activity has been traditionally studied using the R'_{HK} index, defined as the ratio of the emission from the chromosphere in the cores of the Ca II H & K to the total bolometric emission of the star, where the prime denotes that subtraction of the photospheric contribution has been performed. It was first used by Noyes et al. (1984). This index was first measured using observed flux indices in the core of Ca II H & K (corrected from the continuum signal) with the Mount Wilson H-K spectrophotometer (Vaughan et al. 1978). These fluxes were corrected from the photospheric contribution using an empirical calibration with the colour index $B-V$ (Noyes et al. 1984). Finally, the Ca II H and K line-core flux measurements were corrected from the minimum surface flux using a calibration with the colour index $B-V$ (Rutten 1984), thus providing a measurement of the chromospheric contribution associated with magnetic activity. In principle, we could derive R'_{HK} directly from the measured fluxes in Ca II H & K lines using the subtraction technique

$$R'_{\text{HK}} = \frac{F'_H + F'_K}{\sigma T_{\text{eff}}^4}. \quad (4)$$

When the subtraction technique is applied, the residual chromospheric contribution of the reference star is also subtracted from the spectrum of the target star. The source of possible differences between the fluxes obtained using the subtraction technique and those obtained with the traditional method, is the difference in chromospheric emission between our reference stars and those used by Rutten (1984) to compile his calibration. In Fig. 3, we have plotted the total surface flux in the Ca II H & K lines for the reference stars used in this work, and the Rutten (1984) calibration for main sequence stars. The values of total surface flux in the Ca II H & K lines for the reference stars have been obtained from Duncan et al. (1991), Henry et al. (1996), Wright et al. (2004), and Jenkins et al. (2006) and are included in Table 2. We note that all our reference stars have Ca II H & K fluxes close to the lower boundary defined by Rutten (1984) adopted in subsequent studies. The maximum difference between the surface fluxes of the stars used as references in the present study and the Rutten (1984) calibration is 0.2 dex, with the exception of K5 to K7 stars for which it is 0.35 dex. Since these differences account for differences of only 0.2 dex (0.35 dex for K5 to K7 stars) in R'_{HK} , we can assume that the values of R'_{HK} obtained using the subtraction technique are comparable to those obtained with the traditional method.

To determine the effective temperatures needed to convert total flux in Ca II H & K into R'_{HK} , we used the empirical calibrations with the colour index $B-V$ provided by Gray (2008), which holds for the spectral type range of the target stars ($0.00 \leq B-V \leq 1.5$).

4.3. Comparison with previous results

To test whether the transformation is consistent with those values of R'_{HK} computed using photometry (or a technique to mimic photometric results using spectroscopic data), we compared our data to those obtained by Duncan et al. (1991), Strassmeier et al. (2000), Wright et al. (2004), Hall et al. (2007), and Mamajek & Hillenbrand (2008). The comparison is plotted in Fig. 4, where

$$\sigma = \frac{\log R'_{\text{HK}}(\text{other authors}) - \log R'_{\text{HK}}(\text{this work})}{\log R'_{\text{HK}}(\text{this work})}. \quad (5)$$

The dispersion observed in Fig. 4 is compatible with variations in activity levels with time. To determine if there are system-

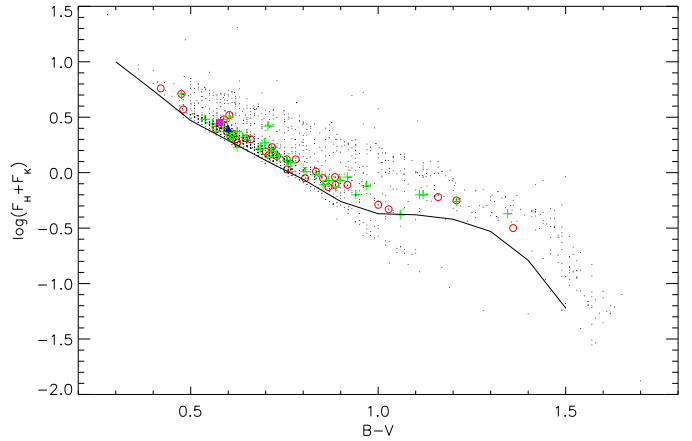


Fig. 3. Ca II H & K surface flux vs colour index $B-V$. Small dots represent Duncan et al. (1991) and Wright et al. (2004) data. To represent the stars considered as reference in this work, we have used different symbols according to the source of $F_H + F_K$ values: circles for Duncan et al. (1991) data, squares for Henry et al. (1996) data, crosses for Wright et al. (2004) data, and triangles for Jenkins et al. (2006) data. The curve represents the surface flux boundary obtained by Rutten (1984).

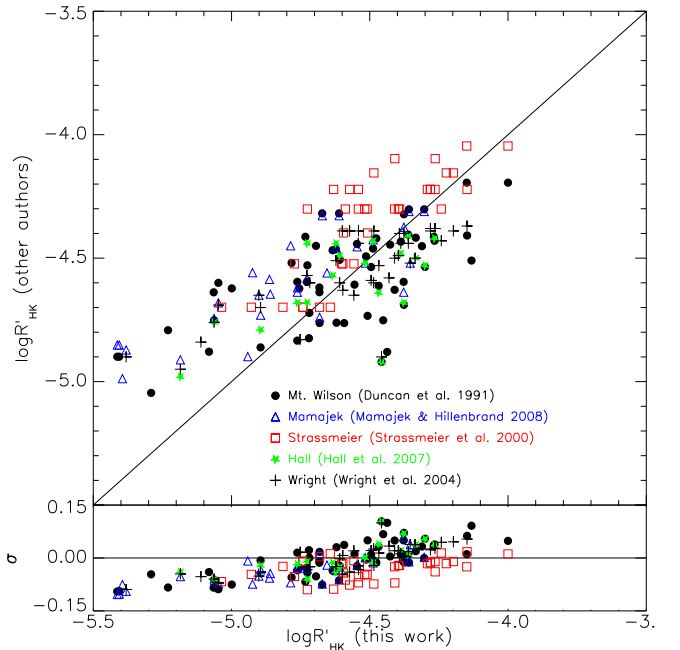


Fig. 4. Comparison of R'_{HK} index obtained in this paper and that obtained with the Mount Wilson H-K spectrophotometer (Vaughan et al. 1978) and similar techniques. Different symbols are used for Duncan et al. (1991), Strassmeier et al. (2000), Wright et al. (2004), Hall et al. (2007), and Mamajek & Hillenbrand (2008) data. In the lower panel, we have plotted σ (as described in the text).

atic differences between our data and any of the five data sets analysed, we have plotted σ in Fig. 4. The closer the value of σ to 0, the smaller the difference between our values and those from other authors. In addition, we performed a Kolmogorov-Smirnov test to determine whether our data and those obtained by other authors are equivalent. The values of the statistical estimator D obtained when applying the Kolmogorov-Smirnov test with Mt. Wilson ($n = 59$), Strassmeier ($n = 37$), Wright ($n = 38$), Hall ($n = 19$) and Mamajek ($n = 31$) data are 0.152,

Table 3. Comparison of the classification of the stars as active or inactive with previous results.

Dataset	# of common stars		# of coincidences	
	Active	Inactive	Active	Inactive
Duncan et al. (1991)	52	90	40	75
Strassmeier et al. (2000)	37	21	31	20
Wright et al. (2004)	34	92	30	84
Hall et al. (2007)	21	35	14	31
Mamajek & Hillenbrand (2008)	27	54	23	47

0.351, 0.236, 0.263 and 0.322, respectively. These results indicate that the null hypothesis, *i. e.*, both samples are equivalent, could not be rejected at a level of significance less than 65 % in the Mt. Wilson, Wright, and Hall cases. This clearly means that $\log R'_{\text{HK}}$ values obtained using the traditional method are equivalent to those obtained in this study. As might be expected, discrepancies are larger when we compare our results with those presented in Mamajek & Hillenbrand (2008), because the latter constitutes a compilation of values obtained from different sources. Differences between our results and Strassmeier et al. (2000) are also larger than the rest. Again this is not surprising, taking into account that the method used to correct from the photospheric contribution is different than in the rest of the cases. The Strassmeier et al. (2000) values therefore do not necessarily reproduce the original $\log R'_{\text{HK}}$ values. It is also important to note that discrepancies are larger for less active stars, in particular for stars with measured $\log R'_{\text{HK}} \leq -4.9$. This result is again expected considering that for stars with low activity levels, errors in the photospheric contribution correction become more apparent.

We also compared our results with those obtained by the mentioned authors (Duncan et al. 1991; Strassmeier et al. 2000; Wright et al. 2004; Hall et al. 2007; Mamajek & Hillenbrand 2008). In Table 3, we summarise the number of active and inactive targets that we share with the mentioned authors as well as the number for which our classification is convergent. As mentioned in Sect. 4.2.1 we classified a star as active when chromospheric features were present in the spectrum. To classify the stars observed by other authors, we used Saar & Brandenburg (1999) criterion to differentiate between active ($\log R'_{\text{HK}} > -4.75$) and inactive ($\log R'_{\text{HK}} \leq -4.75$) stars with the exception of Strassmeier et al. (2000) data, for which the author provides his own classification. For Duncan et al. (1991), we obtained similar results for 84% of the inactive and 77% active stars. We obtained similar results to Strassmeier et al. (2000) data for 95% of the inactive stars and 84% of the active ones. Concerning Wright et al. (2004) and based on the Saar & Brandenburg (1999) criterion, we reached agreement for 88% of the active stars and 91% of the inactive ones. For the Hall et al. (2007) data, we obtained similar results for 89% of the inactive stars and 67% of the active ones. Finally, when comparing our results to those of Mamajek & Hillenbrand (2008), we reached an agreement for 87% of the common inactive stars, and for 85% of the actives ones.

In Table 4, we give details of the values of $\log R'_{\text{HK}}$ found for those stars for which our classification as active or inactive differs from that of Duncan et al. (1991), Strassmeier et al. (2000), Wright et al. (2004), Hall et al. (2007), or Mamajek & Hillenbrand (2008). We note that with the exception of HIP 41484, which was classified as a *high-activity variable* by Hall et al. (2007), in all cases the measured values correspond to the low activity domain ($\log R'_{\text{HK}} \leq -4.40$). It is important to mention that we classify a star as active or inactive after inspecting the spectrum from which the photospheric contribution has

been subtracted. This means that every star showing chromospheric activity features will be considered active, regardless of the weakness of the activity levels that we measure. On the other hand, Saar & Brandenburg (1999) criterion is based on the value obtained after measuring the activity. This implies that some of the stars that we have considered as active (because they show emission features in the spectrum) should be reclassified as inactive after applying the aforementioned criterion. We prefer to maintain our criterion, and consider inactive only those stars that did not exhibit emission features in the subtracted spectrum. Taking this into account, we can consider the agreement between data obtained in the present work and that previously reported as fairly good.

4.4. Spectral types

As mentioned in Sect. 4.2.1, when performing the subtraction technique to measure chromospheric activity the use of a reference non-active star with similar physical properties (temperature and surface gravity) to those of the target star is necessary. Therefore, we were able to determine the spectral types of the target stars by comparing their spectra with those of the reference stars. The process began by assuming a spectral type for each star and applying the subtraction technique using as a reference an inactive star of similar spectral type and luminosity class. We then compared the non-chromospheric lines of the original and morphed spectra to test whether the spectral types of the star and that of the reference were really the same. In this way, we could correct the assumed spectral type of each star. We estimate the errors to be of one spectral subtype.

In theory, if both stars have the same spectral type, the resultant (subtracted) spectrum should be null. In reality, the subtracted spectrum exhibit some noise, because of the small differences in metallicity and/or gravity and when the S/N of one of the spectra is low. Nevertheless, small differences in metallicity (only population I stars were observed) and gravity (the cutoff of ± 1 mag from the Main Sequence (see Sect. 2) corresponds to variations of ± 0.2 in $\log g$) are lower than those produced by the difference of one spectral subtype, which is the estimated error in the spectral type determination. Our results are shown in Table A.1.

5. Discussion

5.1. Flux-flux relationships

Although chromospheric activity has been traditionally studied using the R'_{HK} index, we have already pointed out that longer wavelengths provide noteworthy advantages when exoplanet searches are to be performed. The impact of chromospheric active regions on radial velocity variations appear to be smaller when the red region of the spectrum is considered (Desort et al.

Table 4. Stars for which our classification as active or inactive differs from that of other authors.

HIP	HD	This work		Previous results			
		Activity	$\log R'_{\text{HK}}$	Activity	$\log R'_{\text{HK}}$	Activity	$\log R'_{\text{HK}}$
3765	4628	active	-5.40	inactive	-4.89 ^{1,5}
5286	6660	active	-4.57	inactive	-4.76 ¹
7751	10360	active	-4.94	inactive	-4.90 ⁵
7981	10476	active	-5.19	inactive	-4.95 ³ , -4.98 ⁴ , -4.91 ⁵
10644	13974	inactive	active	-4.64 ^{1,5} , -4.71 ³ , -4.69 ⁴
12929	17230	inactive	active	-4.55 ¹
15442	20619	active	-4.75	inactive	-4.83 ³
15457	20630	inactive	active	-4.41 ^{1,5} , -4.71 ³ , -4.40 ⁴
17420	23356	inactive	active	-4.69 ²
19422	25665	inactive	...	inactive	-4.86 ¹	active	-4.69 ²
19849	26965	active	-5.38	inactive	-4.87 ⁵ , -4.90 ³
20917	28343	active	-4.62	inactive	-4.76 ¹
22449	30652	inactive	...	inactive	-4.79 ¹	active	-4.65 ³
23311	32147	active	-5.29	inactive	-5.75 ¹
36551	59582	active	-4.44	inactive	-4.88 ¹
40693	69830	active*	...	inactive	-4.95 ^{3,5}
42173	72946	inactive	active	-4.46 ¹
41484	71148	inactive	...	inactive	-4.95 ³ , -4.94 ⁴	active	-3.65 ¹
43726	76151	inactive	active	-4.59 ¹ , -4.66 ⁴
46509	81997	inactive	active	-4.67 ⁴
46853	82443	inactive	active	-4.01 ¹ , -4.05 ²
49699	87883	inactive	active	-5.00 ²
56452	100623	active*	...	inactive	-4.89 ^{3,5}
56997	101501	inactive	active	-4.54 ^{1,5} , -4.55 ³ , -4.62 ⁴
64394	114710	active	-5.06	inactive	-4.75 ¹ , -4.76 ^{3,4}	active	-4.74 ⁵
64792	115383	inactive	active	-4.45 ¹ , -4.40 ³ , -4.47 ⁴
67275	120136	active	-4.89	inactive	-4.86 ¹ , -4.79 ³	active	-4.73 ⁵
68337	122120	active	-4.68	inactive	-4.82 ¹
69701	124850	inactive	...	inactive	-4.75 ¹	active	-4.69 ⁴
72875	131582	active	-4.45	inactive	-4.75 ¹
73695	133640	inactive	active	-4.62 ¹ , -4.64 ⁵
81375	149806	inactive	...	inactive	-4.83 ³	active	-4.70 ²
84195	155712	inactive	active	-4.69 ²
85810	159222	active	-4.48	inactive	-4.92 ¹ , -4.90 ³
86400	160346	active	-4.76	inactive	-4.83 ¹
88622	165401	inactive	active	-4.61 ¹
96285	184489	active	-5.08	inactive	-4.88 ¹
97649	187642	inactive	active	-4.47 ¹
99461	191408	active	-5.39	inactive	-4.99 ⁵
101955	196795	inactive	...	inactive	-4.78 ¹	active	-5.00 ²
104092	200779	active	-5.14	inactive	-5.14 ¹
108156	208313	active	-4.68	inactive	-4.76 ¹
114886	219538	active	-4.84	inactive	-4.84 ³

¹ Duncan et al. (1991)² Strassmeier et al. (2000)³ Wright et al. (2004)⁴ Hall et al. (2007)⁵ Mamajek & Hillenbrand (2008)

* Activity features in the spectrum but values not measured due to the lack of a suitable reference star.

2007). Moreover, the S/N in the red region of the spectrum is higher for cool stars. We have measured activity levels using activity tracers throughout the optical spectrum, including the IRT Ca II lines.

After measuring chromospheric activity in different indicator lines, we have analysed the relationships between their fluxes. This approach was first introduced to study the magnetic structure of cool stars (Schrijver 1987; Rutten et al. 1991) by comparing fluxes in chromospheric and coronal indicator lines. Subsequent studies generalised the method and analysed the re-

lationship among different chromospheric indicators. The most widely studied relationship is that between H_{α} core emission and the total surface flux in Ca II H & K lines (Strassmeier et al. 1990; Robinson et al. 1990; Cincunegui et al. 2007; Walkowicz & Hawley 2009). Several studies have obtained fluxes in other chromospheric indicator lines, such as the Ca II infrared triplet, for binary (Montes et al. 1995b, 1996b,a) and single (Thatcher & Robinson 1993; López-Santiago et al. 2005; Busà et al. 2007) stars. The aforementioned studies were either centred on a specific spectral type range (Thatcher & Robinson 1993; Walkowicz

& Hawley 2009) or analysed the relation between total fluxes, instead of that between each of the indicator lines.

We have obtained empirical power-law relations between pairs of chromospheric indicator lines by fitting the data shown in Figs. 5 and Table A.1 to an equation

$$\log F_1 = c_1 + c_2 \log F_2, \quad (6)$$

where F_1 and F_2 are the fluxes of two different lines. We present the coefficients and the correlation coefficient (R) of such relationships in Table 5.

In this context, the present study represents a significant extension in terms of spectral type range and number of stars. Moreover, we present relationships between each pair of chromospheric indicator lines in the optical range. These relationships have an enormous potential given that they permit the transformation between any pair of chromospheric activity indicator lines, in particular the transformation of Ca II H & K fluxes to other more convenient ones. They might be extremely useful when using traditional photometric activity data, *i.e.*, similar to that obtained by Vaughan et al. (1978), or when using spectroscopic data in which not all the chromospheric features are present. We have used them to obtain $\log R'_{\text{HK}}$ when Ca II H or K lines could not be measured (see Sect. 5.2).

5.2. Predicted radial velocity jitter

The most fruitful technique for detecting extrasolar planets has been the radial velocity method. As instrumental improvements and technique refinements have improved precisions in the m s^{-1} domain, the analysis and minimization of the impact of RV noise sources has become more important. There are two different kinds of RV perturbations: the random and systematic measurement effects, and the intrinsic stellar variations. The former can be reduced by improving spectrographs and performing robust statistical analysis. The latter, however, includes several phenomena (Saar 2009) and must be handled carefully. The RV noise sources can lead to a false planet detection (if they produce a periodic signal over a few orbital periods) or prevent planet detection (if the perturbation is larger than the orbital RV variation). Following Narayan et al. (2005), the minimum detectable exoplanet mass with the RV method is

$$M_{\text{min}} \propto M_p N_{\text{obs}}^{-1/2} (\sigma_i^2 + \sigma_{\text{rv}}^2)^{1/2} P^{1/3} M_*^{2/3}, \quad (7)$$

where M_p is the planet mass, M_* is the stellar mass, N is the number of observations, P is the orbital period, and σ_i and σ_{rv} are the *rms* instrumental error and *rms* velocity jitter caused by stellar sources, respectively. Therefore, for a given system, the minimum detectable mass will be limited by the number of observations and the dominant noise source, σ_i or σ_{rv} . Since spectrographs have been improved to achieve $\sigma_i \sim 1 \text{ m s}^{-1}$, the true limiting factor in Eq. 7 is the intrinsic stellar noise.

Stellar RV variations are produced by different magnetic-activity-related phenomena: convection (Saar 2009), starspots (Saar & Donahue 1997), magnetic plage/network (Saar 2003) and flares (Saar 2009; Reiners 2009). Although bisector analysis may sometimes lead to the confirmation of a planet orbiting a star even when RV jitter is present (Sozzetti et al. 2006; Setiawan et al. 2007, 2008), the latter technique is not always successful (Huélamo et al. 2008; Figueira et al. 2009). Several authors have studied the impact of activity on RV jitter using R'_{HK} as a *proxy* (Saar et al. 1998; Santos et al. 2000; Paulson et al. 2002; Saar et al. 2003; Wright 2005; Paulson & Yelda 2006; Santos et al. 2009). In particular, Saar et al. (1998) and Santos et al. (2000)

compiled empirical relationships between σ_{rv} and R'_{HK} for stars in the Lick v_r survey (Marcy & Butler 1998) and the Geneva extrasolar planet search programme. We used these relationships to obtain the expected RV jitter for the active stars in the sample. Results are given in Table A.4. We note that, while Santos et al. (2000) obtained individual relationships for G and K stars, Saar et al. (1998) found that both type of stars exhibited similar trend. Agreement between the values obtained using each method is therefore fairly good except for K stars, which present larger σ_{rv} values for Saar et al. (1998) than for Santos et al. (2000) relationships.

It is important to mention that both relationships were obtained using stars with moderate activity levels ($-5.0 \leq \log R'_{\text{HK}} \leq -4.0$). We assumed that the linear fit holds for more active stars and applied the relations to five stars that have $\log R'_{\text{HK}} > -4.0$. Whether this is valid or not is an open question that must be studied by recalibrating these relations by including a wider variety of activity levels. In our study, we considered chromospheric activity measurements in spectral ranges that contain some advantages for cool stars, *i.e.* the Ca II IRT lines. New calibrations with different indices would be very beneficial to the community. In the context of this aim, our sample represents a large and varied (in terms of activity levels and activity indicators) set of stars but due to the unavailability of σ_{rv} data (not public) we could not perform this analysis.

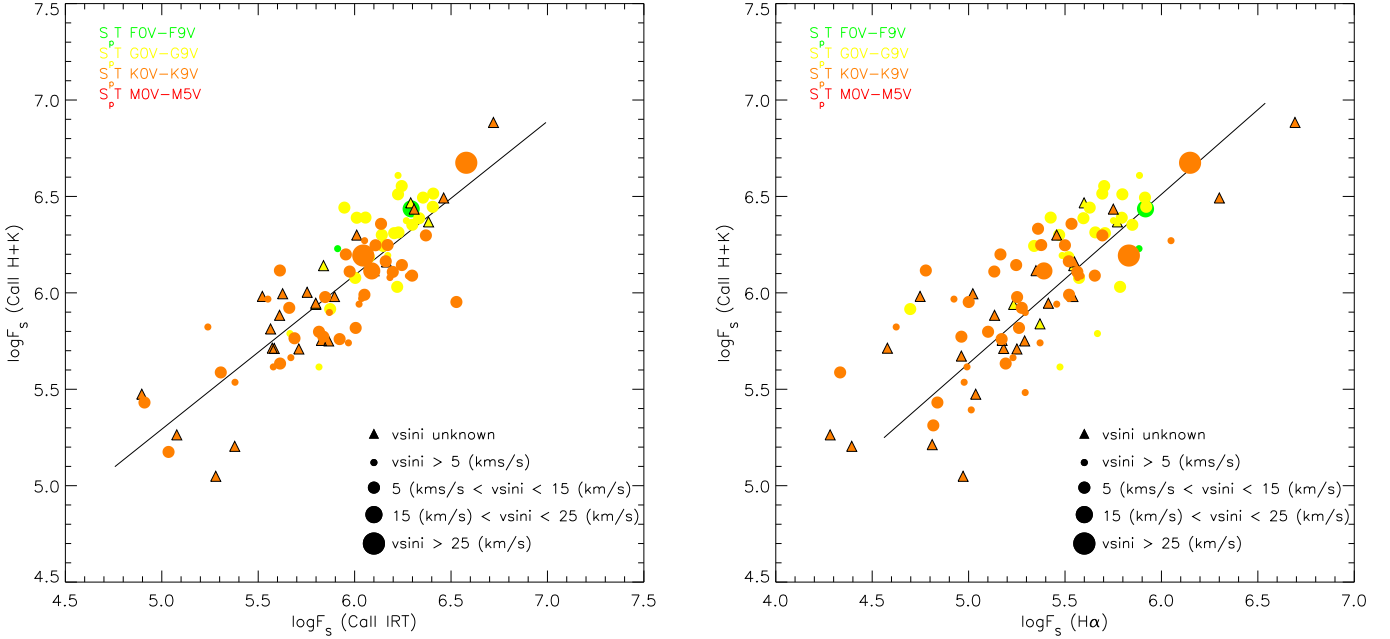
By applying the aforementioned empirical relationships and the derived values of R'_{HK} , we calculated the expected RV jitter for the stars in the sample, which we present in Table A.4. For stars for which both Ca II H and Ca II K could be measured, R'_{HK} could be directly derived as described in Sect. 4.2.2. However, in some cases, measurement of one of the Ca II lines (or both) was not possible due to low S/N or the presence of cosmic rays. In these cases, we used the empirical relationships obtained in Sect. 5.1 to transform the total flux in Ca II IRT into Ca II (H + K) flux. We chose to use the Ca II IRT index because the dispersion between both indices is clearly lower than in the relation between the Ca II (H + K) and H α fluxes. However, when one or more lines in the triplet could not be measured, we used the flux in H α to infer that in Ca II (H + K). It is important to mention that the stars observed with the SARG spectrograph constitute a special case. With the configuration of the spectrograph we used, the spectral range containing Ca II H & K is not available in the spectrum. The photospheric contribution correction for the orders containing the Ca II IRT lines was also less accurate than in the H α order. Consequently, we chose to use the empirical relationship between Ca II (H + K) and H α for these stars. The R'_{HK} values obtained are given in Table A.3. As mentioned in Sect. 4.3, discrepancies between our derived values of $\log R'_{\text{HK}}$ and those obtained using a traditional method become important for stars with low activity levels. Given that the Saar et al. (1998) and Santos et al. (2000) relationships were obtained using traditional $\log R'_{\text{HK}}$ data, the results obtained when applying them to the least active stars should be interpreted carefully. We have marked all stars with $\log R'_{\text{HK}} \leq -4.9$ in Table A.3 with the symbol †.

We cross-correlated our sample with the exoplanet database³ and found that out of the total sample of 371 stars, 17 have confirmed exoplanets orbiting around them. As expected, all of them are either inactive stars, *i.e.*, HIP 1499 (HD 1461 b), HIP 7513 (ν And b), HIP 43587 (55 Cnc b), HIP 49699 (HD 87833 b), HIP 53721 (47 UMa b), HIP 64924 (61 Vir b), HIP 65721 (70 Vir b), HIP 109378 (HD 210277 b) and HIP 116727 (γ Cephei b); or

³ <http://exoplanet.eu>

Table 5. Linear fit coefficients for each flux-flux relationship

$\log F_1$	$\log F_2$	c_1	c_2	R
Ca II H	Ca II K	-0.16 ± 0.20	1.01 ± 0.03	0.897
Ca II H	H α	1.95 ± 0.29	0.69 ± 0.05	0.736
H α	Ca II K	-0.14 ± 0.44	0.95 ± 0.08	0.775
Ca II IRT ($\lambda 8498 \text{ \AA}$)	Ca II IRT ($\lambda 8542 \text{ \AA}$)	-0.15 ± 0.16	1.01 ± 0.03	0.894
H α	Ca II IRT ($\lambda 8542 \text{ \AA}$)	-0.06 ± 0.29	0.98 ± 0.05	0.818
Ca II H	Ca II IRT ($\lambda 8542 \text{ \AA}$)	1.27 ± 0.30	0.80 ± 0.05	0.830
Ca II (H + K)	Ca II IRT ($\lambda 8489 \text{ \AA} + \lambda 8542 \text{ \AA} + \lambda 8662 \text{ \AA}$)	1.30 ± 0.32	0.80 ± 0.05	0.852
Ca II (H + K)	H α	2.37 ± 0.30	0.68 ± 0.06	0.748

**Fig. 5.** Flux-flux relationship between the total flux in H&K Ca II and Ca II IRT (**left**) and the total flux in H&K Ca II and Ca II IRT (**right**). Symbol sizes increase with increasing rotational velocity (triangles are used when $v \sin i$ could not be determined). Colors are used to discern different spectral types.

have very low activity levels, *i.e.*, HIP 3093 (HD 3651 b), HIP 10138 (Gl 86 b), HIP 16537 (ϵ Eri b), HIP 71395 (HD 128331 b), HIP 80337 (HD 147513 b), HIP 99711 (HD 192263 b) and HIP 113357 (51 Peg b). For HIP 40693 (HD 69830 b), chromospheric activity could not be measured because of the lack of an inactive reference star to apply the subtraction technique, but chromospheric features were visible in the spectrum. The stars with known extrasolar planets are marked with † in Table A.1.

5.3. Applicability to transit searches

Transit searches for exoplanets are also affected by the presence of active regions on the surface of a star (Henry et al. 1997; Baliunas et al. 1997; Henry et al. 2000). Aigrain et al. (2004) used a Sun-based model to predict the “stellar background” using chromospheric activity (as given by R'_{HK}). In the solar case, the noise spectrum for chromospheric irradiance variations at frequencies lower than ~ 8 mHz, commonly referred to as “solar background”, is frequently modelled by a sum of power laws, in

which the number of terms, N , varies from one to five depending on the frequency coverage (Andersen et al. 1994), *i.e.*,

$$P(\nu) = \sum_{i=1}^N P_i = \sum_{i=1}^N \frac{A_i}{1 + (B_i \nu)^{C_i}}, \quad (8)$$

where ν is frequency, A_i is the amplitude of the i th component, B_i is its characteristic timescale, and C_i is the slope of the power law. For a given component, the power remains approximately constant on timescales longer than B , and declines for shorter timescales. Each power law corresponds to a separate class of physical phenomena with a different characteristic timescale. The fitting of solar data (Aigrain et al. 2004) uncovers three components. The first component corresponds to active regions ($\tau \approx 1.3 \times 10^5$ s), whose amplitude both increases and correlates with the Ca II K-line index (Andersen et al. 1994; Aigrain et al. 2004). The second component is related to super- and meso-granulation with typical timescales of hours, but no detailed models of these phenomena have been developed to date. The third component is the superposition of variability on timescales of a few minutes, related to granulation and higher frequency effects, such as oscillations and photon noise.

This model can be applied to other stars (Aigrain et al. 2004) to predict the expected “stellar background”. According to Aigrain et al. (2004), the amplitude of the first power law A_1 is correlated with emission in the Ca II H & K lines, *i.e.* R'_{HK} , and can be written as follows

$$A_1 = 2.20 \times 10^{-5} + 3.04R'_{\text{HK}} + 1.90(R'_{\text{HK}})^2 \times 10^5. \quad (9)$$

We refer the reader to Aigrain et al. (2004) for a detailed derivation of the aforementioned formula and the other two parameters (B_i and C_i). Chromospheric activity measurements, such as those presented in this work, can be therefore used as a *proxy* to infer the expected amplitude variation of active stars and thus to establish a lower limit to planet detection.

6. Summary and conclusions

We have used high resolution spectroscopic observations to measure the chromospheric activity and the projected rotational velocities for 371 nearby cool stars. For the fraction presenting chromospheric activity (173 stars out of 371), we have analysed the relationship between pairs of chromospheric activity indicator lines, compiling empirical relations to be used when not all the chromospheric features are included in the spectral range. We have applied these relationships to obtain values of $\log R'_{\text{HK}}$ when the Ca II H & K spectral region was not available in the spectrum.

To test the applicability of the results to planet searches, we have calculated the *RV* jitter one should expect for each of the active stars in the sample. As previously pointed out, those values must be applied carefully because magnetic activity is variable and a simple subtraction of the activity-related “signal” is not possible. They have to be used as an estimation of the activity-related noise one should expect for a star and thus used to set the minimum detectable mass for a planet orbiting the star or to determine the minimal amplitude variation that could indicate the existence of a planet. Our results represent an important resource in terms of target selection for exoplanet searches surveys.

Acknowledgements. R. Martínez-Arnáiz acknowledges support from the Spanish Ministerio de Educación y Ciencia (currently the Ministerio de Ciencia e Innovación), under the grant FPI20061465-00592 (programa nacional Formación Personal Investigador) and projects AYA2008-00695 (Programa Nacional de Astronomía y Astrofísica), AYA2008-01727 (Programa Nacional de Astronomía y Astrofísica), AstroMadrid S2009/ESP-1496. This research has made use of the SIMBAD database and VizieR catalogue access tool, operated at CDS, Strasbourg, France. We also thank the anonymous referee for his/her valuable suggestions on how to improve the manuscript.

References

Aigrain, S., Favata, F., & Gilmore, G. 2004, *A&A*, 414, 1139
 Allende Prieto, C., Barklem, P. S., Lambert, D. L., & Cunha, K. 2004, *A&A*, 420, 183
 Andersen, B. N., Leifsen, T. E., & Toutain, T. 1994, *Sol. Phys.*, 152, 247
 Baliunas, S. L., Henry, G. W., Donahue, R. A., Fekel, F. C., & Soon, W. H. 1997, *ApJ*, 474, L119
 Barden, S. C. 1985, *ApJ*, 295, 162
 Busà, I., Aznar Cuadrado, R., Terranegra, L., Andretta, V., & Gomez, M. T. 2007, *A&A*, 466, 1089
 Cincunegui, C., Díaz, R. F., & Mauas, P. J. D. 2007, *A&A*, 469, 309
 Desort, M., Lagrange, A.-M., Galland, F., Udry, S., & Mayor, M. 2007, *A&A*, 473, 983
 Dommanget, J. & Nys, O. 1994, *Communications de l’Observatoire Royal de Belgique*, 115
 Dommanget, J. & Nys, O. 2002, *VizieR Online Data Catalog*, 1274, 0
 Doyle, L. R., Billingham, J., & DeVincenzi, D. L. 1998, *Acta Astron.*, 42, 599
 Duncan, D. K., Vaughan, A. H., Wilson, O. C., et al. 1991, *ApJ Suppl.*, 76, 383

ESA. 1997, *The Hipparcos and Tycho Catalogues*, ESA SP-1200
 Figueira, P., Pepe, F., Melo, C. H. F., et al. 2009, *ArXiv e-prints*
 Frasca, A. & Catalano, S. 1994, *A&A*, 284, 883
 Gálvez, M. C., Montes, D., Fernández-Figueroa, M. J., de Castro, E., & Cornide, M. 2007, *A&A*, 472, 587
 Gálvez, M. C., Montes, D., Fernández-Figueroa, M. J., De Castro, E., & Cornide, M. 2009, *AJ*, 137, 3965
 Gálvez, M. C., Montes, D., Fernández-Figueroa, M. J., et al. 2002, *A&A*, 389, 524
 Gray, D. F. 2008, *The Observation and Analysis of Stellar Photospheres* (Third Edition, Cambridge University Press)
 Gunn, A. G. & Doyle, J. G. 1997, *A&A*, 318, 60
 Hall, J. C. 1996, *Publications of the ASP*, 108, 313
 Hall, J. C., Lockwood, G. W., & Skiff, B. A. 2007, *AJ*, 133, 862
 Hall, J. C. & Ramcey, L. W. 1992, *AJ*, 104, 1942
 Henry, G. W., Baliunas, S. L., Donahue, R. A., Fekel, F. C., & Soon, W. 2000, *ApJ*, 531, 415
 Henry, G. W., Baliunas, S. L., Donahue, R. A., Soon, W. H., & Saar, S. H. 1997, *ApJ*, 474, 503
 Henry, T. J., Soderblom, D. R., Donahue, R. A., & Baliunas, S. L. 1996, *AJ*, 111, 439
 Høg, E., Fabricius, C., Makarov, V. V., et al. 2000, *A&A*, 355, L27
 Huélamo, N., Figueira, P., Bonfils, X., et al. 2008, *A&A*, 489, L9
 Huenemoerder, D. P. & Barden, S. C. 1984, in *Bulletin of the American Astronomical Society*, Vol. 16, *Bulletin of the American Astronomical Society*, 510
 Huenemoerder, D. P., Buzasi, D. L., & Ramsey, L. W. 1989, *AJ*, 98, 1398
 Jenkins, J. S., Jones, H. R. A., Tinney, C. G., et al. 2006, *MNRAS*, 372, 163
 Kasting, J. F., Whitmire, D. P., & Reynolds, R. T. 1993, *Icarus*, 101, 108
 Kaufer, A., Stahl, O., Tubbesing, S., et al. 2000, in *Proc. SPIE Vol. 4008*, p. 459-466, *Optical and IR Telescope Instrumentation and Detectors*, Masanori Iye; Alan F. Moorwood; Eds., ed. M. Iye & A. F. Moorwood, 459-466
 Kurucz, R. L. 1993, in *Astronomical Society of the Pacific Conference Series*, Vol. 44, *IAU Colloq. 138: Peculiar versus Normal Phenomena in A-type and Related Stars*, ed. M. M. Dworetzky, F. Castellì, & R. Faraggiana, 87-98
 Lázaro, C. & Arévalo, M. J. 1997, *AJ*, 113, 2283
 López-Santiago, J., Montes, D., Fernández-Figueroa, M. J., Gálvez, M. C., & Crespo-Chacón, I. 2005, in *ESA Special Publication*, Vol. 560, *13th Cambridge Workshop on Cool Stars, Stellar Systems and the Sun*, ed. F. Favata, G. A. J. Hussain, & B. Battrick, 775
 López-Santiago, J., Montes, D., Fernández-Figueroa, M. J., & Ramsey, L. W. 2003, *A&A*, 411, 489
 López-Santiago, J., Montes, D., Gálvez-Ortiz, M. C., et al. 2010, *A&A*, in press
 Maldonado, J., Martínez-Arnáiz, R., Eiroa, C., & Montes, D. 2010, in *Proceedings of Pathways towards habitable planets. ASP Conference S.*, Eds., in press
 Mamajek, E. E. & Hillenbrand, L. A. 2008, *ApJ*, 687, 1264
 Marcy, G. W. & Butler, R. P. 1998, *ARA&A*, 36, 57
 Martínez-Arnáiz, R., Maldonado, J., Montes, D., et al. 2009, in *Proceedings of the IAU Symposium 258: The Ages of Stars*, Cambridge University Press
 Melo, C., Pasquini, L., & de Medeiros, J. R. 2004, in *IAU Symposium*, Vol. 215, *Stellar Rotation*, ed. A. Maeder & P. Eenens, 455-459
 Montes, D., de Castro, E., Fernández-Figueroa, M. J., & Cornide, M. 1995a, *A&A Suppl.*, 114, 287
 Montes, D., Fernández-Figueroa, M. J., Cornide, M., & De Castro, E. 1996a, in *Astronomical Society of the Pacific Conference Series*, Vol. 109, *Cool Stars, Stellar Systems, and the Sun*, ed. R. Pallavicini & A. K. Dupree, 657
 Montes, D., Fernández-Figueroa, M. J., Cornide, M., & de Castro, E. 1996b, *A&A*, 312, 221
 Montes, D., Fernández-Figueroa, M. J., de Castro, E., & Cornide, M. 1995b, *A&A*, 294, 165
 Montes, D., Fernández-Figueroa, M. J., De Castro, E., et al. 2000, *A&A Suppl.*, 146, 103
 Montes, D., López-Santiago, J., Fernández-Figueroa, M. J., & Gálvez, M. C. 2001, *A&A*, 379, 976
 Montes, D., Martin, E. L., Fernández-Figueroa, M. J., Cornide, M., & de Castro, E. 1997, *A&AS*, 123, 473
 Montes, D., Martínez-Arnáiz, R., Maldonado, J., & Eiroa, C. 2010, in *Proceedings of Towards Other Earths: perspectives and limitations in the ELT era*, in press
 Narayan, R., Cumming, A., & Lin, D. N. C. 2005, *ApJ*, 620, 1002
 Noyes, R. W., Hartmann, L. W., Baliunas, S. L., Duncan, D. K., & Vaughan, A. H. 1984, *ApJ*, 279, 763
 Paulson, D. B., Cochran, W. D., & Hatzes, A. P. 2004, *AJ*, 127, 3579
 Paulson, D. B., Saar, S. H., Cochran, W. D., & Hatzes, A. P. 2002, *AJ*, 124, 572
 Paulson, D. B. & Yelda, S. 2006, *PASP*, 118, 706
 Pfeiffer, M. J., Frank, C., Baumüller, D., Fuhrmann, K., & Gehren, T. 1998, *A&A Suppl.*, 130, 381

- Pourbaix, D., Tokovinin, A. A., Batten, A. H., et al. 2004, *A&A*, 424, 727
- Queloz, D., Allain, S., Mermilliod, J.-C., Bouvier, J., & Mayor, M. 1998, *A&A*, 335, 183
- Reiners, A. 2009, *A&A*, 498, 853
- Reiners, A., Bean, J. L., Huber, K. F., et al. 2009, arXiv:0909.0002v1
- Robinson, R. D., Cram, L. E., & Giampapa, M. S. 1990, *ApJS*, 74, 891
- Rutten, R. G. M. 1984, *A&A*, 130, 353
- Rutten, R. G. M., Schrijver, C. J., Lemmens, A. F. P., & Zwaan, C. 1991, *A&A*, 252, 203
- Saar, S. H. 2003, in *Astronomical Society of the Pacific Conference Series*, Vol. 294, *Scientific Frontiers in Research on Extrasolar Planets*, ed. D. Deming & S. Seager, 65–70
- Saar, S. H. 2009, in *American Institute of Physics Conference Series*, Vol. 1094, *American Institute of Physics Conference Series*, ed. E. Stempels, 152–161
- Saar, S. H. & Brandenburg, A. 1999, *ApJ*, 524, 295
- Saar, S. H., Butler, R. P., & Marcy, G. W. 1998, *ApJ*, 498, L153
- Saar, S. H. & Donahue, R. A. 1997, *ApJ*, 485, 319
- Saar, S. H. & Fischer, D. 2000, *ApJ*, 534, L105
- Saar, S. H., Hatzes, A., Cochran, W., & Paulson, D. 2003, in *The Future of Cool-Star Astrophysics: 12th Cambridge Workshop on Cool Stars, Stellar Systems, and the Sun (2001 July 30 - August 3)*, eds. A. Brown, G.M. Harper, and T.R. Ayres, (University of Colorado), 2003, p. 694-698., ed. A. Brown, G. M. Harper, & T. R. Ayres, Vol. 12, 694–698
- Santos, N. C., Gomes da Silva, J., Lovis, C., & Melo, C. 2009, ArXiv e-prints
- Santos, N. C., Mayor, M., Naef, D., et al. 2000, *A&A*, 361, 265
- Sbordone, L. 2005, *Memorie della Societa Astronomica Italiana Supplement*, 8, 61
- Sbordone, L., Bonifacio, P., Castelli, F., & Kurucz, R. L. 2004, *Memorie della Societa Astronomica Italiana Supplement*, 5, 93
- Schrijver, C. J. 1987, *A&A*, 172, 111
- Setiawan, J., Henning, T., Launhardt, R., et al. 2008, *Nature*, 451, 38
- Setiawan, J., Weise, P., Henning, T., et al. 2007, *ApJ*, 660, L145
- Soderblom, D. R., Pendleton, J., & Pallavicini, R. 1989, *AJ*, 97, 539
- Sozzetti, A., Udry, S., Zucker, S., et al. 2006, *A&A*, 449, 417
- Strassmeier, K., Washuettl, A., Granzer, T., Scheck, M., & Weber, M. 2000, *A&AS*, 142, 275
- Strassmeier, K. G., Fekel, F. C., Bopp, B. W., Dempsey, R. C., & Henry, G. W. 1990, *ApJS*, 72, 191
- Thatcher, J. D. & Robinson, R. D. 1993, *MNRAS*, 262, 1
- Tull, R. G., MacQueen, P. J., Sneden, C., & Lambert, D. L. 1995, *Publications of the ASP*, 107, 251
- Turnbull, M. C. & Tarter, J. C. 2003, *ApJ Suppl.*, 145, 181
- van Leeuwen, F. 2007, *Hipparcos, the New Reduction of the Raw Data (Springer)*, 449
- Vaughan, A. H., Preston, G. W., & Wilson, O. C. 1978, *PASP*, 90, 267
- Walkowicz, L. M. & Hawley, S. L. 2009, *AJ*, 137, 3297
- Wright, J. T. 2005, *PASP*, 117, 657
- Wright, J. T., Marcy, G. W., Butler, R. P., & Vogt, S. S. 2004, *ApJS*, 152, 261

Appendix A: Tables of results

The stellar and line parameters are published in electronic format only. available at CDS, Table A.1, contains the Hipparcos number (Col. #1), the spectrograph used to observe the star (Col. #2), the modified julian date (MJD) of the observation (Col. #3), the right ascension and declination (Col. #4 and #5), colour index ($B-V$) (Col. #6), spectral type (Col. #7), and projected rotational velocity, $v \sin i$ (Col. #8). Col. #9 specifies whether the star may be classified as active or non active. We note that for some stars in Col. #8, only upper limits are given. As mentioned in the text, for very slowly rotating stars, the value of σ_0 can be higher than that of σ_{obs} . In those cases, we give the minimum value that could be measured with the same spectrograph and for a star of the same spectral type.

The chromospheric activity results are listed in two different tables. Table A.2 contains the excess emission EW as measured in the subtracted spectrum, whereas Table A.3 includes the excess fluxes derived in this work. In both tables, Cols. #1, #2, and #3 contain the Hipparcos number of the star, the spectrograph used to observe it, and the modified julian date of the observation, respectively. In Cols. #4, #5, #6, #7, #8, and #9, excess emission (or fluxes) for Ca II K, Ca II H, H α , and Ca II IRT $\lambda 4898\text{\AA}$, Ca II IRT $\lambda 8542\text{\AA}$ and Ca II IRT $\lambda 8662\text{\AA}$ are given. Table A.3 has an additional column containing $\log R'_{\text{HK}}$. As mentioned in the text, for those stars with measured values of both Ca II H and Ca II K lines, $\log R'_{\text{HK}}$ was derived directly as described in Sect. 4.2.2. When it was not possible to measure one or both of the Ca II lines, we used the empirical relationships between the total flux in Ca II (H + K) and H α or Ca II IRT obtained in the present work (see Fig. 5 and Table 5). Given that the relationship between Ca II (H + K) and Ca II IRT clearly exhibits lower dispersion, we used it when possible, *i.e.* when measuring the three lines in the Ca II infrared triplet was possible. In the remaining cases, including all the stars observed with SARG (infrared orders are strongly affected by fringing), we used the relationship between Ca II (H + K) and H α .

Predicted radial velocity variations, *i.e.*, jitter (based on Saar et al. 1998; Santos et al. 2000), are given in Table A.4. It contains only those stars for which $\log R'_{\text{HK}}$ could be derived. Columns #1, #2, and #3 contain the same information as that of Tables A.2 and A.3. The spectral type and $\log R'_{\text{HK}}$ for each star are listed in Cols. #4 and #5. Columns #6 and #7 contain the σ_{rv} values (within 1σ) obtained using Saar et al. (1998) and Santos et al. (2000) relationships, respectively.

As online material we have also included Fig. A.1 with plots of the flux-flux relationships among different chromospheric activity indicators.

Table A.1. Stellar parameters of the stars.

HIP	Spectrograph	MJD (days)	RA (J2000)	DEC (J2000)	$B - V$ (mag)	SpT	$v \sin i$ (km s ⁻¹)	ACTIVE
171	McDonald	52164.3858	00 02 09.65	+27 05 04.2	0.690	G5Vb	≤ 4.07	Not Active
544	McDonald	52031.3248	00 06 36.53	+29 01 19.0	0.749	G8V	5.72	Active
544	SARG	54780.9561	00 06 36.53	+29 01 19.0	0.749	G8V	8.07	Active
910	SARG	54777.8430	00 11 15.91	-15 28 02.4	0.489	F5V	4.88	Not Active
1499†	FOCES	53578.1286	00 18 41.62	-08 03 09.5	0.680	G1.5V	4.18	Not Active
1532	FOCES	54089.7731	00 19 05.58	-09 57 50.8	1.305	K5V	≤ 0.53	Not Active
1598	FOCES	53576.1488	00 20 00.51	+38 13 41.0	0.625	G0V	3.74	Not Active
1599	FEROS	52030.4120	00 20 01.91	-64 52 39.4	0.576	F9V	≤ 3.23	Not Active
1803	SARG	54777.9856	00 22 51.55	-12 12 34.5	0.675	G3V	9.94	Active
2021	FEROS	52030.2567	00 25 39.20	-77 15 18.1	0.618	G0V	2.64	Not Active
2941	SARG	54777.9574	00 37 19.79	-24 46 02.0	0.717	G5V	5.54	Not Active
3093†★	FOCES	53577.1854	00 39 22.09	+21 15 04.9	0.850	K0.5V	11.97	Active
3093†★	McDonald	51880.1295	00 39 22.09	+21 15 04.9	0.850	K0.5V	6.79	Not Active
3206	FOCES	53579.0491	00 40 49.00	+40 11 19.7	0.956	K3/K4V	9.16	Not Active
3418	FOCES	53580.1213	00 43 33.00	+34 50 43.6	1.058	K5V	0.53	Active*
3535	FOCES	53579.1710	00 45 04.92	+01 47 12.9	1.005	K3V	≤ 3.35	Not Active
3765★	McDonald	52164.3977	00 48 22.53	+05 17 00.2	0.885	K2V	6.30	Active
3765★	FOCES	53747.7686	00 48 22.53	+05 17 00.2	0.885	K2V	9.04	Active
3765★	SARG	54107.8938	00 48 22.53	+05 17 00.2	0.885	K2V	4.78	Not Active
3821	McDonald	52164.4538	00 49 05.10	+57 48 59.6	0.582	G0VSB	≤ 3.15	Not Active
3979	FOCES	53579.1354	00 51 10.69	-05 02 20.4	0.668	G1.5V	13.97	Not Active
3998	FOCES	53577.0654	00 51 21.72	+18 44 23.6	1.237	K3V	≤ 3.35	Not Active
4148	FEROS	51834.1339	00 53 00.72	-30 21 25.2	0.911	K2V	3.52	Active
4845	SARG	54778.9878	01 02 21.12	-10 25 24.3	1.177	K7V	≤ 3.21	Active
5286	FOCES	53576.1601	01 07 37.81	+22 57 22.2	1.114	K3V	≤ 3.35	Active
5336	McDonald	51789.1451	01 08 12.92	+54 55 27.2	0.704	G5Vb	4.17	Not Active
5799	FOCES	53577.1530	01 14 23.97	-07 55 24.6	0.713	F6V	13.04	Not Active
5944	FOCES	53576.1764	01 16 29.34	+42 56 22.2	0.583	G0V	8.78	Active
5957	FOCES	53577.0880	01 16 39.08	+25 19 54.2	1.372	K7V	≤ 3.68	Low S/N
6290	SARG	54107.9171	01 20 41.06	+57 19 36.7	1.437	K7V	≤ 3.21	Active
7235	SARG	54780.9662	01 33 15.63	-24 10 39.3	0.766	G8V	4.88	Active
7339	SARG	54779.9914	01 34 33.88	+68 56 52.3	0.682	G7V	3.27	Not Active
7513†	McDonald	51883.1803	01 36 47.98	+41 24 23.0	0.544	F8V	10.73	Not Active
7576	FOCES	53577.1583	01 37 35.37	-06 45 36.7	0.793	G8V	0.45	Active
7751	FEROS	51834.1456	01 39 47.24	-56 11 47.2	0.895	K0V	5.64	Active
7918	McDonald	52206.3054	01 41 46.52	+42 36 49.7	0.620	G2V	≤ 4.07	Not Active
7981★	SARG	54779.9355	01 42 29.95	+20 16 12.5	0.836	K1V	5.98	Not Active
7981★	FOCES	53578.1869	01 42 29.95	+20 16 12.5	0.836	K1V	≤ 1.20	Active
7981★	McDonald	51880.1781	01 42 29.95	+20 16 12.5	0.836	K1V	7.01	Not Active
8102	McDonald	51880.1671	01 44 05.13	-15 56 22.4	0.727	G8V	≤ 3.26	Not Active
8275	FOCES	54086.7647	01 46 38.70	+12 24 43.0	1.012	K3/K4V	9.01	Active
8362	McDonald	51883.2217	01 47 44.06	+63 51 11.2	0.797	K0V	2.67	Active
8486	FOCES	53748.8161	01 49 23.43	-10 42 11.9	0.639	G1V	3.34	Active
8768	SARG	54778.0142	01 52 48.64	-22 26 05.5	1.376	K7V	≤ 3.21	Active
9269	FOCES	53748.8369	01 59 06.46	+33 12 37.9	0.786	G8V	14.54	Not Active
9269	SARG	54779.9417	01 59 06.46	+33 12 37.9	0.786	G8V	3.87	Not Active
10138†	FEROS	51834.1664	02 10 24.00	-50 49 31.1	0.812	K0V	0.18	Active
10337	SARG	54780.0100	02 13 11.93	-21 11 47.7	1.362	K7V	≤ 3.21	Active
10416	FOCES	54086.7855	02 14 13.58	-03 38 04.8	1.073	K3/K4V	8.12	Active
10644	McDonald	51880.1997	02 17 02.42	+34 13 29.4	0.606	G0.5V	3.93	Not Active
10798	McDonald	52206.3310	02 18 58.65	-25 56 48.4	0.726	G8V	≤ 3.26	Not Active
11072	SARG	54780.0327	02 22 32.42	-23 48 58.7	0.613	G2V	4.22	Not Active
11452	FOCES	54087.9694	02 27 45.81	+04 25 53.6	1.394	K7V	10.18	Low S/N
11565	SARG	54780.2041	02 29 01.31	-19 58 46.6	1.186	K5V	5.30	Active
12110	SARG	54780.0623	02 36 00.72	-23 31 16.9	1.061	K3V	10.85	Active
12114	FOCES	54086.7803	02 36 03.83	+06 53 00.1	0.918	K3V	≤ 3.35	Not Active
12114	SARG	54778.0541	02 36 03.83	+06 53 00.1	0.918	K3V	6.45	Not Active
12843	McDonald	52164.4842	02 45 05.98	-18 34 21.5	0.486	F5/F6V	28.02	Not Active
12929	FOCES	54086.8010	02 46 17.12	+11 46 32.7	1.170	K5V	8.11	Not Active
13258	FOCES	54086.8172	02 50 36.69	+15 42 39.2	1.198	K5V	9.26	Active
13402	McDonald	52207.4006	02 52 31.89	-12 46 09.3	0.876	K1V	7.74	Active
13402	SARG	54779.0488	02 52 31.89	-12 46 09.3	0.876	K1V	9.96	Active
13976	SARG	54778.0715	03 00 02.62	+07 44 58.9	0.933	K3/K4V	8.86	Active
14150	SARG	54779.0891	03 02 25.87	+26 36 34.7	0.715	G8V	4.08	Not Active
14286	FOCES	53747.8359	03 04 08.75	+61 42 27.1	0.653	G1.5V	16.48	Not Active
14632	McDonald	51880.2222	03 09 02.88	+49 36 48.6	0.606	G0V	3.15	Not Active
14879	McDonald	51883.2713	03 12 04.28	-28 59 20.8	0.511	F8IV	4.41	Not Active
15099	FOCES	53747.8508	03 14 46.99	+08 58 54.4	0.896	K0V	≤ 1.20	Active*
15330	FEROS	51834.2315	03 17 44.47	-62 34 36.8	0.641	G1V	≤ 2.64	Active

† stars with known exoplanets

★ stars with chromospheric variations during our observations

* stars classified as active by visual inspection but for which chromospheric activity could not be measured

Table A.1. continue

HIP	Spectrograph	MJD (days)	RA (J2000)	DEC (J2000)	$B - V$ (mag)	SpT	$v \sin i$ (km s ⁻¹)	ACTIVE
15371	FEROS	51834.2390	03 18 11.14	-62 30 28.6	0.600	G1V	≤ 2.64	Not Active
15442	SARG	54780.1170	03 19 01.75	-02 50 34.6	0.647	G4V	3.20	Active
15457	McDonald	51880.2509	03 19 21.54	+03 22 11.9	0.674	G5Vvar	5.86	Not Active
15510	FEROS	51834.2471	03 19 53.22	-43 04 17.6	0.711	G8V	≤ 0.18	Not Active
15673	FOCES	54086.8639	03 21 55.05	+52 19 55.8	1.032	K2V	≤ 3.04	Active
15919	FOCES	53747.8508	03 24 59.87	-05 21 42.8	1.145	K5V	≤ 0.53	Active
16134	SARG	54779.0552	03 27 52.07	-19 48 18.8	1.337	K7V	≤ 3.85	Active
16134	FOCES	54091.9052	03 27 52.07	-19 48 18.8	1.337	K7V	≤ 3.21	Active*
16537†	McDonald	51833.9938	03 32 56.42	-09 27 29.9	0.887	K2V	4.08	Active
16852	McDonald	51883.2557	03 36 52.52	+00 24 10.2	0.573	F9V	2.67	Not Active
17147	FOCES	53748.8576	03 40 21.66	-03 12 59.3	0.538	G0V	9.70	Not Active
17378	McDonald	52206.3787	03 43 14.96	-09 45 54.7	0.922	K0IV	≤ 6.79	Not Active
17420	McDonald	52207.4446	03 43 55.15	-19 06 40.6	0.915	K2V	3.03	Active
17496	FOCES	54086.8866	03 44 50.94	+11 55 10.9	1.194	K5V	7.33	Active*
17651	SARG	54778.0619	03 46 50.99	-23 14 54.4	0.731	F7V	16.25	Not Active
18324	FOCES	53748.9323	03 55 03.31	+61 10 02.7	0.858	K1V	10.29	Not Active
18774	SARG	54779.1053	04 01 18.81	+76 09 38.5	1.129	K4V	8.41	Active
18859	SARG	54780.1408	04 02 36.66	-00 16 05.9	0.520	F7V	20.24	Active
19076	SARG	54780.1482	04 05 20.15	+22 00 33.2	0.646	G5V	5.52	Active
19335	SARG	54780.1552	04 08 36.49	+38 02 24.8	0.529	F7V	20.81	Active
19422	SARG	54778.1206	04 09 34.92	+69 32 31.6	0.957	K3/K4V	6.26	Not Active
19832	FOCES	54087.9871	04 15 09.48	-04 25 05.1	1.149	K5V	8.14	Active
19849	McDonald	51880.2760	04 15 17.64	-07 38 40.4	0.820	K0V	≤ 4.06	Active
20917	FOCES	54086.9422	04 29 00.17	+21 55 20.2	1.357	K5V	1.11	Active
22263	McDonald	52207.4280	04 47 36.21	-16 56 05.5	0.638	G1V	4.07	Active
22449	McDonald	51883.3250	04 49 50.14	+06 57 40.5	0.477	F6V	19.22	Not Active
23311	McDonald	52207.4662	05 00 48.68	-05 45 03.5	1.069	K3V	5.18	Active
23693	FEROS	51834.2547	05 05 30.69	-57 28 22.8	0.518	F7V	18.34	Active
23786	FOCES	53747.9144	05 06 42.05	+14 26 48.5	0.804	K0V	≤ 1.20	Active
24786	SARG	54780.1623	05 18 50.24	-18 07 48.7	0.574	G0.5V	4.38	Not Active
24813	McDonald	51880.3379	05 19 08.08	+40 06 02.4	0.627	G0V	≤ 3.15	Not Active
24819	FOCES	53748.9549	05 19 12.25	-03 04 26.9	1.021	K3V	3.69	Active
24874	FOCES	54086.9907	05 19 59.47	-15 50 24.5	1.014	K3V	7.37	Active
25220	FOCES	53748.9746	05 23 38.23	+17 19 26.9	1.121	K5V	≤ 0.53	Active
25623	FOCES	54087.0273	05 28 26.28	-03 29 51.4	1.182	K4V	≤ 3.35	Active
26505	FOCES	53747.9719	05 38 12.38	+51 26 43.7	0.827	K0V	1.20	Not Active
26779	McDonald	52030.0849	05 41 20.33	+53 28 56.4	0.844	K1V	4.06	Active
27072	FEROS	51834.2811	05 44 27.97	-22 26 51.0	0.498	F7V	9.84	Not Active
27207	SARG	54779.1315	05 46 01.53	+37 17 09.2	0.846	K5V	4.00	Not Active
27207	FOCES	53749.0129	05 46 01.53	+37 17 09.2	0.846	K5V	12.05	Not Active
27435	SARG	54194.8500	05 48 34.90	-04 05 38.7	0.639	G5V	2.61	Not Active
27913	McDonald	51882.3464	05 54 23.08	+20 16 35.1	0.599	G0V	10.79	Active
28103	SARG	54107.0756	05 56 24.32	-14 10 04.9	0.833	F1V	16.99	Not Active
29067	FOCES	54088.0550	06 07 55.33	+67 58 37.5	1.258	K5V	≤ 0.53	Active
29271	FEROS	51834.2617	06 10 14.20	-74 45 09.1	0.730	G5V	0.32	Not Active
29432	FOCES	54086.0365	06 12 00.45	+06 47 01.3	0.635	G4V	1.49	Not Active
29525	FOCES	53747.9540	06 13 12.46	+10 37 40.3	0.667	G1.5V	12.09	Active
29568	SARG	54778.1689	06 13 45.33	-23 51 43.9	0.702	G5V	9.63	Active
29650	SARG	54193.8451	06 14 50.94	+19 09 24.8	0.709	F6V	5.67	Not Active
29800	SARG	54193.8509	06 16 26.57	+12 16 18.2	0.730	F5IV-V	20.92	Active
29860	SARG	54193.8555	06 17 16.25	+05 05 58.9	0.611	G0.5Vb	2.98	Not Active
32010	FOCES	54086.0581	06 41 15.58	+23 57 30.2	1.028	K2V	7.40	Active
32423	FOCES	54086.0836	06 46 05.37	+32 33 19.6	0.989	K3V	3.35	Active
32439	SARG	54778.1944	06 46 14.47	+79 33 58.6	0.517	F8V	6.63	Not Active
32480	FOCES	54086.0365	06 46 44.34	+43 34 37.3	0.570	G0V	5.03	Not Active
32919	FOCES	54086.0995	06 51 32.60	+47 22 10.2	1.206	K5V	10.46	Active
32984	FOCES	54088.0194	06 52 18.37	-05 10 25.3	1.067	K3V	8.07	Active
33277	FOCES	54087.0522	06 55 18.69	+25 22 32.3	0.599	G0V	≤ 1.89	Not Active
33373	FOCES	54086.1177	06 56 28.03	+40 04 31.4	1.113	K3/K4V	6.91	Active
33537	FOCES	54087.0571	06 58 11.72	+22 28 32.3	0.633	G5V	≤ 3.01	Not Active
33560	SARG	54193.8607	06 58 26.02	-12 59 29.3	1.115	K5V	7.97	Active
33852	FOCES	54087.0680	07 01 38.11	+48 22 47.0	0.997	K3/K4V	6.59	Active
33955	SARG	54192.8556	07 02 43.04	-06 47 54.5	1.159	K5V	6.72	Not Active
34017	FOCES	54087.0835	07 03 30.35	+29 20 20.7	0.601	G4V	1.92	Not Active
35136	FOCES	54088.0145	07 15 50.11	+47 14 25.5	0.583	G0V	≤ 1.89	Not Active
36357	FOCES	54164.9213	07 29 01.66	+31 59 36.3	0.946	K2V	7.14	Active
36357	SARG	54107.0827	07 29 01.66	+31 59 36.3	0.946	K2V	7.38	Active
36366	FOCES	54133.0217	07 29 06.61	+31 47 02.7	0.333	F0V	56.66	Not Active
36366	SARG	54778.2122	07 29 06.61	+31 47 02.7	0.333	F0V	42.32	Not Active
36366	FOCES	54088.1352	07 29 06.61	+31 47 02.7	0.333	F0V	50.74	Not Active

† stars with known exoplanets

★ stars with chromospheric variations during our observations

* stars classified as active by visual inspection but for which chromospheric activity could not be measured

Table A.1. continue

HIP	Spectrograph	MJD (days)	RA (J2000)	DEC (J2000)	$B - V$ (mag)	SpT	$v \sin i$ (km s ⁻¹)	ACTIVE
36439	FOCES	54088.1291	07 29 55.86	+49 40 21.6	0.696	F6V	5.88	Not Active
36551	FOCES	54086.1369	07 31 07.67	+14 36 53.5	1.141	K2V	≤ 3.04	Active
36827	SARG	54193.8830	07 34 26.21	-06 53 47.7	0.871	K2V	8.76	Active
37279	McDonald	51880.3830	07 39 18.54	+05 13 39.0	0.432	F5IV-V	5.38	Not Active
37288	SARG	54780.1812	07 39 23.12	+02 11 03.3	1.397	M0V	...	Low S/N
37349	McDonald	51883.3603	07 39 59.29	-03 35 48.6	0.944	K1V	9.50	Active
37349	FOCES	53748.0933	07 39 59.29	-03 35 48.6	0.944	K1V	4.63	Active
37349	SARG	54193.8960	07 39 59.29	-03 35 48.6	0.944	K1V	7.31	Active
38657	FOCES	54087.1403	07 54 54.01	+19 14 14.8	0.979	K2	6.36	Not Active
38784	SARG	54778.2232	07 56 18.87	+80 15 55.2	0.732	G8V	4.27	Not Active
38931	FOCES	53749.0318	07 57 57.88	-00 48 51.9	1.021	K5V	≤ 0.53	Not Active
39157	FOCES	54088.0799	08 00 32.24	+29 12 54.7	0.714	G8V	5.65	Not Active
40035	SARG	54778.2756	08 10 39.98	-13 47 57.7	0.495	F7V	11.26	Not Active
40118	FOCES	54087.2768	08 11 38.96	+32 27 31.3	0.657	G4V	≤ 1.49	Not Active
40170	FOCES	54158.0979	08 12 14.55	+51 54 27.3	1.497	K5V	≤ 0.53	Active
40375	SARG	54192.8698	08 14 36.17	+13 01 21.3	1.192	K5	4.38	Not Active
40671	FOCES	54086.1612	08 18 10.97	+30 36 10.1	1.077	K4V	8.45	Low S/N
40671	FOCES	54164.9814	08 18 10.97	+30 36 10.1	1.077	K4V	3.81	Active
40693†	McDonald	51880.4285	08 18 23.78	-12 37 47.2	0.771	K0V	≤ 6.79	Active*
40843	FOCES	54088.1499	08 20 03.87	+27 13 07.0	0.479	F6V	4.45	Not Active
41484	FOCES	54164.9640	08 27 36.80	+45 39 13.8	0.624	G5V	12.37	Not Active
41926	McDonald	52030.1102	08 32 52.26	-31 30 09.7	0.774	K0V	≤ 6.79	Not Active
42074	FOCES	54087.1283	08 34 31.76	-00 43 34.0	0.791	G8V	5.60	Active
42074	SARG	54193.9536	08 34 31.76	-00 43 34.0	0.791	G8V	6.34	Active
42173	FOCES	53748.1111	08 35 51.34	+06 37 23.2	0.695	G5V	3.23	Not Active
42333	FOCES	53749.0569	08 37 50.47	-06 48 25.2	0.654	G1.5V	9.44	Active
42438	McDonald	51883.5354	08 39 11.74	+65 01 14.5	0.617	G1.5Vb	11.21	Active
42499	FOCES	53574.9531	08 39 50.86	+11 31 26.0	0.836	K1V	≤ 3.18	Not Active
42808	FEROS	52046.9654	08 43 18.26	-38 52 59.5	0.926	K2V	9.63	Active
43557	FOCES	53749.0723	08 52 16.30	+08 03 48.6	0.627	G0	≤ 1.89	Active
43587†	McDonald	51880.5005	08 52 36.13	+28 19 53.0	0.873	G8V	2.27	Not Active
43726	SARG	54193.9604	08 54 18.19	-05 26 04.3	0.671	G3V	3.66	Not Active
43726	FOCES	54086.1561	08 54 18.19	-05 26 04.3	0.671	G3V	3.58	Not Active
44248	FOCES	54091.1468	09 00 38.75	+41 47 00.4	0.705	F5V	21.17	Not Active
44897	SARG	54779.1457	09 08 51.20	+33 52 57.0	0.604	F9V	5.86	Active
45038	SARG	54779.1571	09 10 23.53	+67 08 03.3	0.498	F6IV	7.55	Not Active
45170	FOCES	53748.1456	09 12 17.87	+14 59 43.6	0.750	G9V	16.32	Not Active
45333	SARG	54779.1643	09 14 20.55	+61 25 24.2	0.602	F9V	5.59	Not Active
45383	FOCES	53748.1605	09 14 53.72	+04 26 34.4	1.010	K0V	41.20	Active
45617	FOCES	53748.1832	09 17 53.42	+28 33 42.3	1.002	K0V	≤ 1.20	Active
45839	FOCES	54087.1669	09 20 44.53	-05 45 13.3	1.191	K5V	7.73	Not Active
46509	SARG	54779.2324	09 29 08.84	-02 46 08.2	0.411	F6V	30.56	Not Active
46509	FOCES	54164.9473	09 29 08.84	-02 46 08.2	0.411	F6V	14.04	Not Active
46580	SARG	54193.9665	09 29 55.12	+05 39 17.5	0.994	K3V	8.39	Active
46580	FOCES	54087.1896	09 29 55.12	+05 39 17.5	0.994	K3V	8.85	Active
46816	FOCES	54161.0253	09 32 25.72	-11 11 05.0	0.911	K0V	29.03	Active
46816	SARG	54193.9734	09 32 25.72	-11 11 05.0	0.911	K0V	30.42	Active
46843	SARG	54193.9834	09 32 43.86	+26 59 20.9	0.783	K0V	10.57	Active
46843	FOCES	54161.0562	09 32 43.86	+26 59 20.9	0.783	K0V	29.71	Active
46853	McDonald	51880.4889	09 32 52.33	+51 40 43.0	0.487	K0V	8.77	Not Active
47080	McDonald	52031.1226	09 35 40.03	+35 48 38.8	0.779	G8V	6.72	Active
47080	FOCES	53749.1406	09 35 40.03	+35 48 38.8	0.779	G8V	7.22	Active
47592	SARG	54779.2669	09 42 14.67	-23 54 58.4	0.538	G0V	7.08	Not Active
48113	SARG	54192.8958	09 48 35.18	+46 01 16.4	0.624	G2V	3.97	Not Active
48113	FOCES	54086.0303	09 48 35.18	+46 01 16.4	0.624	G2V	1.89	Not Active
48411	SARG	53785.1132	09 52 11.61	+03 13 18.5	1.162	K5	≤ 1.90	Active*
49081	FOCES	54086.2050	10 01 01.02	+31 55 29.0	0.675	G1V	3.08	Not Active
49366	SARG	53786.1106	10 04 37.77	-11 43 46.7	0.913	K0	8.22	Active
49699†	SARG	54194.0124	10 08 43.18	+34 14 32.7	0.964	F6V	3.67	Not Active
49699†	FOCES	53749.1488	10 08 43.18	+34 14 32.7	0.964	F6V	≤ 1.20	Not Active
49908	SARG	54194.0217	10 11 23.36	+49 27 19.7	1.319	K7V	≤ 3.21	Active
49908	FOCES	54086.2131	10 11 23.36	+49 27 19.7	1.319	K7V	5.21	Low S/N
49986	SARG	54779.2385	10 12 17.76	-03 44 42.3	1.359	M1.5	...	Active*
50125	SARG	53785.1372	10 13 57.30	+52 30 30.9	1.122	K5	2.85	Not Active
50384	FOCES	54088.1414	10 17 14.80	+23 06 23.2	0.503	F8Vbw	2.16	Not Active
50505	SARG	53786.1322	10 18 51.90	+44 02 56.6	0.686	K0V	1.72	Not Active
51459	McDonald	51880.5129	10 30 37.76	+55 58 50.2	0.532	F8V	≤ 3.41	Not Active
51502	SARG	54780.2195	10 31 05.02	+82 33 30.7	0.783	F2V	41.65	Not Active
51525	SARG	53786.1408	10 31 24.69	+45 31 39.0	1.339	K7V	≤ 3.21	Active
51933	FOCES	54164.9551	10 36 32.22	-12 13 42.6	0.523	F7V	31.06	Not Active

† stars with known exoplanets

★ stars with chromospheric variations during our observations

* stars classified as active by visual inspection but for which chromospheric activity could not be measured

Table A.1. continue

HIP	Spectrograph	MJD (days)	RA (J2000)	DEC (J2000)	$B - V$ (mag)	SpT	$v \sin i$ (km s ⁻¹)	ACTIVE
52369	SARG	54106.1490	10 42 13.18	-13 47 14.3	0.629	G2/G3V	3.80	Not Active
52369	FOCES	54167.9622	10 42 13.18	-13 47 14.3	0.629	G2/G3V	10.64	Not Active
53486	SARG	53786.1585	10 56 30.95	+07 23 19.2	0.924	K0	7.85	Active
53721†	McDonald	52031.1341	10 59 28.22	+40 25 48.4	0.622	G0V	≤ 3.15	Not Active
54155	SARG	53786.1684	11 04 41.58	-04 13 15.0	0.837	G8V	9.46	Active
54155	FOCES	54158.1320	11 04 41.58	-04 13 15.0	0.837	G8V	≤ 0.45	Active
54426	FOCES	54087.2019	11 08 14.17	+38 25 35.5	0.964	K0V	5.74	Active
54646★	FOCES	54086.2260	11 11 04.77	+30 26 47.4	1.344	K8V	5.83	Active
54646★	SARG	54780.2266	11 11 04.77	+30 26 47.4	1.344	K8V	≤ 3.21	Not Active
54646★	FOCES	54159.0846	11 11 04.77	+30 26 47.4	1.344	K8V	≤ 0.53	Not Active
54651	FOCES	54167.9786	11 11 11.26	-10 57 08.4	1.089	K5V	≤ 1.90	Not Active
54651	SARG	54106.1567	11 11 11.26	-10 57 08.4	1.089	K5V	≤ 0.53	Not Active
54745	FOCES	54086.2729	11 12 32.53	+35 48 52.0	0.620	G1V	7.74	Active
54810	SARG	54106.1858	11 13 13.42	+04 28 56.7	1.228	K5V	5.31	Active
54906	FOCES	54087.2432	11 14 33.23	+25 42 37.0	0.824	K1V	3.18	Not Active
55210	FOCES	54087.2567	11 18 21.55	-05 04 01.0	0.756	G8V	1.52	Not Active
56242	FOCES	54087.2704	11 31 45.14	+14 21 53.9	0.581	G0V	3.59	Not Active
56452	McDonald	52030.1374	11 34 29.95	-32 50 00.0	0.804	K0V	≤ 6.79	Active*
56997	McDonald	52031.1440	11 41 03.03	+34 12 09.2	0.737	G8Vvar	≤ 3.26	Not Active
57443	FEROS	52045.9778	11 46 32.25	-40 30 04.8	0.664	G3/G5V	≤ 0.32	Not Active
57494	FOCES	54156.0187	11 47 03.96	-11 49 26.0	1.196	K3/K4V	7.27	Active
57757	McDonald	52030.1547	11 50 41.29	+01 45 55.4	0.563	F8V	3.41	Not Active
57939	SARG	54780.2555	11 52 55.82	+37 43 58.1	0.745	G8Vp	≤ 3.26	Not Active
57939	FOCES	54156.0864	11 52 55.82	+37 43 58.1	0.745	G8Vp	9.28	Not Active
58576	McDonald	52030.1657	12 00 44.37	-10 26 41.4	0.772	G8IV-V	≤ 3.26	Not Active
59000	FOCES	54158.1703	12 05 50.67	-18 52 28.1	1.403	K7V	3.68	Low S/N
59000	SARG	54194.0305	12 05 50.67	-18 52 28.1	1.403	K7V	≤ 3.21	Active
59280	FOCES	54156.0998	12 09 37.50	+40 15 07.8	0.786	K0V	≤ 1.20	Active
60866★	FOCES	54228.9530	12 28 31.49	-18 17 48.7	1.165	K5V	≤ 0.53	Active
60866★	SARG	54194.0543	12 28 31.49	-18 17 48.7	1.165	K5V	3.19	Not Active
61317	McDonald	52030.1888	12 33 45.09	+41 21 24.4	0.595	G0V	≤ 3.15	Not Active
61901	SARG	54108.2284	12 41 06.41	+15 22 39.3	1.095	K5V	3.60	Low S/N
61941	McDonald	52031.1932	12 41 40.00	-01 26 58.3	0.368	F0V	31.36	Not Active
62207	FOCES	54156.1221	12 44 59.68	+39 16 42.9	0.557	G0V	8.11	Not Active
62523★	SARG	54194.1269	12 48 47.26	+24 50 25.7	0.706	G7V	6.24	Not Active
62523★	FOCES	53575.8536	12 48 47.26	+24 50 25.7	0.706	G7V	11.97	Active
62523★	FOCES	54132.2376	12 48 47.26	+24 50 25.7	0.706	G7V	13.60	Not Active
63257	SARG	54108.2639	12 57 44.17	-14 27 48.8	1.109	K5V	6.91	Not Active
64241	McDonald	52030.2129	13 09 59.55	+17 31 44.8	0.455	F5V	21.47	Not Active
64394	McDonald	52030.2579	13 11 52.92	+27 52 33.7	0.588	G1V	4.72	Active
64792	McDonald	51883.2234	13 16 46.71	+09 25 25.3	0.587	G0Vs	10.64	Not Active
64797	McDonald	52030.2286	13 16 50.67	+17 01 04.1	0.910	K2V	2.86	Active
64924†	SARG	54195.0981	13 18 24.97	-18 18 31.0	0.709	G5V	4.09	Not Active
64924†	McDonald	52030.2464	13 18 24.97	-18 18 31.0	0.709	G5V	1.35	Not Active
65352	SARG	53786.1888	13 23 39.15	+02 43 22.2	0.780	G5	3.34	Not Active
65515	FOCES	54132.1649	13 25 45.76	+56 58 13.7	0.804	K0V	≤ 1.20	Active
65721†	FOCES	54156.1333	13 28 25.95	+13 46 48.7	0.711	G5V	4.83	Not Active
66147	SARG	53786.1989	13 33 32.70	+08 35 11.5	1.028	K3/K4V	8.66	Active
66252	FOCES	54168.0938	13 34 43.38	-08 20 30.5	1.196	K5V	≤ 0.53	Active
66886	SARG	53786.2148	13 42 26.20	-01 41 09.2	1.223	K5V	1.90	Not Active
67105	SARG	53786.2384	13 45 14.76	+08 50 10.4	1.042	K2	6.76	Active
67275	SARG	54108.3087	13 47 16.04	+17 27 24.4	0.501	F6IV	17.86	Active
67422	McDonald	52030.2748	13 49 04.28	+26 58 48.5	1.104	K2	6.27	Active
67927	McDonald	52030.3480	13 54 41.12	+18 23 54.9	0.607	G0IV	15.43	Not Active
68030	SARG	54106.2362	13 55 50.17	+14 03 23.3	0.510	F6V	3.66	Not Active
68184	McDonald	52030.3291	13 57 32.10	+61 29 32.4	1.037	K3V	7.43	Not Active
68337	FOCES	53577.8595	13 59 19.50	+22 52 11.0	1.149	K5V	≤ 0.53	Active
68682	FOCES	53578.8527	14 03 32.30	+10 47 15.1	0.737	G8V	≤ 0.45	Not Active
69357	FOCES	53578.0216	14 11 46.32	-12 36 40.8	0.861	K0V	11.71	Active
69414	FOCES	53578.8591	14 12 45.33	-03 19 09.5	0.747	G8V	18.16	Not Active
69526	FOCES	53578.9125	14 13 57.35	+30 13 00.3	1.053	K2V	9.43	Active
69701	FOCES	54156.1416	14 16 00.88	-05 59 58.3	0.521	F7V	4.39	Not Active
69962	SARG	54108.2822	14 18 58.28	-06 36 09.3	1.316	K7V	3.21	Active
69962	FOCES	54156.1471	14 18 58.28	-06 36 09.3	1.316	K7V	9.38	Active*
69972	FEROS	52177.0088	14 19 05.36	-59 22 37.4	1.020	K3V	3.97	Not Active
70016	SARG	53786.2551	14 19 35.23	-05 09 03.2	0.867	K1V	8.15	Not Active
70218	SARG	53786.2988	14 21 57.64	+29 37 49.3	1.238	K5V	≤ 1.90	Active
70218	FOCES	54159.1693	14 21 57.64	+29 37 49.3	1.238	K5V	10.40	Active
70319	FOCES	54156.1724	14 23 15.15	+01 14 33.8	0.637	G1V	≤ 3.08	Not Active
71284	SARG	54108.3110	14 34 40.69	+29 44 41.3	0.803	F3Vvvar	7.32	Not Active

† stars with known exoplanets

★ stars with chromospheric variations during our observations

* stars classified as active by visual inspection but for which chromospheric activity could not be measured

Table A.1. continue

HIP	Spectrograph	MJD (days)	RA (J2000)	DEC (J2000)	$B - V$ (mag)	SpT	$v \sin i$ (km s ⁻¹)	ACTIVE
71395†	SARG	54194.1338	14 36 00.44	+09 44 49.7	0.965	K2V	9.22	Active
71395†	FOCES	53577.8799	14 36 00.44	+09 44 49.7	0.965	K2V	9.39	Active
71681	FEROS	52045.1062	14 39 39.39	-60 50 22.1	0.900	K1V	≤ 3.52	Not Active
71683	FEROS	52045.1030	14 39 40.90	-60 50 06.5	0.710	G2V	≤ 2.64	Not Active
71743	SARG	54193.0776	14 40 31.17	-16 12 32.9	0.709	G8V	6.19	Active
72146	FOCES	53575.8597	14 45 24.32	+13 50 48.7	0.929	K0V	7.68	Active
72146	FOCES	54132.2205	14 45 24.32	+13 50 48.7	0.929	K0V	12.04	Low S/N
72146	SARG	54194.1582	14 45 24.32	+13 50 48.7	0.929	K0V	6.00	Active
72237	FOCES	54159.2162	14 46 23.35	+16 29 56.2	1.358	K5V	≤ 1.90	Active
72237	SARG	53786.2752	14 46 23.35	+16 29 56.2	1.358	K5V	≤ 0.53	Active
72567	FOCES	54168.1225	14 50 15.72	+23 54 42.4	0.592	G2V	8.54	Active
72603	SARG	54193.0831	14 50 41.26	-15 59 49.5	0.763	F4V	5.95	Not Active
72659	McDonald	52030.3731	14 51 23.28	+19 06 02.3	0.764	G8V	3.26	Active
72848	McDonald	52164.0668	14 53 24.04	+19 09 08.2	0.844	K1V	6.35	Active
72875	FOCES	53577.8968	14 53 42.09	+23 20 42.6	0.961	K0V	4.00	Active
72981	SARG	54193.0870	14 54 53.67	+09 56 40.1	1.377	M1	...	Low S/N
73184	SARG	54194.1436	14 57 27.35	-21 24 40.6	1.092	K4V	7.68	Active
73457	FOCES	54156.1866	15 00 43.42	-11 08 02.3	1.472	K7V	≤ 3.68	Not Active
73695	McDonald	52030.3967	15 03 47.68	+47 39 14.5	0.641	G0V	≤ 3.15	Not Active
73786	FOCES	53577.9150	15 04 53.88	+05 38 21.6	1.333	K7V	≤ 3.68	Not Active
73996	FOCES	53575.8734	15 07 17.95	+24 52 10.5	0.724	F6V	11.15	Not Active
74537	SARG	53786.2673	15 13 51.64	-01 21 00.6	0.761	K0V	2.12	Not Active
74702	SARG	54108.2523	15 15 59.06	+00 47 48.1	0.827	K0	8.07	Active
75201	SARG	54193.0544	15 22 04.27	-04 46 38.7	1.297	K7V	≤ 3.21	Active
75253	FOCES	54161.1805	15 22 36.73	-10 39 38.3	0.971	K3/K4V	≤ 3.35	Active
75277	FOCES	53576.9457	15 22 46.98	+18 55 07.6	0.804	G8V	≤ 0.45	Not Active
75542	SARG	54195.1035	15 25 59.04	-26 42 20.7	1.117	K3/K4V	6.80	Active
75809	FOCES	54160.1481	15 29 11.97	+80 26 54.0	0.648	G8V	11.09	Active
76779	SARG	54195.1198	15 40 34.47	-18 02 57.3	1.337	K7V	≤ 3.21	Active
77052	FOCES	54158.2301	15 44 01.85	+02 30 55.9	0.678	G2.5V	11.01	Not Active
77257	McDonald	52032.2461	15 46 26.75	+07 21 11.7	0.609	G0Vvar	≤ 3.15	Not Active
77408★	FOCES	54158.2014	15 48 09.57	+01 34 19.7	0.796	G8V	7.61	Not Active
77408★	FOCES	53575.9293	15 48 09.57	+01 34 19.7	0.796	G8V	≤ 0.45	Active
77408★	SARG	54193.1507	15 48 09.57	+01 34 19.7	0.796	G8V	7.48	Active
77952	FEROS	52045.1226	15 55 08.81	-63 25 47.1	0.324	F1V	69.63	Not Active
78072	FOCES	53579.9391	15 56 26.99	+15 39 53.0	0.478	F6V	11.13	Not Active
78072	McDonald	52030.4041	15 56 26.99	+15 39 53.0	0.478	F6V	11.71	Not Active
78709	SARG	54193.1431	16 04 04.03	+25 15 11.3	0.760	G8V	4.35	Not Active
78775	McDonald	52030.4155	16 04 57.22	+39 09 23.0	0.738	G8V	≤ 3.26	Not Active
78843	SARG	54194.1958	16 05 40.29	-20 26 57.1	1.059	K3/K4V	6.24	Not Active
79190	FEROS	52180.0646	16 09 42.94	-56 26 45.5	0.837	K1V	≤ 3.97	Not Active
79492	FOCES	53575.9778	16 13 18.34	+13 31 40.5	0.756	G8V	2.24	Not Active
79672	McDonald	52164.0986	16 15 37.13	-08 22 05.7	0.658	G1V	≤ 4.07	Not Active
80337†	FEROS	52045.1772	16 24 01.24	-39 11 34.8	0.633	G3/G5V	≤ 0.32	Active
80366	SARG	54193.2128	16 24 19.94	-13 38 28.2	0.974	K2V	5.89	Active
80644	FOCES	53574.8662	16 27 57.05	+07 18 21.9	1.209	K7V	≤ 3.68	Not Active
80686	FEROS	52045.2054	16 28 27.80	-70 05 04.8	0.556	F9V	3.23	Active
80725	FOCES	53579.9305	16 28 52.88	+18 24 47.2	0.834	K2V	4.12	Active
81300	McDonald	52164.1210	16 36 21.18	-02 19 25.8	0.844	K0V _k	4.12	Active
81375	FOCES	53574.8765	16 37 08.37	+00 15 15.0	0.827	K0	5.66	Not Active
81693	McDonald	52030.4342	16 41 17.48	+31 36 06.8	0.652	G0IV	3.11	Not Active
82588	FOCES	53576.9600	16 52 59.22	-00 01 22.1	0.751	G8V	10.60	Active
83591	SARG	54195.2015	17 05 03.93	-05 03 49.5	1.120	K5V	≤ 1.90	Not Active
83601	SARG	54195.2462	17 05 16.83	+00 42 12.1	0.578	F9V	8.00	Active
84195	FOCES	53579.9452	17 12 37.56	+18 21 05.3	0.940	K0V	10.77	Not Active
84195	SARG	54195.2119	17 12 37.56	+18 21 05.3	0.940	K0V	6.40	Not Active
84405	McDonald	52208.0394	17 15 21.29	-26 36 00.2	0.861	K2V	5.12	Active
84720	FEROS	52048.1876	17 19 02.95	-46 38 11.4	0.764	G8V	...	Not Active
84862	McDonald	52030.4428	17 20 39.47	+32 28 13.0	0.616	G0V	≤ 3.15	Not Active
85235	McDonald	52030.4468	17 25 00.90	+67 18 24.1	0.773	K0V	≤ 6.79	Not Active
85295	SARG	54193.2589	17 25 45.57	+02 06 51.5	1.354	K7V	≤ 3.21	Active
85561	SARG	54194.2041	17 29 06.74	-23 50 09.4	1.324	K5V	≤ 1.90	Active
85810★	SARG	54193.2741	17 32 01.16	+34 16 15.6	0.648	G5V	5.12	Active
85810★	FOCES	54132.2478	17 32 01.16	+34 16 15.6	0.648	G5V	3.01	Not Active
86036	McDonald	52030.4566	17 34 59.25	+61 52 33.0	0.601	G0Va	5.61	Active
86400	McDonald	52032.3071	17 39 17.02	+03 33 19.7	0.957	K3V	3.37	Active
86722	FOCES	53574.8860	17 43 15.72	+21 36 38.6	0.755	K0V	≤ 1.20	Not Active
86974	McDonald	52030.4693	17 46 27.72	+27 43 21.0	0.751	G5IV	≤ 5.86	Not Active
87579	FOCES	53574.8992	17 53 29.98	+21 19 30.5	0.950	K0V	15.78	Active
88175	SARG	54195.2729	18 00 28.92	-03 41 24.6	0.770	F3V	51.51	Not Active

† stars with known exoplanets

★ stars with chromospheric variations during our observations

* stars classified as active by visual inspection but for which chromospheric activity could not be measured

Table A.1. continue

HIP	Spectrograph	MJD (days)	RA (J2000)	DEC (J2000)	$B - V$ (mag)	SpT	$v \sin i$ (km s ⁻¹)	ACTIVE
88601	McDonald	52164.1787	18 05 27.21	+02 30 08.8	0.860	K1V	≤ 4.06	Active
88622	FOCES	53578.9512	18 05 37.47	+04 39 28.6	0.593	G0V	13.90	Not Active
88972	McDonald	52030.4780	18 09 37.65	+38 27 32.1	0.886	K2V	≤ 4.06	Not Active
88972	SARG	54195.2463	18 09 37.65	+38 27 32.1	0.886	K2V	4.82	Not Active
89937	McDonald	52030.4614	18 21 02.34	+72 44 01.3	0.509	F7V	6.01	Not Active
90656	FOCES	53574.9158	18 29 52.31	-01 49 03.5	1.072	K3V	11.33	Not Active
90790	McDonald	52208.0867	18 31 19.05	-18 54 30.0	0.864	K1V	≤ 4.06	Active
91009	SARG	54779.8159	18 33 55.60	+51 43 11.7	1.183	K6Ve	8.81	Active
91438	FEROS	52046.2542	18 38 53.45	-21 03 05.4	0.664	G5V	≤ 0.32	Not Active
92043	FOCES	53574.9531	18 45 39.73	+20 32 49.6	0.475	F6V	14.08	Not Active
92200	FOCES	53574.9577	18 47 27.33	-03 38 21.0	1.226	K7V	≤ 3.68	Active
92283	FOCES	53578.9782	18 48 29.15	+10 44 47.4	1.128	K3/K4V	≤ 3.35	Active
93017	SARG	54779.8858	18 57 01.47	+32 54 05.8	0.590	F9V	6.80	Not Active
93871	FOCES	53574.9827	19 07 02.23	+07 37 03.8	1.050	K5V	4.07	Not Active
95319	FOCES	53576.0730	19 23 33.96	+33 13 17.7	0.805	G8V	0.00	Not Active
96085	FOCES	53578.0463	19 32 06.56	-11 16 29.9	0.923	K2V	3.04	Active
96100	McDonald	52030.4861	19 32 20.59	+69 39 55.4	0.804	K0V	≤ 6.79	Not Active
96285	FOCES	53575.0438	19 34 39.53	+04 34 54.3	1.355	K7V	≤ 3.68	Active
98036	McDonald	52164.2366	19 55 18.77	+06 24 28.6	0.850	G9.5V	22.28	Not Active
98677	FOCES	53575.0687	20 02 34.25	+15 35 36.6	0.723	G0V	10.87	Not Active
98819	FOCES	53575.0956	20 04 06.47	+17 04 16.2	0.609	G1V	8.06	Not Active
98819	SARG	54195.2659	20 04 06.47	+17 04 16.2	0.609	G1V	5.38	Not Active
98819	FOCES	54228.1518	20 04 06.47	+17 04 16.2	0.609	G1V	8.27	Not Active
98828	FOCES	53575.0823	20 04 10.09	+25 47 25.2	0.934	K0V	≤ 1.20	Active
99240	FEROS	51834.9776	20 08 41.86	-66 10 45.6	0.751	G5IV-Vvar	≤ 0.32	Not Active
99316	FOCES	53578.0824	20 09 34.30	+16 48 19.2	0.825	K0	4.06	Not Active
99452	FOCES	53575.1133	20 11 06.33	+16 11 13.3	0.837	K1V	6.41	Not Active
99461	FEROS	51833.9874	20 11 11.61	-36 05 50.6	0.868	K3V	≤ 3.97	Active
99711†	FOCES	53575.9912	20 13 59.88	-00 52 03.1	0.936	K4V	5.72	Active
99764	FOCES	53576.0317	20 14 28.18	-07 16 52.8	1.291	K6V	3.85	Active
99825	FEROS	51834.0083	20 15 16.58	-27 01 57.1	0.878	K2V	≤ 3.97	Not Active
101345	FOCES	53578.9946	20 32 23.51	-09 51 13.1	0.698	G2.5IV	1.91	Not Active
101955	FOCES	53579.9626	20 39 37.20	+04 58 18.7	1.219	K5V	≤ 0.53	Not Active
101997	SARG	54779.7904	20 40 11.44	-23 46 30.0	0.729	G8/K0V	3.50	Not Active
102422	McDonald	52030.4905	20 45 17.27	+61 50 12.5	0.912	K0IV	≤ 6.79	Not Active
102485	SARG	54779.8091	20 46 05.77	-25 16 13.9	0.725	F5V	34.94	Not Active
103256	FOCES	53576.0317	20 55 06.53	+13 10 33.1	1.025	K2V	≤ 3.04	Active
104092	FOCES	53576.0519	21 05 19.70	+07 04 14.4	1.215	K6V	14.33	Active
104214	SARG	54777.8548	21 06 50.84	+38 44 29.4	1.069	K5V	4.72	Not Active
104217	SARG	54777.8623	21 06 52.19	+38 44 03.9	1.303	K7V	≤ 3.21	Not Active
104239	FOCES	53579.0004	21 07 10.15	-13 55 22.1	0.903	K1IV	5.57	Active
104858	FOCES	54089.7671	21 14 28.79	+10 00 27.8	0.508	F5V+...	16.87	Not Active
105038	FOCES	53576.0819	21 16 32.38	+09 23 38.8	1.003	K5V	1.53	Active
105152	FOCES	53576.0981	21 18 02.70	+00 09 43.3	1.028	K5V	≤ 0.53	Not Active
105858	FEROS	51833.9938	21 26 26.49	-65 22 05.3	0.491	F6V	≤ 9.84	Not Active
106147	FOCES	53580.0879	21 30 02.15	-12 30 34.0	1.233	K7V	≤ 3.68	Active*
106400	SARG	54778.8327	21 33 00.61	+62 00 07.1	1.158	K5V	9.09	Active
107310	FOCES	54229.1363	21 44 08.40	+28 44 35.6	0.504	F6V	5.45	Not Active
107350	SARG	54777.8715	21 44 31.19	+14 46 20.0	0.581	G4V	12.81	Active
108028	FOCES	53576.1120	21 53 05.36	+20 55 50.8	0.936	K0V	≤ 1.20	Active
108156	FOCES	53575.1412	21 54 44.89	+32 19 44.9	0.925	K0V	≤ 1.20	Active
109176	McDonald	52164.2581	22 07 00.47	+25 20 42.2	0.713	F5V	5.42	Not Active
109378†	SARG	54777.8864	22 09 29.82	-07 32 51.2	0.757	G4V	3.98	Not Active
109527	FOCES	53578.0943	22 11 11.89	+36 15 25.0	0.809	G8V	13.20	Active
110109	FEROS	51834.0002	22 18 15.18	-53 37 31.9	0.600	G3V	≤ 0.32	Not Active
110778	SARG	54777.9046	22 26 34.15	-16 44 31.7	0.617	G1V	11.78	Active
111449	SARG	54778.8827	22 34 41.50	-20 42 28.3	0.713	F7V	33.31	Not Active
111888	FOCES	53576.1296	22 39 50.66	+04 06 57.1	0.910	K2V	≤ 3.04	Active
112190	FOCES	53577.0266	22 43 21.39	-06 24 00.4	0.968	K3/K4V	≤ 3.35	Not Active
112447	FOCES	53577.0599	22 46 41.44	+12 10 26.7	0.501	F6V	12.67	Not Active
112870	FOCES	53577.0413	22 51 26.11	+13 58 10.2	0.848	G8V	≤ 0.45	Not Active
113357†	SARG	54777.8102	22 57 27.85	+20 46 07.3	0.665	G5V	4.99	Not Active
113576	SARG	54777.9334	23 00 16.69	-22 31 28.2	1.351	K7V	≤ 3.21	Active
113718	FOCES	53579.0086	23 01 51.31	-03 50 53.6	0.948	K4V	5.73	Not Active
114622	McDonald	52164.3198	23 13 14.74	+57 10 03.5	1.000	K3Vvar	6.94	Not Active
114886	FOCES	53575.1545	23 16 17.91	+30 40 12.0	0.898	K1V	≤ 3.18	Active
115162	FOCES	53576.9955	23 19 39.50	+42 15 10.4	0.733	G0	7.19	Active
115331	FOCES	53578.1064	23 21 36.00	+44 05 50.5	0.797	G8V	11.55	Active
115341	FOCES	53575.1704	23 21 44.29	+45 10 34.4	1.046	K5V	≤ 0.53	Active
115445	FOCES	53580.1105	23 23 04.63	-10 45 53.6	0.902	K0V	8.46	Not Active

† stars with known exoplanets

★ stars with chromospheric variations during our observations

* stars classified as active by visual inspection but for which chromospheric activity could not be measured

Table A.1. continue

HIP	Spectrograph	MJD (days)	RA (J2000)	DEC (J2000)	$B - V$ (mag)	SpT	$v \sin i$ (km s ⁻¹)	ACTIVE
116613	FOCES	53578.1185	23 37 58.19	+46 11 58.1	0.649	G0V	8.28	Active
116727†	McDonald	52164.3603	23 39 20.98	+77 37 55.1	1.029	K1IV	≤ 4.06	Not Active
116771	McDonald	51880.1089	23 39 56.82	+05 37 38.5	0.514	F7V	6.67	Not Active
120005	SARG	54779.1742	09 14 26.19	+52 41 16.7	1.420	K7V	≤ 3.21	Active

† stars with known exoplanets

★ stars with chromospheric variations during our observations

* stars classified as active by visual inspection but for which chromospheric activity could not be measured

Table A.2. Excess emission in different chromospheric activity indicator lines for the active stars in the sample.

HIP	Spectrograph	MJD (days)	EW (Å) in the subtrated spectrum					
			Ca II		$H\alpha$	Ca II IRT		
			K	H		$\lambda 8498$	$\lambda 8542$	$\lambda 8662$
544	SARG	54780.9561	0.056 ± 0.016	0.239 ± 0.067	0.220 ± 0.105	0.228 ± 0.084
544	McDonald	52031.3248	0.112 ± 0.008	0.089 ± 0.008	0.115 ± 0.036	0.133 ± 0.023	0.151 ± 0.020	0.164 ± 0.006
1803	SARG	54777.9856	0.135 ± 0.013	0.177 ± 0.081	0.227 ± 0.066	...
3093	FOCES	53577.1854	0.062 ± 0.004
3765	FOCES	53747.7686	0.035 ± 0.030	0.319 ± 0.019	0.004 ± 0.011
3765	McDonald	52164.3977	0.032 ± 0.006	0.023 ± 0.006	0.009 ± 0.025	0.019 ± 0.010	0.033 ± 0.003	0.023 ± 0.006
4148	FEROS	51834.1339	0.124 ± 0.007	0.093 ± 0.009	0.066 ± 0.015	0.095 ± 0.013	0.140 ± 0.014	0.087 ± 0.006
4845	SARG	54778.9878	0.073 ± 0.017	0.050 ± 0.020	0.073 ± 0.101	0.063 ± 0.087
5286	FOCES	53576.1601	...	0.150 ± 0.178	0.060 ± 0.022	0.080 ± 0.017	0.111 ± 0.017	0.119 ± 0.018
5944	FOCES	53576.1764	0.119 ± 0.014	0.095 ± 0.012	0.077 ± 0.015	0.072 ± 0.070	0.077 ± 0.008	0.064 ± 0.013
6290	SARG	54107.9171	0.131 ± 0.018	0.070 ± 0.073	0.070 ± 0.123	0.062 ± 0.049
7235	SARG	54780.9662	0.039 ± 0.022
7576	FOCES	53577.1583	0.249 ± 0.032	0.296 ± 0.043	0.119 ± 0.017	0.154 ± 0.018	0.194 ± 0.015	0.188 ± 0.016
7751	FEROS	51834.1456	0.047 ± 0.016	0.029 ± 0.022	0.018 ± 0.011
7981	FOCES	53578.1869	0.042 ± 0.047	0.036 ± 0.033
8275	FOCES	54086.7647	0.278 ± 0.362	0.336 ± 0.301	0.120 ± 0.079	0.123 ± 0.019	0.174 ± 0.020	0.162 ± 0.018
8362	McDonald	51883.2217	0.058 ± 0.007	0.038 ± 0.005	0.021 ± 0.008	0.037 ± 0.005	0.052 ± 0.005	0.021 ± 0.004
8486	FOCES	53748.8161	0.210 ± 0.110	0.250 ± 0.080	0.110 ± 0.020	0.090 ± 0.020	0.180 ± 0.020	0.110 ± 0.020
8768	SARG	54778.0142	0.068 ± 0.025	0.034 ± 0.087	0.088 ± 0.054	0.079 ± 0.109
10138	FEROS	51834.1664	0.050 ± 0.016	0.026 ± 0.021	0.043 ± 0.010
10337	SARG	54780.0100	0.050 ± 0.031	0.065 ± 0.021	0.141 ± 0.063	0.186 ± 0.069
10416	FOCES	54086.7855	0.543 ± 0.126	0.670 ± 0.160	0.140 ± 0.026	0.183 ± 0.016	0.284 ± 0.014	0.184 ± 0.022
11565	SARG	54780.2041	0.065 ± 0.022	0.062 ± 0.087	0.103 ± 0.048	0.099 ± 0.081
12110	SARG	54780.0623	0.112 ± 0.019	0.133 ± 0.070	0.217 ± 0.069	0.180 ± 0.061
13258	FOCES	54086.8172	0.036 ± 0.020	0.074 ± 0.013	0.096 ± 0.017	0.053 ± 0.016
13402	McDonald	52207.4006	0.377 ± 0.004	0.291 ± 0.005	0.128 ± 0.011	0.212 ± 0.005	0.294 ± 0.008	0.264 ± 0.005
13402	SARG	54779.0488	0.128 ± 0.022	0.243 ± 0.077	0.295 ± 0.032	0.296 ± 0.116
13976	SARG	54778.0715	0.113 ± 0.015	0.120 ± 0.053	0.125 ± 0.023	0.112 ± 0.034
15330	FEROS	51834.2315	0.058 ± 0.007	0.041 ± 0.004	0.025 ± 0.005	0.042 ± 0.007	0.058 ± 0.007	0.043 ± 0.004
15442	SARG	54780.1170	0.037 ± 0.022	0.100 ± 0.108	0.111 ± 0.087	0.106 ± 0.099
15673	FOCES	54086.8639	0.125 ± 0.956	0.493 ± 0.307	0.119 ± 0.026	0.103 ± 0.031	0.115 ± 0.024	0.102 ± 0.030
15919	FOCES	53747.8508	0.440 ± 0.138	0.314 ± 0.119	...	0.054 ± 0.033	0.069 ± 0.027	0.060 ± 0.036
16134	SARG	54779.0552	0.062 ± 0.024	0.090 ± 0.030	0.124 ± 0.054	0.158 ± 0.059
16537	McDonald	51833.9938	0.189 ± 0.004	0.141 ± 0.010	0.088 ± 0.016	0.094 ± 0.005	0.153 ± 0.006	0.117 ± 0.006
17420	McDonald	52207.4446	0.081 ± 0.007	0.057 ± 0.010	0.027 ± 0.013	0.018 ± 0.004	0.035 ± 0.018	0.031 ± 0.006
18774	SARG	54779.1053	0.068 ± 0.021	0.107 ± 0.077	0.196 ± 0.090	0.226 ± 0.082
18859	SARG	54780.1408	0.069 ± 0.010	0.220 ± 0.029	0.286 ± 0.033	0.235 ± 0.056
19076	SARG	54780.1482	0.169 ± 0.023	0.135 ± 0.124	0.144 ± 0.091	0.121 ± 0.142
19335	SARG	54780.1552	0.045 ± 0.005	0.226 ± 0.051	0.267 ± 0.036	0.210 ± 0.035
19832	FOCES	54087.9871	0.049 ± 0.013	0.046 ± 0.013	0.075 ± 0.014	0.036 ± 0.105
19849	McDonald	51880.2760	0.026 ± 0.004	0.022 ± 0.005	0.004 ± 0.024	0.010 ± 0.009	0.011 ± 0.010	0.015 ± 0.005
20917	FOCES	54086.9422	0.647 ± 0.366	0.766 ± 0.400	0.146 ± 0.022	0.113 ± 0.014	0.113 ± 0.013	0.101 ± 0.141
22263	McDonald	52207.4280	0.099 ± 0.004	0.077 ± 0.009	0.044 ± 0.009	0.096 ± 0.008	0.124 ± 0.007	0.115 ± 0.004
23311	McDonald	52207.4662	0.072 ± 0.004	0.050 ± 0.008	...	0.011 ± 0.005	0.025 ± 0.004	0.012 ± 0.007
23693	FEROS	51834.2547	0.094 ± 0.008	0.083 ± 0.007	0.087 ± 0.008	0.088 ± 0.008	0.152 ± 0.009	0.127 ± 0.006
23786	FOCES	53747.9144	0.133 ± 0.037	...	0.084 ± 0.025	0.132 ± 0.017	0.150 ± 0.015	0.129 ± 0.021
24819	FOCES	53748.9549	0.411 ± 0.078	0.198 ± 0.044	0.031 ± 0.011	0.046 ± 0.009	0.047 ± 0.009	0.054 ± 0.007
24874	FOCES	54086.9907	0.775 ± 0.097	0.672 ± 0.209	0.125 ± 0.030	0.170 ± 0.020	0.213 ± 0.016	0.178 ± 0.016
25220	FOCES	53748.9746	1.123 ± 0.687	0.940 ± 0.340	0.136 ± 0.019	0.142 ± 0.018	0.179 ± 0.015	0.175 ± 0.017
25623	FOCES	54087.0273	...	0.433 ± 0.132	0.060 ± 0.032	0.035 ± 0.017	0.070 ± 0.020	0.078 ± 0.020
26779	McDonald	52030.0849	0.200 ± 0.004	0.149 ± 0.008	0.088 ± 0.021	0.134 ± 0.012	0.199 ± 0.012	0.144 ± 0.006
27913	McDonald	51882.3464	0.119 ± 0.012	0.093 ± 0.012	0.091 ± 0.014	0.110 ± 0.010	0.162 ± 0.007	0.151 ± 0.005
29067	FOCES	54088.0550	0.926 ± 0.445	0.789 ± 0.743	0.174 ± 0.018	0.101 ± 0.014	0.140 ± 0.012	0.137 ± 0.018
29525	FOCES	53747.9540	0.198 ± 0.032	0.158 ± 0.027	0.065 ± 0.015	0.009 ± 0.008	0.109 ± 0.009	0.091 ± 0.008
29568	SARG	54778.1689	0.120 ± 0.011	0.163 ± 0.080	0.204 ± 0.085	0.113 ± 0.088
29800	SARG	54193.8509	0.080 ± 0.005	0.157 ± 0.059	0.137 ± 0.023	...
32010	FOCES	54086.0581	0.622 ± 0.165	0.263 ± 0.092	0.023 ± 0.027	0.045 ± 0.020	0.072 ± 0.016	0.054 ± 0.038
32423	FOCES	54086.0836	0.073 ± 0.020	0.067 ± 0.022	0.067 ± 0.019
32919	FOCES	54086.0995	...	0.515 ± 0.357	...	0.011 ± 0.010	0.032 ± 0.012	0.014 ± 0.012
32984	FOCES	54088.0194	0.644 ± 0.120	0.399 ± 0.134	0.057 ± 0.024	0.112 ± 0.013	0.149 ± 0.012	0.159 ± 0.016
33373	FOCES	54086.1177	0.397 ± 0.071	0.437 ± 0.101	0.088 ± 0.028	0.081 ± 0.015	0.076 ± 0.015	0.063 ± 0.015
33560	SARG	54193.8607	0.278 ± 0.034	0.141 ± 0.087	0.161 ± 0.093	0.152 ± 0.115
33852	FOCES	54087.0680	0.250 ± 0.067	0.098 ± 0.083	0.032 ± 0.018	0.078 ± 0.009	0.108 ± 0.011	0.087 ± 0.012
36357	SARG	54107.0827	0.094 ± 0.010	0.169 ± 0.049	0.310 ± 0.070	0.273 ± 0.060
36357	FOCES	54164.9213	0.485 ± 0.239	0.333 ± 0.089	0.097 ± 0.023	0.146 ± 0.014	0.178 ± 0.016	0.147 ± 0.014
36551	FOCES	54086.1369	0.728 ± 0.207	0.362 ± 0.149	0.028 ± 0.038	0.041 ± 0.013	0.067 ± 0.023	0.058 ± 0.014
36827	SARG	54193.8830	0.191 ± 0.011	0.131 ± 0.045	0.155 ± 0.043	0.122 ± 0.033
37349	SARG	54193.8960	0.069 ± 0.024	0.166 ± 0.050	0.172 ± 0.046	0.171 ± 0.043
37349	McDonald	51883.3603	0.241 ± 0.005	0.197 ± 0.006	0.055 ± 0.011	0.105 ± 0.009	0.141 ± 0.017	0.012 ± 0.007
37349	FOCES	53748.0933	0.520 ± 0.106	0.338 ± 0.098	0.344 ± 0.008	0.163 ± 0.004	0.127 ± 0.011	0.122 ± 0.015
40170	FOCES	54158.0979	0.473 ± 2.664	0.180 ± 0.749	0.114 ± 0.022	0.063 ± 0.017	0.067 ± 0.016	0.037 ± 0.075

Table A.2. continue

HIP	Spectrograph	MJD (days)	EW (Å) in the subtrated spectrum					
			Ca II		$H\alpha$	Ca II IRT		
			K	H		$\lambda 8498$	$\lambda 8542$	$\lambda 8662$
40671	FOCES	54164.9814	0.317 ± 0.105	0.246 ± 0.132	0.018 ± 0.030	0.009 ± 0.016	0.035 ± 0.020	0.034 ± 0.018
42074	FOCES	54087.1283	0.331 ± 0.074	0.225 ± 0.066	0.082 ± 0.025	0.172 ± 0.022	0.245 ± 0.015	0.205 ± 0.026
42074	SARG	54193.9536	0.179 ± 0.022	0.089 ± 0.161	0.708 ± 0.074	0.160 ± 0.046
42333	FOCES	53749.0569	0.181 ± 0.021	0.118 ± 0.024	0.040 ± 0.011	0.082 ± 0.009	0.086 ± 0.008	0.096 ± 0.007
42438	McDonald	51883.5354	0.157 ± 0.003	0.129 ± 0.008	0.113 ± 0.017	0.153 ± 0.006	0.209 ± 0.006	0.194 ± 0.002
42808	FEROS	52046.9654	0.303 ± 0.009	0.216 ± 0.009	0.132 ± 0.012	0.248 ± 0.042	0.233 ± 0.011	0.226 ± 0.008
43557	FOCES	53749.0723	0.081 ± 0.015	0.067 ± 0.016	0.049 ± 0.008	0.041 ± 0.009	0.067 ± 0.007	0.045 ± 0.006
44897	SARG	54779.1457	0.099 ± 0.011	0.136 ± 0.049	0.119 ± 0.038	0.099 ± 0.067
45383	FOCES	53748.1605	0.556 ± 0.132	0.417 ± 0.064	0.245 ± 0.023	0.141 ± 0.013	0.181 ± 0.012	0.129 ± 0.013
45617	FOCES	53748.1832	0.294 ± 0.122	0.309 ± 0.038	...	0.073 ± 0.009	0.086 ± 0.011	0.068 ± 0.011
46580	FOCES	54087.1896	0.616 ± 0.302	0.407 ± 0.151	0.083 ± 0.022	0.142 ± 0.015	0.223 ± 0.018	0.222 ± 0.011
46580	SARG	54193.9665	0.036 ± 0.017	0.093 ± 0.064	0.110 ± 0.092	0.081 ± 0.054
46816	SARG	54193.9734	1.507 ± 0.017	0.728 ± 0.040	0.702 ± 0.061	0.845 ± 0.076
46816	FOCES	54161.0253	1.489 ± 0.136	1.530 ± 0.125	1.389 ± 0.015	0.528 ± 0.013	0.701 ± 0.009	0.594 ± 0.010
46843	SARG	54193.9834	0.264 ± 0.017	0.274 ± 0.054	0.412 ± 0.066	0.327 ± 0.105
46843	FOCES	54161.0562	0.464 ± 0.023	0.571 ± 0.036	0.288 ± 0.015	0.282 ± 0.007	0.436 ± 0.012	0.359 ± 0.012
47080	McDonald	52031.1226	0.098 ± 0.005	0.079 ± 0.010	0.010 ± 0.016	0.057 ± 0.011	0.094 ± 0.016	0.060 ± 0.007
47080	FOCES	53749.1406	0.281 ± 0.036	0.149 ± 0.023	0.060 ± 0.010	0.082 ± 0.008	0.168 ± 0.009	0.140 ± 0.009
49366	SARG	53786.1106	0.069 ± 0.020	0.128 ± 0.044	0.150 ± 0.073	0.157 ± 0.095
49908	SARG	54194.0217	0.016 ± 0.027	0.032 ± 0.084	0.026 ± 0.077	0.107 ± 0.081
51525	SARG	53786.1408	0.025 ± 0.035	0.099 ± 0.079	0.096 ± 0.066	0.112 ± 0.131
53486	SARG	53786.1585	0.059 ± 0.016	0.128 ± 0.083	0.124 ± 0.056	0.119 ± 0.100
54155	SARG	53786.1684	0.108 ± 0.021	0.254 ± 0.097	0.219 ± 0.077	0.243 ± 0.111
54155	FOCES	54158.1320	0.349 ± 0.039	0.305 ± 0.072	0.138 ± 0.022	0.210 ± 0.013	0.265 ± 0.016	0.272 ± 0.015
54426	FOCES	54087.2019	0.196 ± 0.108	0.097 ± 0.112	...	0.066 ± 0.019	0.068 ± 0.016	0.051 ± 0.017
54646	FOCES	54086.2260	0.421 ± 0.371	0.360 ± 0.298	0.057 ± 0.018	0.010 ± 0.011	0.030 ± 0.013	0.016 ± 0.013
54745	FOCES	54086.2729	0.132 ± 0.225	0.240 ± 0.452	0.069 ± 0.016	0.108 ± 0.013	0.141 ± 0.009	0.137 ± 0.018
54810	SARG	54106.1858	0.085 ± 0.024	0.170 ± 0.041	0.177 ± 0.064	0.124 ± 0.063
57494	FOCES	54156.0187	0.402 ± 0.335	0.163 ± 0.202	0.012 ± 0.032	0.022 ± 0.010	0.051 ± 0.013	0.038 ± 0.014
59000	SARG	54194.0305	0.334 ± 0.025	0.152 ± 0.043	0.192 ± 0.045	0.301 ± 0.064
59280	FOCES	54156.0998	0.143 ± 0.041	0.146 ± 0.019	0.046 ± 0.012	0.081 ± 0.011	0.175 ± 0.014	0.103 ± 0.012
60866	FOCES	54228.9530	0.010 ± 0.010	0.021 ± 0.015	0.013 ± 0.016	0.026 ± 0.012
62523	FOCES	53575.8536	0.199 ± 0.135	0.116 ± 0.086	0.086 ± 0.012	0.086 ± 0.016	0.168 ± 0.016	0.149 ± 0.012
64394	McDonald	52030.2579	0.031 ± 0.012	0.024 ± 0.013	0.059 ± 0.017	0.036 ± 0.007	0.023 ± 0.007	0.037 ± 0.005
64797	McDonald	52030.2286	0.201 ± 0.005	0.143 ± 0.005	0.081 ± 0.026	0.098 ± 0.007	0.140 ± 0.013	0.128 ± 0.004
65515	FOCES	54132.1649	0.349 ± 0.019	0.308 ± 0.020	0.122 ± 0.012	0.157 ± 0.010	0.263 ± 0.013	0.177 ± 0.011
66147	SARG	53786.1989	0.040 ± 0.030	0.050 ± 0.961	0.059 ± 0.081	0.061 ± 0.103
66252	FOCES	54168.0938	2.508 ± 0.549	2.031 ± 0.211	1.148 ± 0.014	0.441 ± 0.015	0.658 ± 0.017	0.478 ± 0.013
67105	SARG	53786.2384	0.116 ± 0.041	0.071 ± 0.071	0.106 ± 0.084	0.109 ± 0.101
67275	SARG	54108.3087	0.026 ± 0.009
67422	McDonald	52030.2748	0.331 ± 0.007	0.221 ± 0.004	0.068 ± 0.007	0.110 ± 0.010	0.157 ± 0.013	0.127 ± 0.004
68337	FOCES	53577.8595	0.040 ± 0.017	0.092 ± 0.032	0.104 ± 0.021	0.161 ± 0.016
69357	FOCES	53578.0216	0.373 ± 0.199	0.303 ± 0.064	0.057 ± 0.022	0.174 ± 0.022	0.151 ± 0.017	...
69526	FOCES	53578.9125	0.715 ± 0.206	0.483 ± 0.126	0.059 ± 0.023	0.115 ± 0.017	0.143 ± 0.015	0.134 ± 0.019
69962	SARG	54108.2822	0.032 ± 0.020	0.043 ± 0.068	0.060 ± 0.075	0.067 ± 0.073
70218	SARG	53786.2988	0.149 ± 0.035	0.198 ± 0.138	0.194 ± 0.062	0.219 ± 0.109
70218	FOCES	54159.1693	0.704 ± 0.596	0.463 ± 0.478	0.117 ± 0.021	0.159 ± 0.015	0.215 ± 0.009	0.216 ± 0.013
71395	SARG	54194.1338	0.077 ± 0.025	0.176 ± 0.042	0.197 ± 0.053	0.191 ± 0.056
71395	FOCES	53577.8799	0.431 ± 0.186	0.274 ± 0.074	0.057 ± 0.036	0.180 ± 0.015	0.264 ± 0.013	0.222 ± 0.011
71743	SARG	54193.0776	0.081 ± 0.032	0.066 ± 0.051	0.082 ± 0.027	0.072 ± 0.070
72146	FOCES	53575.8597	0.088 ± 0.084	0.097 ± 0.055	0.046 ± 0.023	0.039 ± 0.016	0.062 ± 0.019	0.046 ± 0.037
72146	SARG	54194.1582	0.035 ± 0.017	0.066 ± 0.070	0.079 ± 0.052	0.108 ± 0.065
72237	FOCES	54159.2162	0.719 ± 0.635	0.864 ± 0.130	0.131 ± 0.017	0.073 ± 0.011	0.114 ± 0.011	0.082 ± 0.010
72237	SARG	53786.2752	0.080 ± 0.023	0.093 ± 0.067	0.095 ± 0.073	0.110 ± 0.114
72567	FOCES	54168.1225	0.147 ± 0.035	0.150 ± 0.029	0.080 ± 0.011	0.080 ± 0.008	0.160 ± 0.008	0.113 ± 0.010
72659	McDonald	52030.3731	0.050 ± 0.004	0.033 ± 0.007	0.058 ± 0.006	0.052 ± 0.010	0.071 ± 0.006	0.058 ± 0.005
72848	McDonald	52164.0668	0.212 ± 0.005	0.162 ± 0.009	0.087 ± 0.020	0.148 ± 0.010	0.175 ± 0.007	0.170 ± 0.004
72875	FOCES	53577.8968	0.355 ± 0.215	0.252 ± 0.078	0.122 ± 0.023	0.229 ± 0.015	0.241 ± 0.013	0.244 ± 0.018
73184	SARG	54194.1436	0.052 ± 0.019	0.049 ± 0.087	0.040 ± 0.045	0.063 ± 0.062
74702	SARG	54108.2523	0.131 ± 0.027	0.110 ± 0.040	0.135 ± 0.066	0.139 ± 0.096
75201	SARG	54193.0544	0.077 ± 0.021	0.058 ± 0.065	0.114 ± 0.045	0.255 ± 0.090
75253	FOCES	54161.1805	...	0.261 ± 0.055	0.026 ± 0.018	0.047 ± 0.012	0.047 ± 0.014	0.046 ± 0.012
75542	SARG	54195.1035	0.023 ± 0.034	0.031 ± 0.086	0.066 ± 0.058	0.068 ± 0.087
75809	FOCES	54160.1481	...	0.369 ± 0.082	0.115 ± 0.019	0.221 ± 0.017	0.304 ± 0.014	0.248 ± 0.011
76779	SARG	54195.1198	0.035 ± 0.025	0.045 ± 0.032	0.084 ± 0.044	0.105 ± 0.079
77408	SARG	54193.1507	0.084 ± 0.024	0.121 ± 0.060	0.124 ± 0.064	0.116 ± 0.065
77408	FOCES	53575.9293	0.393 ± 0.058	0.288 ± 0.043	0.084 ± 0.023	0.145 ± 0.015	0.214 ± 0.015	0.207 ± 0.013
80337	FEROS	52045.1772	0.031 ± 0.047	0.045 ± 0.038	0.033 ± 0.014	0.025 ± 0.021
80366	SARG	54193.2128	0.056 ± 0.012	0.047 ± 0.062	0.064 ± 0.077	0.075 ± 0.072
80686	FEROS	52045.2054	0.076 ± 0.005	0.055 ± 0.004	0.089 ± 0.006	0.061 ± 0.019	0.047 ± 0.010	0.054 ± 0.006
80725	FOCES	53579.9305	0.211 ± 0.105	...	0.077 ± 0.020	0.049 ± 0.026	0.052 ± 0.021	0.036 ± 0.019
81300	McDonald	52164.1210	0.128 ± 0.004	0.102 ± 0.008	0.047 ± 0.009	0.076 ± 0.013	0.090 ± 0.010	0.065 ± 0.005

Table A.2. continue

HIP	Spectrograph	MJD (days)	EW (Å) in the subtrated spectrum					
			Ca II		$H\alpha$	Ca II IRT		
			K	H		$\lambda 8498$	$\lambda 8542$	$\lambda 8662$
82588	FOCES	53576.9600	0.207 ± 0.057	0.183 ± 0.046	0.086 ± 0.015	0.146 ± 0.016	0.152 ± 0.014	0.158 ± 0.019
83601	SARG	54195.2462	0.093 ± 0.017	0.155 ± 0.080	0.152 ± 0.077	0.153 ± 0.070
84405	McDonald	52208.0394	0.019 ± 0.009	0.077 ± 0.012	0.085 ± 0.013	0.096 ± 0.005
85295	SARG	54193.2589	0.043 ± 0.025	0.032 ± 0.074	0.057 ± 0.054	0.110 ± 0.085
85561	SARG	54194.2041	0.124 ± 0.018	0.122 ± 0.054	0.110 ± 0.062	0.101 ± 0.055
85810	SARG	54193.2741	0.099 ± 0.023	0.054 ± 0.076	0.062 ± 0.100	0.072 ± 0.108
86036	McDonald	52030.4566	0.063 ± 0.011	0.051 ± 0.005	0.049 ± 0.006	0.065 ± 0.013	0.081 ± 0.007	0.068 ± 0.005
86400	McDonald	52032.3071	0.072 ± 0.006	0.049 ± 0.006	0.033 ± 0.011	0.016 ± 0.004
87579	FOCES	53574.8992	0.328 ± 0.108	0.287 ± 0.065	0.076 ± 0.021	0.142 ± 0.015	0.170 ± 0.019	0.141 ± 0.012
88601	McDonald	52164.1787	0.103 ± 0.005	0.073 ± 0.006	0.049 ± 0.018	0.065 ± 0.014	0.085 ± 0.007	0.086 ± 0.005
90790	McDonald	52208.0867	0.093 ± 0.008	0.071 ± 0.007	0.045 ± 0.012	0.051 ± 0.009	0.064 ± 0.008	0.051 ± 0.004
91009	SARG	54779.8159	1.470 ± 0.034	0.526 ± 0.069	0.780 ± 0.035	0.783 ± 0.052
92200	FOCES	53574.9577	0.458 ± 0.152	0.409 ± 0.100	0.023 ± 0.014	0.060 ± 0.002	0.090 ± 0.021	0.063 ± 0.009
92283	FOCES	53578.9782	0.045 ± 0.014	0.083 ± 0.012	0.127 ± 0.015	0.094 ± 0.006
96085	FOCES	53578.0463	0.075 ± 0.020	0.140 ± 0.018	0.194 ± 0.014	0.148 ± 0.008
96285	FOCES	53575.0438	0.184 ± 0.127	0.302 ± 0.109	0.021 ± 0.017	0.051 ± 0.013	0.055 ± 0.011	0.061 ± 0.012
98828	FOCES	53575.0823	0.094 ± 0.070	0.112 ± 0.058	0.027 ± 0.031
99461	FEROS	51833.9874	0.028 ± 0.008	0.025 ± 0.016	0.016 ± 0.012	0.018 ± 0.031	0.002 ± 0.012	0.005 ± 0.005
99711	FOCES	53575.9912	0.218 ± 0.085	0.179 ± 0.056	0.030 ± 0.034	0.988 ± 0.017	0.145 ± 0.015	0.086 ± 0.011
99764	FOCES	53576.0317	...	0.145 ± 0.182	0.044 ± 0.029
103256	FOCES	53576.0317	0.265 ± 0.103	0.393 ± 0.098	0.039 ± 0.020	0.043 ± 0.020	0.072 ± 0.015	0.060 ± 0.013
104092	FOCES	53576.0519	...	0.262 ± 0.309	0.007 ± 0.015	0.013 ± 0.021	0.030 ± 0.016	0.023 ± 0.012
104239	FOCES	53579.0004	0.128 ± 0.100	0.111 ± 0.119	0.035 ± 0.025	0.062 ± 0.015	0.090 ± 0.013	0.073 ± 0.012
105038	FOCES	53576.0819	...	0.077 ± 0.060	0.041 ± 0.025	0.060 ± 0.017	0.063 ± 0.015	0.060 ± 0.014
106400	SARG	54778.8327	0.484 ± 0.019	0.335 ± 0.072	0.468 ± 0.055	0.519 ± 0.074
107350	SARG	54777.8715	0.098 ± 0.018	0.189 ± 0.052	0.151 ± 0.077	0.176 ± 0.046
108028	FOCES	53576.1120	0.322 ± 0.058	0.317 ± 0.070	0.106 ± 0.015	0.138 ± 0.019	0.211 ± 0.014	0.180 ± 0.012
108156	FOCES	53575.1412	0.194 ± 0.078	0.128 ± 0.060	0.040 ± 0.015	0.060 ± 0.020	0.036 ± 0.017	0.049 ± 0.011
109527	FOCES	53578.0943	0.228 ± 0.045	0.205 ± 0.024	0.048 ± 0.014	0.132 ± 0.010	0.141 ± 0.013	0.142 ± 0.009
110778	SARG	54777.9046	0.113 ± 0.011	0.098 ± 0.081	0.136 ± 0.077	0.135 ± 0.070
111888	FOCES	53576.1296	0.207 ± 0.112	0.170 ± 0.054	0.098 ± 0.019	0.066 ± 0.021	0.116 ± 0.015	0.090 ± 0.013
113576	SARG	54777.9334	0.058 ± 0.020	0.068 ± 0.049	0.108 ± 0.060	0.153 ± 0.075
114886	FOCES	53575.1545	0.069 ± 0.041	0.041 ± 0.023	0.030 ± 0.016	0.003 ± 0.018	0.010 ± 0.014	0.014 ± 0.012
115162	FOCES	53576.9955	0.329 ± 0.085	0.214 ± 0.038	0.148 ± 0.021	0.185 ± 0.014	0.195 ± 0.013	0.214 ± 0.014
115331	FOCES	53578.1064	0.468 ± 0.038	0.298 ± 0.036	0.105 ± 0.008	0.206 ± 0.013	0.276 ± 0.016	0.260 ± 0.010
115341	FOCES	53575.1704	0.215 ± 0.071	0.201 ± 0.037	0.059 ± 0.028	0.102 ± 0.027	0.119 ± 0.021	0.068 ± 0.015
115445	FOCES	53580.1105	0.040 ± 0.014	0.049 ± 0.026	0.039 ± 0.022	0.048 ± 0.012
116613	FOCES	53578.1185	0.101 ± 0.094	0.081 ± 0.048	0.048 ± 0.016	0.066 ± 0.013	0.118 ± 0.010	0.089 ± 0.007
120005	SARG	54779.1742	0.133 ± 0.027	0.138 ± 0.039	0.174 ± 0.048	0.284 ± 0.077

Table A.3. Excess flux in different chromospheric activity indicator lines for the active stars in the sample.

HIP	Spectrograph	MJD (days)	$\log F_S$ (erg cm ⁻² s ⁻¹) in the subtrated spectrum						$\log R'_{HK}$
			Ca II		$H\alpha$	Ca II IRT			
			K	H		$\lambda 8498$	$\lambda 8542$	$\lambda 8662$	
544	SARG	54780.9561	5.47 ± 0.12	5.95 ± 0.12	5.91 ± 0.21	5.93 ± 0.16	-4.61
544	McDonald	52031.3248	5.78 ± 0.03	5.68 ± 0.04	5.79 ± 0.14	5.69 ± 0.08	5.75 ± 0.06	5.79 ± 0.02	-4.67
1803	SARG	54777.9856	5.94 ± 0.04	5.87 ± 0.20	5.98 ± 0.13	...	-4.36
3093	FOCES	53577.1854	5.32 ± 0.03
3765	FOCES	53747.7686	5.00 ± 0.37	5.96 ± 0.03	4.13 ± 1.38	-5.41
3765	McDonald	52164.3977	4.95 ± 0.08	4.81 ± 0.12	4.55 ± 1.18	4.76 ± 0.22	4.99 ± 0.04	4.83 ± 0.12	-5.41
4148	FEROS	51834.1339	5.50 ± 0.03	5.37 ± 0.04	5.37 ± 0.10	5.44 ± 0.06	5.61 ± 0.04	5.40 ± 0.03	-4.83
4845	SARG	54778.9878	5.12 ± 0.10	4.97 ± 0.17	5.14 ± 0.60	5.07 ± 0.60	-4.54
5286	FOCES	53576.1601	...	5.17 ± 0.52	5.11 ± 0.16	5.22 ± 0.09	5.36 ± 0.06	5.39 ± 0.07	-4.59
5944	FOCES	53576.1764	6.13 ± 0.05	6.04 ± 0.06	5.79 ± 0.08	5.54 ± 0.43	5.57 ± 0.04	5.49 ± 0.09	-4.47
6290	SARG	54107.9171	5.10 ± 0.06	4.94 ± 0.45	4.94 ± 0.76	4.89 ± 0.34	-4.40
7235	SARG	54780.9662	5.30 ± 0.25	-4.72
7576	FOCES	53577.1583	6.03 ± 0.06	6.11 ± 0.06	5.75 ± 0.06	5.73 ± 0.05	5.83 ± 0.03	5.81 ± 0.04	-4.29
7751	FEROS	51834.1456	5.10 ± 0.15	4.89 ± 0.34	4.82 ± 0.27	-4.94
7981	FOCES	53578.1869	5.18 ± 0.49	5.11 ± 0.39	-5.19
8275	FOCES	54086.7647	5.65 ± 0.57	5.73 ± 0.39	5.52 ± 0.28	5.48 ± 0.07	5.63 ± 0.05	5.60 ± 0.05	-4.51
8362	McDonald	51883.2217	5.40 ± 0.05	5.22 ± 0.06	4.99 ± 0.17	5.10 ± 0.05	5.26 ± 0.04	4.86 ± 0.07	-5.05
8486	FOCES	53748.8161	6.27 ± 0.23	6.34 ± 0.14	5.89 ± 0.08	5.60 ± 0.10	5.90 ± 0.05	5.69 ± 0.08	-4.19
8768	SARG	54778.0142	4.88 ± 0.16	4.67 ± 1.12	5.09 ± 0.26	5.04 ± 0.60	-4.59
10138	FEROS	51834.1664	5.30 ± 0.14	5.02 ± 0.35	5.29 ± 0.10	-4.68
10337	SARG	54780.0100	4.76 ± 0.27	4.96 ± 0.14	5.30 ± 0.19	5.42 ± 0.16	-4.68
10416	FOCES	54086.7855	5.81 ± 0.10	5.91 ± 0.10	5.52 ± 0.08	5.61 ± 0.04	5.80 ± 0.02	5.61 ± 0.05	-4.30
11565	SARG	54780.2041	5.07 ± 0.15	5.06 ± 0.61	5.28 ± 0.20	5.27 ± 0.35	-4.58
12110	SARG	54780.0623	5.44 ± 0.07	5.48 ± 0.23	5.69 ± 0.14	5.61 ± 0.15	-4.40
13258	FOCES	54086.8172	4.79 ± 0.24	5.13 ± 0.08	5.24 ± 0.08	4.98 ± 0.13	-4.76
13402	McDonald	52207.4006	6.05 ± 0.01	5.94 ± 0.01	5.69 ± 0.04	5.81 ± 0.01	5.95 ± 0.01	5.90 ± 0.01	-4.30
13402	SARG	54779.0488	5.70 ± 0.07	5.87 ± 0.14	5.95 ± 0.05	5.95 ± 0.17	-4.36
13976	SARG	54778.0715	5.58 ± 0.06	5.52 ± 0.19	5.54 ± 0.08	5.49 ± 0.13	-4.40
15330	FEROS	51834.2315	5.71 ± 0.05	5.56 ± 0.04	5.23 ± 0.09	5.27 ± 0.07	5.41 ± 0.05	5.27 ± 0.04	-4.86
15442	SARG	54780.1170	5.40 ± 0.26	5.64 ± 0.47	5.69 ± 0.34	5.67 ± 0.41	-4.75
15673	FOCES	54086.8639	5.26 ± 3.33	5.86 ± 0.27	5.49 ± 0.09	5.39 ± 0.13	5.44 ± 0.09	5.38 ± 0.13	-4.54
15919	FOCES	53747.8508	5.58 ± 0.14	5.43 ± 0.16	...	5.03 ± 0.26	5.14 ± 0.17	5.08 ± 0.26	-4.60
16134	SARG	54779.0552	4.88 ± 0.17	5.12 ± 0.14	5.26 ± 0.19	5.37 ± 0.16	-4.61
16537	McDonald	51833.9938	5.73 ± 0.01	5.60 ± 0.03	5.52 ± 0.08	5.45 ± 0.03	5.66 ± 0.02	5.54 ± 0.02	-4.62
17420	McDonald	52207.4446	5.30 ± 0.04	5.15 ± 0.08	4.98 ± 0.21	4.71 ± 0.09	5.00 ± 0.23	4.95 ± 0.09	-5.04
18774	SARG	54779.1053	5.15 ± 0.14	5.34 ± 0.31	5.60 ± 0.20	5.66 ± 0.16	-4.56
18859	SARG	54780.1408	5.81 ± 0.06	6.07 ± 0.06	6.18 ± 0.05	6.10 ± 0.10	-4.60
19076	SARG	54780.1482	6.07 ± 0.06	5.77 ± 0.40	5.80 ± 0.27	5.72 ± 0.51	-4.30
19335	SARG	54780.1552	5.61 ± 0.05	6.07 ± 0.10	6.15 ± 0.06	6.04 ± 0.07	-4.73
19832	FOCES	54087.9871	4.98 ± 0.11	4.96 ± 0.12	5.17 ± 0.08	4.85 ± 1.29	-4.66
19849	McDonald	51880.2760	5.00 ± 0.07	4.92 ± 0.11	4.28 ± 2.46	4.52 ± 0.41	4.55 ± 0.41	4.71 ± 0.15	-5.38
20917	FOCES	54086.9422	5.32 ± 0.25	5.40 ± 0.23	5.23 ± 0.06	5.21 ± 0.06	5.21 ± 0.05	5.16 ± 0.60	-4.62
22263	McDonald	52207.4280	5.94 ± 0.02	5.83 ± 0.05	5.49 ± 0.08	5.63 ± 0.04	5.74 ± 0.02	5.71 ± 0.01	-4.61
23311	McDonald	52207.4662	4.95 ± 0.03	4.79 ± 0.07	...	4.40 ± 0.21	4.75 ± 0.07	4.43 ± 0.26	-5.29
23693	FEROS	51834.2547	6.16 ± 0.04	6.10 ± 0.04	5.92 ± 0.04	5.67 ± 0.04	5.91 ± 0.02	5.83 ± 0.02	-4.49
23786	FOCES	53747.9144	5.74 ± 0.12	...	5.59 ± 0.13	5.65 ± 0.06	5.71 ± 0.04	5.64 ± 0.07	-4.49
24819	FOCES	53748.9549	5.80 ± 0.08	5.48 ± 0.10	4.92 ± 0.16	5.05 ± 0.08	5.06 ± 0.08	5.11 ± 0.06	-4.53
24874	FOCES	54086.9907	6.09 ± 0.05	6.02 ± 0.14	5.53 ± 0.10	5.62 ± 0.05	5.72 ± 0.03	5.64 ± 0.04	-4.14
25220	FOCES	53748.9746	6.04 ± 0.27	5.96 ± 0.16	5.46 ± 0.06	5.47 ± 0.05	5.57 ± 0.04	5.56 ± 0.04	-4.13
25623	FOCES	54087.0273	...	5.50 ± 0.13	5.04 ± 0.23	4.82 ± 0.21	5.12 ± 0.12	5.17 ± 0.11	-4.60
26779	McDonald	52030.0849	5.84 ± 0.01	5.71 ± 0.02	5.57 ± 0.10	5.63 ± 0.04	5.80 ± 0.03	5.66 ± 0.02	-4.55
27913	McDonald	51882.3464	6.10 ± 0.04	5.99 ± 0.05	5.85 ± 0.07	5.72 ± 0.04	5.88 ± 0.02	5.85 ± 0.01	-4.49
29067	FOCES	54088.0550	5.68 ± 0.21	5.61 ± 0.41	5.41 ± 0.04	5.22 ± 0.06	5.37 ± 0.04	5.36 ± 0.06	-4.40
29525	FOCES	53747.9540	6.19 ± 0.07	6.09 ± 0.07	5.63 ± 0.10	4.59 ± 0.37	5.67 ± 0.03	5.58 ± 0.04	-4.33
29568	SARG	54778.1689	5.85 ± 0.04	5.81 ± 0.21	5.91 ± 0.18	5.66 ± 0.34	-4.39
29800	SARG	54193.8509	5.65 ± 0.03	5.78 ± 0.16	5.72 ± 0.07	...	-4.51
32010	FOCES	54086.0581	5.96 ± 0.12	5.59 ± 0.15	4.78 ± 0.51	5.04 ± 0.19	5.23 ± 0.10	5.11 ± 0.31	-4.38
32423	FOCES	54086.0836	5.27 ± 0.12	5.23 ± 0.14	5.23 ± 0.12	-4.64
32919	FOCES	54086.0995	...	5.53 ± 0.30	...	4.31 ± 0.38	4.76 ± 0.16	4.40 ± 0.37	-5.06
32984	FOCES	54088.0194	5.90 ± 0.08	5.69 ± 0.15	5.13 ± 0.18	5.40 ± 0.05	5.52 ± 0.04	5.55 ± 0.04	-4.36
33373	FOCES	54086.1177	5.60 ± 0.08	5.64 ± 0.10	5.28 ± 0.14	5.23 ± 0.08	5.20 ± 0.09	5.12 ± 0.10	-4.51
33560	SARG	54193.8607	5.77 ± 0.05	5.47 ± 0.27	5.53 ± 0.25	5.50 ± 0.33	-4.14
33852	FOCES	54087.0680	5.63 ± 0.12	5.22 ± 0.37	4.96 ± 0.24	5.29 ± 0.05	5.43 ± 0.05	5.34 ± 0.06	-4.74
36357	SARG	54107.0827	5.48 ± 0.05	5.66 ± 0.12	5.93 ± 0.10	5.87 ± 0.10	-4.45
36357	FOCES	54164.9213	6.02 ± 0.21	5.86 ± 0.12	5.50 ± 0.10	5.60 ± 0.04	5.69 ± 0.04	5.60 ± 0.04	-4.30
36551	FOCES	54086.1369	5.81 ± 0.12	5.50 ± 0.18	4.75 ± 0.60	4.91 ± 0.13	5.13 ± 0.15	5.07 ± 0.11	-4.44
36827	SARG	54193.8830	5.87 ± 0.02	5.60 ± 0.15	5.68 ± 0.12	5.57 ± 0.12	-4.24
37349	SARG	54193.8960	5.35 ± 0.15	5.66 ± 0.13	5.67 ± 0.12	5.67 ± 0.11	-4.54
37349	McDonald	51883.3603	5.72 ± 0.01	5.63 ± 0.01	5.25 ± 0.09	5.46 ± 0.04	5.58 ± 0.05	4.53 ± 0.26	-4.57
37349	FOCES	53748.0933	6.05 ± 0.09	5.87 ± 0.13	6.05 ± 0.01	5.65 ± 0.01	5.54 ± 0.04	5.52 ± 0.05	-4.28
40170	FOCES	54158.0979	4.91 ± 2.45	4.49 ± 1.81	4.97 ± 0.09	4.85 ± 0.12	4.88 ± 0.10	4.63 ± 0.87	-5.15

Table A.3. continue

HIP	Spectrograph	MJD (days)	$\log F_S$ (erg cm ⁻² s ⁻¹) in the subtrated spectrum						$\log R'_{HK}$
			Ca II			Ca II IRT			
			K	H	H α	$\lambda 8498$	$\lambda 8542$	$\lambda 8662$	
40671	FOCES	54164.9814	5.57 ± 0.14	5.46 ± 0.23	4.62 ± 0.73	4.31 ± 0.76	4.89 ± 0.25	4.88 ± 0.23	-4.64
42074	FOCES	54087.1283	6.16 ± 0.10	5.99 ± 0.13	5.60 ± 0.13	5.78 ± 0.05	5.93 ± 0.03	5.85 ± 0.06	-4.28
42074	SARG	54193.9536	5.93 ± 0.05	5.49 ± 0.79	6.39 ± 0.05	5.74 ± 0.13	-4.26
42333	FOCES	53749.0569	6.17 ± 0.05	5.99 ± 0.09	5.43 ± 0.12	5.55 ± 0.05	5.57 ± 0.04	5.62 ± 0.03	-4.40
42438	McDonald	51883.5354	6.19 ± 0.01	6.10 ± 0.03	5.92 ± 0.07	5.84 ± 0.02	5.98 ± 0.01	5.95 ± 0.01	-4.38
42808	FEROS	52046.9654	5.86 ± 0.01	5.71 ± 0.02	5.65 ± 0.04	5.84 ± 0.07	5.82 ± 0.02	5.80 ± 0.02	-4.48
43557	FOCES	53749.0723	5.88 ± 0.08	5.80 ± 0.10	5.54 ± 0.07	5.27 ± 0.10	5.48 ± 0.04	5.30 ± 0.06	-4.67
44897	SARG	54779.1457	5.88 ± 0.05	5.80 ± 0.16	5.74 ± 0.14	5.67 ± 0.29	-4.47
45383	FOCES	53748.1605	5.95 ± 0.10	5.83 ± 0.07	5.83 ± 0.04	5.54 ± 0.04	5.65 ± 0.03	5.50 ± 0.04	-4.31
45617	FOCES	53748.1832	5.69 ± 0.18	5.71 ± 0.05	...	5.26 ± 0.06	5.33 ± 0.05	5.23 ± 0.07	-4.51
46580	FOCES	54087.1896	6.03 ± 0.21	5.85 ± 0.16	5.38 ± 0.11	5.55 ± 0.05	5.75 ± 0.03	5.75 ± 0.02	-4.27
46580	SARG	54193.9665	5.02 ± 0.21	5.37 ± 0.30	5.44 ± 0.36	5.31 ± 0.29	-4.73
46816	SARG	54193.9734	6.73 ± 0.01	6.32 ± 0.02	6.31 ± 0.04	6.39 ± 0.04	-3.63
46816	FOCES	54161.0253	6.58 ± 0.04	6.59 ± 0.04	6.69 ± 0.01	6.18 ± 0.01	6.30 ± 0.01	6.23 ± 0.01	-3.69
46843	SARG	54193.9834	6.11 ± 0.03	5.98 ± 0.09	6.16 ± 0.07	6.06 ± 0.14	-4.15
46843	FOCES	54161.0562	6.33 ± 0.02	6.42 ± 0.03	6.15 ± 0.02	6.00 ± 0.01	6.19 ± 0.01	6.10 ± 0.01	-4.00
47080	McDonald	52031.1226	5.66 ± 0.02	5.57 ± 0.05	4.70 ± 0.69	5.30 ± 0.09	5.52 ± 0.08	5.33 ± 0.05	-4.76
47080	FOCES	53749.1406	6.12 ± 0.05	5.84 ± 0.07	5.47 ± 0.07	5.46 ± 0.04	5.77 ± 0.02	5.70 ± 0.03	-4.38
49366	SARG	53786.1106	5.39 ± 0.12	5.56 ± 0.15	5.63 ± 0.21	5.65 ± 0.26	-4.54
49908	SARG	54194.0217	4.32 ± 0.71	4.68 ± 1.14	4.60 ± 1.28	5.21 ± 0.33	-5.00
51525	SARG	53786.1408	4.48 ± 0.61	5.16 ± 0.35	5.15 ± 0.30	5.22 ± 0.51	-4.88
53486	SARG	53786.1585	5.30 ± 0.12	5.56 ± 0.28	5.54 ± 0.19	5.52 ± 0.36	-4.59
54155	SARG	53786.1684	5.66 ± 0.08	5.91 ± 0.17	5.85 ± 0.15	5.90 ± 0.20	-4.41
54155	FOCES	54158.1320	6.10 ± 0.05	6.04 ± 0.10	5.77 ± 0.07	5.83 ± 0.03	5.93 ± 0.03	5.94 ± 0.02	-4.26
54426	FOCES	54087.2019	5.59 ± 0.24	5.29 ± 0.50	...	5.24 ± 0.12	5.25 ± 0.10	5.13 ± 0.14	-4.77
54646	FOCES	54086.2260	5.16 ± 0.38	5.10 ± 0.36	4.84 ± 0.14	4.18 ± 0.45	4.64 ± 0.20	4.36 ± 0.37	-4.86
54745	FOCES	54086.2729	6.10 ± 0.74	6.36 ± 0.82	5.70 ± 0.10	5.69 ± 0.05	5.81 ± 0.03	5.79 ± 0.06	-4.27
54810	SARG	54106.1858	5.13 ± 0.12	5.47 ± 0.11	5.49 ± 0.16	5.34 ± 0.22	-4.50
57494	FOCES	54156.0187	5.44 ± 0.36	5.05 ± 0.54	4.33 ± 1.11	4.60 ± 0.19	4.97 ± 0.12	4.84 ± 0.17	-4.80
59000	SARG	54194.0305	5.54 ± 0.03	5.30 ± 0.12	5.41 ± 0.10	5.60 ± 0.09	-4.12
59280	FOCES	54156.0998	5.81 ± 0.12	5.82 ± 0.06	5.35 ± 0.11	5.45 ± 0.06	5.79 ± 0.03	5.56 ± 0.05	-4.56
60866	FOCES	54228.9530	4.26 ± 0.45	4.62 ± 0.30	4.41 ± 0.53	4.71 ± 0.20	-5.14
62523	FOCES	53575.8536	6.11 ± 0.29	5.88 ± 0.32	5.71 ± 0.06	5.53 ± 0.08	5.83 ± 0.04	5.77 ± 0.04	-4.43
64394	McDonald	52030.2579	5.54 ± 0.17	5.43 ± 0.24	5.67 ± 0.13	5.24 ± 0.08	5.05 ± 0.12	5.25 ± 0.05	-5.06
64797	McDonald	52030.2286	5.71 ± 0.01	5.56 ± 0.02	5.46 ± 0.14	5.45 ± 0.03	5.61 ± 0.04	5.57 ± 0.01	-4.63
65515	FOCES	54132.1649	6.16 ± 0.02	6.10 ± 0.03	5.75 ± 0.04	5.73 ± 0.03	5.95 ± 0.02	5.78 ± 0.03	-4.22
66147	SARG	53786.1989	5.03 ± 0.32	5.08 ± 8.35	5.15 ± 0.60	5.16 ± 0.74	-4.70
66252	FOCES	54168.0938	6.23 ± 0.10	6.14 ± 0.05	6.30 ± 0.01	5.91 ± 0.01	6.08 ± 0.01	5.94 ± 0.01	-3.89
67105	SARG	53786.2384	5.47 ± 0.15	5.22 ± 0.44	5.39 ± 0.35	5.41 ± 0.40	-4.39
67275	SARG	54108.3087	5.41 ± 0.14	-4.90
67422	McDonald	52030.2748	5.54 ± 0.01	5.36 ± 0.01	5.17 ± 0.05	5.37 ± 0.04	5.52 ± 0.04	5.43 ± 0.02	-4.68
68337	FOCES	53577.8595	4.89 ± 0.18	5.26 ± 0.15	5.31 ± 0.09	5.50 ± 0.04	-4.72
69357	FOCES	53578.0216	6.07 ± 0.23	5.98 ± 0.09	5.36 ± 0.17	5.73 ± 0.05	5.67 ± 0.05	...	-4.60
69526	FOCES	53578.9125	5.98 ± 0.13	5.80 ± 0.11	5.17 ± 0.17	5.42 ± 0.06	5.52 ± 0.05	5.49 ± 0.06	-4.28
69962	SARG	54108.2822	4.61 ± 0.27	4.81 ± 0.69	4.96 ± 0.54	5.01 ± 0.47	-4.80
70218	SARG	53786.2988	5.37 ± 0.10	5.53 ± 0.30	5.52 ± 0.14	5.58 ± 0.22	-4.34
70218	FOCES	54159.1693	5.60 ± 0.37	5.42 ± 0.45	5.26 ± 0.08	5.43 ± 0.04	5.57 ± 0.02	5.57 ± 0.03	-4.54
71395	SARG	54194.1338	5.38 ± 0.14	5.67 ± 0.10	5.72 ± 0.12	5.70 ± 0.13	-4.51
71395	FOCES	53577.8799	5.93 ± 0.19	5.73 ± 0.12	5.25 ± 0.27	5.68 ± 0.04	5.84 ± 0.02	5.77 ± 0.02	-4.39
71743	SARG	54193.0776	5.68 ± 0.17	5.42 ± 0.34	5.51 ± 0.14	5.45 ± 0.42	-4.51
72146	FOCES	53575.8597	5.31 ± 0.41	5.35 ± 0.25	5.19 ± 0.22	5.04 ± 0.18	5.24 ± 0.14	5.11 ± 0.35	-4.93
72146	SARG	54194.1582	5.07 ± 0.22	5.27 ± 0.46	5.34 ± 0.28	5.48 ± 0.26	-4.74
72237	FOCES	54159.2162	5.37 ± 0.38	5.45 ± 0.07	5.18 ± 0.06	5.02 ± 0.06	5.21 ± 0.04	5.07 ± 0.06	-4.57
72237	SARG	53786.2752	4.97 ± 0.13	5.12 ± 0.31	5.13 ± 0.33	5.19 ± 0.45	-4.54
72567	FOCES	54168.1225	6.21 ± 0.10	6.21 ± 0.08	5.80 ± 0.06	5.58 ± 0.04	5.88 ± 0.02	5.73 ± 0.04	-4.34
72659	McDonald	52030.3731	5.40 ± 0.04	5.21 ± 0.09	5.47 ± 0.04	5.27 ± 0.08	5.41 ± 0.04	5.32 ± 0.04	-5.07
72848	McDonald	52164.0668	5.86 ± 0.01	5.74 ± 0.02	5.56 ± 0.10	5.68 ± 0.03	5.75 ± 0.02	5.74 ± 0.01	-4.52
72875	FOCES	53577.8968	5.86 ± 0.26	5.71 ± 0.14	5.58 ± 0.08	5.78 ± 0.03	5.81 ± 0.02	5.81 ± 0.03	-4.45
73184	SARG	54194.1436	5.07 ± 0.16	5.03 ± 0.77	4.93 ± 0.49	5.13 ± 0.43	-4.63
74702	SARG	54108.2523	5.76 ± 0.09	5.56 ± 0.16	5.65 ± 0.21	5.66 ± 0.30	-4.35
75201	SARG	54193.0544	5.01 ± 0.12	4.96 ± 0.49	5.25 ± 0.17	5.60 ± 0.15	-4.54
75253	FOCES	54161.1805	...	5.70 ± 0.09	4.90 ± 0.31	5.09 ± 0.11	5.09 ± 0.12	5.08 ± 0.11	-4.83
75542	SARG	54195.1035	4.68 ± 0.65	4.81 ± 1.19	5.14 ± 0.38	5.15 ± 0.55	-4.88
75809	FOCES	54160.1481	...	6.49 ± 0.10	5.90 ± 0.07	5.98 ± 0.03	6.12 ± 0.02	6.03 ± 0.02	-4.41
76779	SARG	54195.1198	4.63 ± 0.31	4.82 ± 0.30	5.09 ± 0.23	5.19 ± 0.33	-4.78
77408	SARG	54193.1507	5.60 ± 0.12	5.62 ± 0.21	5.63 ± 0.22	5.60 ± 0.24	-4.49
77408	FOCES	53575.9293	6.23 ± 0.06	6.09 ± 0.06	5.60 ± 0.12	5.70 ± 0.04	5.87 ± 0.03	5.85 ± 0.03	-4.20
80337	FEROS	52045.1772	5.45 ± 0.67	5.61 ± 0.36	5.37 ± 0.19	5.05 ± 0.37	-4.79
80366	SARG	54193.2128	5.23 ± 0.09	5.08 ± 0.58	5.22 ± 0.53	5.29 ± 0.41	-4.60
80686	FEROS	52045.2054	5.99 ± 0.03	5.85 ± 0.04	5.88 ± 0.03	5.49 ± 0.14	5.37 ± 0.09	5.44 ± 0.05	-4.65
80725	FOCES	53579.9305	5.88 ± 0.22	...	5.52 ± 0.11	5.20 ± 0.23	5.23 ± 0.18	5.07 ± 0.23	-4.51
81300	McDonald	52164.1210	5.64 ± 0.01	5.54 ± 0.03	5.29 ± 0.08	5.38 ± 0.07	5.46 ± 0.05	5.32 ± 0.03	-4.73

Table A.3. continue

HIP	Spectrograph	MJD (days)	$\log F_S$ (erg cm ⁻² s ⁻¹) in the subtrated spectrum						$\log R'_{HK}$
			Ca II			Ca II IRT			
			K	H	H α	$\lambda 8498$	$\lambda 8542$	$\lambda 8662$	
82588	FOCES	53576.9600	6.04 ± 0.12	5.99 ± 0.11	5.66 ± 0.08	5.73 ± 0.05	5.75 ± 0.04	5.77 ± 0.05	-4.39
83601	SARG	54195.2462	5.88 ± 0.08	5.88 ± 0.23	5.87 ± 0.22	5.87 ± 0.20	-4.50
84405	McDonald	52208.0394	4.88 ± 0.22	5.38 ± 0.07	5.42 ± 0.06	5.48 ± 0.02	-4.92
85295	SARG	54193.2589	4.70 ± 0.26	4.66 ± 0.99	4.91 ± 0.42	5.20 ± 0.33	-4.72
85561	SARG	54194.2041	5.19 ± 0.06	5.26 ± 0.19	5.22 ± 0.24	5.18 ± 0.24	-4.40
85810	SARG	54193.2741	5.83 ± 0.10	5.37 ± 0.62	5.43 ± 0.71	5.50 ± 0.65	-4.46
86036	McDonald	52030.4566	5.82 ± 0.08	5.73 ± 0.05	5.57 ± 0.05	5.48 ± 0.09	5.58 ± 0.04	5.51 ± 0.03	-4.76
86400	McDonald	52032.3071	5.17 ± 0.04	5.00 ± 0.05	5.01 ± 0.15	4.63 ± 0.11	-4.76
87579	FOCES	53574.8992	5.84 ± 0.14	5.78 ± 0.10	5.39 ± 0.12	5.59 ± 0.05	5.66 ± 0.05	5.58 ± 0.04	-4.43
88601	McDonald	52164.1787	5.52 ± 0.02	5.37 ± 0.03	5.29 ± 0.16	5.30 ± 0.09	5.42 ± 0.03	5.43 ± 0.03	-4.86
90790	McDonald	52208.0867	5.46 ± 0.04	5.34 ± 0.04	5.25 ± 0.12	5.20 ± 0.08	5.30 ± 0.06	5.20 ± 0.04	-4.90
91009	SARG	54779.8159	6.42 ± 0.01	5.99 ± 0.06	6.16 ± 0.02	6.17 ± 0.03	-3.66
92200	FOCES	53574.9577	5.44 ± 0.14	5.39 ± 0.11	4.58 ± 0.25	5.02 ± 0.01	5.20 ± 0.10	5.04 ± 0.06	-4.65
92283	FOCES	53578.9782	4.96 ± 0.14	5.23 ± 0.06	5.41 ± 0.05	5.28 ± 0.03	-4.68
96085	FOCES	53578.0463	5.41 ± 0.11	5.60 ± 0.06	5.74 ± 0.03	5.62 ± 0.02	-4.52
96285	FOCES	53575.0438	4.78 ± 0.30	5.00 ± 0.16	4.39 ± 0.35	4.87 ± 0.11	4.90 ± 0.09	4.94 ± 0.09	-5.08
98828	FOCES	53575.0823	5.33 ± 0.32	5.41 ± 0.22	4.96 ± 0.49	-4.81
99461	FEROS	51833.9874	4.94 ± 0.13	4.88 ± 0.28	4.81 ± 0.32	4.74 ± 0.75	3.89 ± 2.12	4.20 ± 0.44	-5.39
99711	FOCES	53575.9912	5.69 ± 0.17	5.61 ± 0.14	5.00 ± 0.48	6.44 ± 0.01	5.60 ± 0.05	5.38 ± 0.06	-4.60
99764	FOCES	53576.0317	...	4.81 ± 0.54	4.78 ± 0.29	-4.71
103256	FOCES	53576.0317	5.60 ± 0.17	5.77 ± 0.11	5.02 ± 0.22	5.02 ± 0.20	5.24 ± 0.09	5.16 ± 0.09	-4.50
104092	FOCES	53576.0519	...	5.22 ± 0.51	4.08 ± 0.90	4.38 ± 0.67	4.72 ± 0.24	4.62 ± 0.23	-5.23
104239	FOCES	53579.0004	5.53 ± 0.34	5.47 ± 0.46	5.10 ± 0.32	5.25 ± 0.10	5.42 ± 0.06	5.33 ± 0.07	-4.78
105038	FOCES	53576.0819	...	5.11 ± 0.34	5.07 ± 0.27	5.17 ± 0.13	5.19 ± 0.11	5.17 ± 0.10	-4.69
106400	SARG	54778.8327	5.97 ± 0.02	5.81 ± 0.09	5.96 ± 0.05	6.00 ± 0.06	-3.98
107350	SARG	54777.8715	5.90 ± 0.08	5.96 ± 0.12	5.86 ± 0.22	5.93 ± 0.11	-4.48
108028	FOCES	53576.1120	5.86 ± 0.08	5.86 ± 0.10	5.55 ± 0.06	5.58 ± 0.06	5.77 ± 0.03	5.70 ± 0.03	-4.40
108156	FOCES	53575.1412	5.66 ± 0.17	5.48 ± 0.20	5.13 ± 0.17	5.23 ± 0.14	5.00 ± 0.21	5.14 ± 0.10	-4.68
109527	FOCES	53578.0943	5.96 ± 0.08	5.92 ± 0.05	5.34 ± 0.13	5.65 ± 0.03	5.68 ± 0.04	5.68 ± 0.03	-4.41
110778	SARG	54777.9046	5.92 ± 0.04	5.65 ± 0.36	5.79 ± 0.25	5.79 ± 0.23	-4.43
111888	FOCES	53576.1296	5.72 ± 0.24	5.64 ± 0.14	5.54 ± 0.08	5.28 ± 0.14	5.53 ± 0.06	5.42 ± 0.06	-4.59
113576	SARG	54777.9334	4.84 ± 0.15	4.99 ± 0.31	5.19 ± 0.24	5.34 ± 0.21	-4.63
114886	FOCES	53575.1545	5.27 ± 0.26	5.05 ± 0.24	5.04 ± 0.24	3.92 ± 2.82	4.46 ± 0.63	4.62 ± 0.35	-5.11
115162	FOCES	53576.9955	6.28 ± 0.11	6.09 ± 0.08	5.91 ± 0.06	5.85 ± 0.03	5.87 ± 0.03	5.91 ± 0.03	-4.22
115331	FOCES	53578.1064	6.30 ± 0.03	6.10 ± 0.05	5.69 ± 0.03	5.85 ± 0.03	5.98 ± 0.03	5.95 ± 0.02	-4.15
115341	FOCES	53575.1704	5.47 ± 0.14	5.44 ± 0.08	5.17 ± 0.20	5.38 ± 0.11	5.44 ± 0.08	5.20 ± 0.10	-4.73
115445	FOCES	53580.1105	5.16 ± 0.15	5.16 ± 0.23	5.05 ± 0.25	5.15 ± 0.11	-4.70
116613	FOCES	53578.1185	5.93 ± 0.41	5.83 ± 0.26	5.52 ± 0.15	5.46 ± 0.08	5.71 ± 0.04	5.59 ± 0.03	-4.61
120005	SARG	54779.1742	5.12 ± 0.09	5.25 ± 0.12	5.35 ± 0.12	5.56 ± 0.12	-4.39

Table A.4. Predicted radial velocity jitter.

HIP	Spectrograph	MJD (days)	SpT	$\log R'_{\text{HK}}$	σ_{rv}^1 (m s^{-1})	σ_{rv}^2 (m s^{-1})
544	SARG	54780.9561	G8V	-4.61	5 - 18	8 - 19
544	McDonald	52031.3248	G8V	-4.67	5 - 15	7 - 18
1803	SARG	54777.9856	G3V	-4.36	11 - 34	11 - 26
3765‡	FOCES	53747.7686	K2V	-5.41	0 - 2	4 - 10
3765‡	McDonald	52164.3977	K2V	-5.41	0 - 2	4 - 10
4148	FEROS	51834.1339	K2V	-4.83	3 - 10	5 - 12
4845	SARG	54778.9878	K7V	-4.54	6 - 21	5 - 13
5286	FOCES	53576.1601	K3V	-4.59	6 - 19	5 - 13
5944	FOCES	53576.1764	G0V	-4.47	8 - 26	10 - 23
6290	SARG	54107.9171	K7V	-4.40	10 - 31	6 - 14
7235	SARG	54780.9662	G8V	-4.72	4 - 14	7 - 17
7576	FOCES	53577.1583	G8V	-4.29	13 - 41	12 - 29
7751‡	FEROS	51834.1456	K0V	-4.94	2 - 8	5 - 12
7981‡	FOCES	53578.1869	K1V	-5.19	1 - 4	4 - 11
8275	FOCES	54086.7647	K3/K4V	-4.51	7 - 23	5 - 13
8362‡	McDonald	51883.2217	K0V	-5.05	1 - 6	4 - 11
8486	FOCES	53748.8161	G1V	-4.19	16 - 53	14 - 33
8768	SARG	54778.0142	K7V	-4.59	6 - 19	5 - 13
10138	FEROS	51834.1664	K0V	-4.68	4 - 15	5 - 13
10337	SARG	54780.0100	K7V	-4.68	4 - 15	5 - 13
10416	FOCES	54086.7855	K3/K4V	-4.30	12 - 40	6 - 14
11565	SARG	54780.2041	K5V	-4.58	6 - 20	5 - 13
12110	SARG	54780.0623	K3V	-4.40	9 - 31	6 - 14
13258	FOCES	54086.8172	K5V	-4.76	4 - 12	5 - 12
13402	McDonald	52207.4006	K1V	-4.30	12 - 40	6 - 14
13402	SARG	54779.0488	K1V	-4.36	11 - 35	6 - 14
13976	SARG	54778.0715	K3/K4V	-4.40	10 - 31	6 - 14
15330	FEROS	51834.2315	G1V	-4.86	3 - 9	6 - 14
15442	SARG	54780.1170	G4V	-4.75	4 - 12	7 - 16
15673	FOCES	54086.8639	K2V	-4.54	7 - 22	5 - 13
15919	FOCES	53747.8508	K5V	-4.60	5 - 18	5 - 13
16134	SARG	54779.0552	K7V	-4.61	5 - 18	5 - 13
16537	McDonald	51833.9938	K2V	-4.62	5 - 17	5 - 13
17420‡	McDonald	52207.4446	K2V	-5.04	1 - 6	4 - 11
18774	SARG	54779.1053	K4V	-4.56	6 - 21	5 - 13
18859	SARG	54780.1408	F7V	-4.60	11 - 74	12 - 27
19076	SARG	54780.1482	G5V	-4.30	12 - 40	12 - 28
19335	SARG	54780.1552	F7V	-4.73	6 - 45	9 - 21
19832	FOCES	54087.9871	K5V	-4.66	5 - 16	5 - 13
19849‡	McDonald	51880.2760	K0V	-5.38	0 - 2	4 - 10
20917	FOCES	54086.9422	K5V	-4.62	5 - 18	5 - 13
22263	McDonald	52207.4280	G1V	-4.61	5 - 18	8 - 19
23311‡	McDonald	52207.4662	K3V	-5.29	1 - 3	4 - 11
23693	FEROS	51834.2547	F7V	-4.49	17 - 114	15 - 32
23786	FOCES	53747.9144	K0V	-4.49	8 - 25	5 - 14
24819	FOCES	53748.9549	K3V	-4.53	7 - 22	5 - 13
24874	FOCES	54086.9907	K3V	-4.14	19 - 60	6 - 15
25220	FOCES	53748.9746	K5V	-4.13	19 - 62	6 - 15
25623	FOCES	54087.0273	K4V	-4.60	6 - 19	5 - 13
26779	McDonald	52030.0849	K1V	-4.55	6 - 21	5 - 13
27913	McDonald	51882.3464	G0V	-4.49	7 - 25	9 - 22
29067	FOCES	54088.0550	K5V	-4.40	9 - 31	6 - 14
29525	FOCES	53747.9540	G1.5V	-4.33	11 - 37	12 - 27
29568	SARG	54778.1689	G5V	-4.39	10 - 32	11 - 25
29800	SARG	54193.8509	F5IV-V	-4.51	16 - 106	14 - 31
32010	FOCES	54086.0581	K2V	-4.38	10 - 33	6 - 14
32423	FOCES	54086.0836	K3V	-4.64	5 - 17	5 - 13
32919‡	FOCES	54086.0995	K5V	-5.06	1 - 5	4 - 11
32984	FOCES	54088.0194	K3V	-4.36	11 - 35	6 - 14
33373	FOCES	54086.1177	K3/K4V	-4.51	7 - 23	5 - 13
33560	SARG	54193.8607	K5V	-4.14	19 - 60	6 - 15
33852	FOCES	54087.0680	K3/K4V	-4.74	4 - 13	5 - 13
36357	SARG	54107.0827	K2V	-4.45	8 - 27	5 - 14
36357	FOCES	54164.9213	K2V	-4.30	12 - 40	6 - 14
36551	FOCES	54086.1369	K2V	-4.44	9 - 28	5 - 14
36827	SARG	54193.8830	K2V	-4.24	14 - 47	6 - 15
37349	SARG	54193.8960	K1V	-4.54	6 - 22	5 - 13
37349	McDonald	51883.3603	K1V	-4.57	6 - 20	5 - 13
37349	FOCES	53748.0933	K1V	-4.28	13 - 42	6 - 14
40170‡	FOCES	54158.0979	K5V	-5.15	1 - 4	4 - 11

¹ Saar et al. (1998) ‡Stars with $\log R'_{\text{HK}} \leq -4.9$ ² Santos et al. (2000)

Table A.4. continue

HIP	Spectrograph	MJD (days)	SpT	$\log R'_{\text{HK}}$	σ_{rv}^1 (m s^{-1})	σ_{rv}^2 (m s^{-1})
40671	FOCES	54164.9814	K4V	-4.64	5 - 17	5 - 13
42074	FOCES	54087.1283	G8V	-4.28	13 - 42	12 - 29
42074	SARG	54193.9536	G8V	-4.26	14 - 44	13 - 30
42333	FOCES	53749.0569	G1.5V	-4.40	10 - 31	11 - 25
42438	McDonald	51883.5354	G1.5Vb	-4.38	10 - 33	11 - 26
42808	FEROS	52046.9654	K2V	-4.48	8 - 26	5 - 14
43557	FOCES	53749.0723	G0	-4.67	5 - 15	7 - 18
44897	SARG	54779.1457	F9V	-4.47	18 - 124	15 - 34
45383	FOCES	53748.1605	K0V	-4.31	12 - 39	6 - 14
45617	FOCES	53748.1832	K0V	-4.51	7 - 24	5 - 13
46580	FOCES	54087.1896	K3V	-4.27	13 - 44	6 - 15
46580	SARG	54193.9665	K3V	-4.73	4 - 13	5 - 13
46816	SARG	54193.9734	K0V	-3.63	70 - 221	7 - 18
46816	FOCES	54161.0253	K0V	-3.69	59 - 189	7 - 17
46843	SARG	54193.9834	K0V	-4.15	18 - 59	6 - 15
46843	FOCES	54161.0562	K0V	-4.00	27 - 86	6 - 16
47080	McDonald	52031.1226	G8V	-4.76	3 - 12	7 - 16
47080	FOCES	53749.1406	G8V	-4.38	10 - 33	11 - 26
49366	SARG	53786.1106	K0	-4.54	6 - 22	5 - 13
49908‡	SARG	54194.0217	K7V	-5.00	2 - 6	5 - 12
51525	SARG	53786.1408	K7V	-4.88	2 - 9	5 - 12
53486	SARG	53786.1585	K0	-4.59	6 - 19	5 - 13
54155	SARG	53786.1684	G8V	-4.41	9 - 30	11 - 25
54155	FOCES	54158.1320	G8V	-4.26	14 - 44	13 - 30
54426	FOCES	54087.2019	K0V	-4.77	3 - 12	5 - 12
54646	FOCES	54086.2260	K8V	-4.86	3 - 9	5 - 12
54745	FOCES	54086.2729	G1V	-4.27	14 - 44	13 - 30
54810	SARG	54106.1858	K5V	-4.50	7 - 24	5 - 14
57494	FOCES	54156.0187	K3/K4V	-4.80	3 - 11	5 - 12
59000	SARG	54194.0305	K7V	-4.12	20 - 64	6 - 15
59280	FOCES	54156.0998	K0V	-4.56	6 - 21	5 - 13
60866‡	FOCES	54228.9530	K5V	-5.14	1 - 4	4 - 11
62523	FOCES	53575.8536	G7V	-4.43	9 - 29	10 - 24
64394‡	McDonald	52030.2579	G1V	-5.06	1 - 5	4 - 11
64797	McDonald	52030.2286	K2V	-4.63	5 - 17	5 - 13
65515	FOCES	54132.1649	K0V	-4.22	15 - 49	6 - 15
66147	SARG	53786.1989	K3/K4V	-4.70	4 - 14	5 - 13
66252	FOCES	54168.0938	K5V	-3.89	36 - 114	7 - 16
67105	SARG	53786.2384	K2	-4.39	10 - 32	6 - 14
67275	SARG	54108.3087	F6IV	-4.90	3 - 23	7 - 16
67422	McDonald	52030.2748	K2	-4.68	4 - 15	5 - 13
68337	FOCES	53577.8595	K5V	-4.72	4 - 14	5 - 13
69357	FOCES	53578.0216	K0V	-4.60	6 - 19	5 - 13
69526	FOCES	53578.9125	K2V	-4.28	13 - 43	6 - 14
69962	SARG	54108.2822	K7V	-4.80	3 - 11	5 - 12
70218	SARG	53786.2988	K5V	-4.34	11 - 36	6 - 14
70218	FOCES	54159.1693	K5V	-4.54	7 - 22	5 - 13
71395	SARG	54194.1338	K2V	-4.51	7 - 23	5 - 13
71395	FOCES	53577.8799	K2V	-4.39	10 - 32	6 - 14
71743	SARG	54193.0776	G8V	-4.51	7 - 23	9 - 22
72146‡	FOCES	53575.8597	K0V	-4.93	2 - 8	5 - 12
72146	SARG	54194.1582	K0V	-4.74	4 - 13	5 - 13
72237	FOCES	54159.2162	K5V	-4.57	6 - 20	5 - 13
72237	SARG	53786.2752	K5V	-4.54	7 - 22	5 - 13
72567	FOCES	54168.1225	G2V	-4.34	11 - 37	12 - 27
72659‡	McDonald	52030.3731	G8V	-5.07	1 - 5	4 - 10
72848	McDonald	52164.0668	K1V	-4.52	7 - 23	5 - 13
72875	FOCES	53577.8968	K0V	-4.45	8 - 27	5 - 14
73184	SARG	54194.1436	K4V	-4.63	5 - 17	5 - 13
74702	SARG	54108.2523	K0	-4.35	11 - 35	6 - 14
75201	SARG	54193.0544	K7V	-4.54	6 - 22	5 - 13
75253	FOCES	54161.1805	K3/K4V	-4.83	3 - 10	5 - 12
75542	SARG	54195.1035	K3/K4V	-4.88	2 - 9	5 - 12
75809	FOCES	54160.1481	G8V	-4.41	9 - 30	10 - 25
76779	SARG	54195.1198	K7V	-4.78	3 - 12	5 - 12
77408	SARG	54193.1507	G8V	-4.49	8 - 25	10 - 22
77408	FOCES	53575.9293	G8V	-4.20	16 - 52	14 - 33
80337	FEROS	52045.1772	G3/G5V	-4.79	3 - 11	6 - 15
80366	SARG	54193.2128	K2V	-4.60	5 - 18	5 - 13
80686	FEROS	52045.2054	F9V	-4.65	9 - 59	11 - 24
80725	FOCES	53579.9305	K2V	-4.51	7 - 23	5 - 13

¹ Saar et al. (1998) ‡Stars with $\log R'_{\text{HK}} \leq -4.9$ ² Santos et al. (2000)

Table A.4. continue

HIP	Spectrograph	MJD (days)	SpT	$\log R'_{\text{HK}}$	σ_{rv}^1 (m s^{-1})	σ_{rv}^2 (m s^{-1})
81300	McDonald	52164.1210	K0Vk	-4.73	4 - 13	5 - 13
82588	FOCES	53576.9600	G8V	-4.39	10 - 32	11 - 25
83601	SARG	54195.2462	F9V	-4.50	16 - 111	14 - 32
84405‡	McDonald	52208.0394	K2V	-4.92	2 - 8	5 - 12
85295	SARG	54193.2589	K7V	-4.72	4 - 14	5 - 13
85561	SARG	54194.2041	K5V	-4.40	9 - 31	6 - 14
85810	SARG	54193.2741	G5V	-4.46	8 - 27	10 - 23
86036	McDonald	52030.4566	G0Va	-4.76	3 - 12	7 - 16
86400	McDonald	52032.3071	K3V	-4.76	3 - 12	5 - 12
87579	FOCES	53574.8992	K0V	-4.43	9 - 29	5 - 14
88601	McDonald	52164.1787	K1V	-4.86	3 - 9	5 - 12
90790	McDonald	52208.0867	K1V	-4.90	2 - 8	5 - 12
91009	SARG	54779.8159	K6Ve	-3.66	65 - 207	7 - 18
92200	FOCES	53574.9577	K7V	-4.65	5 - 16	5 - 13
92283	FOCES	53578.9782	K3/K4V	-4.68	4 - 15	5 - 13
96085	FOCES	53578.0463	K2V	-4.52	7 - 23	5 - 13
96285‡	FOCES	53575.0438	K7V	-5.08	1 - 5	4 - 11
98828	FOCES	53575.0823	K0V	-4.81	3 - 11	5 - 12
99461‡	FEROS	51833.9874	K3V	-5.39	0 - 2	4 - 10
99711	FOCES	53575.9912	K4V	-4.60	5 - 18	5 - 13
99764	FOCES	53576.0317	K6V	-4.71	4 - 14	5 - 13
103256	FOCES	53576.0317	K2V	-4.50	7 - 24	5 - 14
104092‡	FOCES	53576.0519	K6V	-5.23	1 - 3	4 - 11
104239	FOCES	53579.0004	K1IV	-4.78	3 - 11	5 - 12
105038	FOCES	53576.0819	K5V	-4.69	4 - 14	5 - 13
106400	SARG	54778.8327	K5V	-3.98	28 - 91	6 - 16
107350	SARG	54777.8715	G4V	-4.48	8 - 25	10 - 23
108028	FOCES	53576.1120	K0V	-4.40	10 - 31	6 - 14
108156	FOCES	53575.1412	K0V	-4.68	4 - 15	5 - 13
109527	FOCES	53578.0943	G8V	-4.41	9 - 30	11 - 25
110778	SARG	54777.9046	G1V	-4.43	9 - 29	10 - 24
111888	FOCES	53576.1296	K2V	-4.59	6 - 19	5 - 13
113576	SARG	54777.9334	K7V	-4.63	5 - 17	5 - 13
114886‡	FOCES	53575.1545	K1V	-5.11	1 - 5	4 - 11
115162	FOCES	53576.9955	G0	-4.22	15 - 49	13 - 31
115331	FOCES	53578.1064	G8V	-4.15	18 - 59	15 - 35
115341	FOCES	53575.1704	K5V	-4.73	4 - 13	5 - 13
115445	FOCES	53580.1105	K0V	-4.70	4 - 14	5 - 13
116613	FOCES	53578.1185	G0V	-4.61	5 - 18	8 - 19
120005	SARG	54779.1742	K7V	-4.39	10 - 32	6 - 14

¹ Saar et al. (1998) ‡Stars with $\log R'_{\text{HK}} \leq -4.9$ ² Santos et al. (2000)

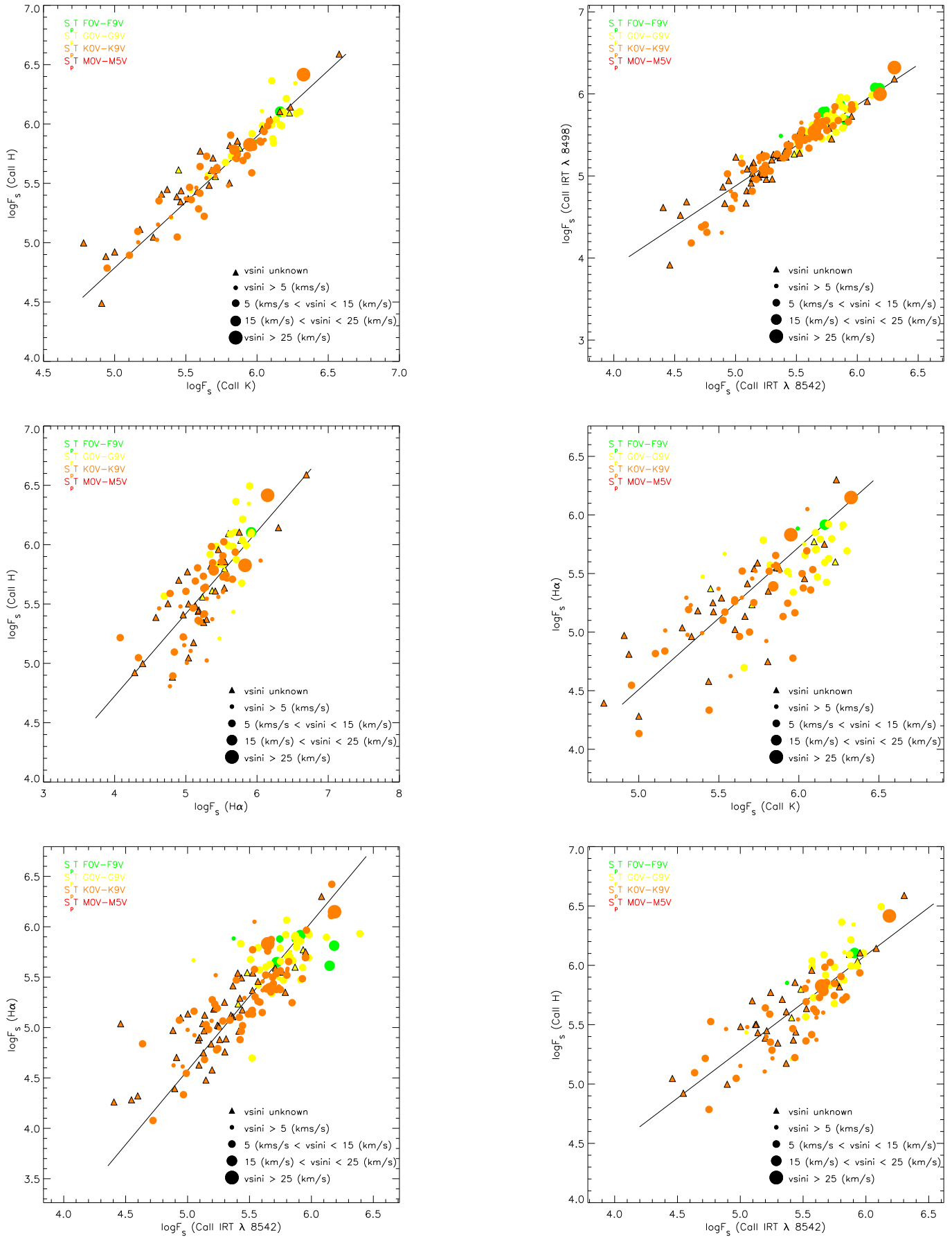


Fig. A.1. Flux-flux relationships among different chromospheric activity indicators. Symbol thickness increases with increasing rotational velocity (triangles are used when $v \sin i$ could not be determined). Colors are used to discern different spectral types.